February 1994
NSRP 0407

THE NATIONAL SHIPBUILDING RESEARCH PROGRAM

Advanced Cutting Technology

U.S. DEPARTMENT OF THE NAVY
CARDEROCK DIVISION, NAVAL SURFACE WARFARE CENTER

in cooperation with
Peterson Builders, Inc.

Report Documentation Page

Form Approved
OMB No. 0704-0188

1. REPORT DATE	2. REPORT TYPE	3. DATES COVERED
FEB 1994	**N/A**	**-**

4. TITLE AND SUBTITLE	5a. CONTRACT NUMBER
The National Shipbuilding Research Program, Advanced Cutting Technology	5b. GRANT NUMBER
	5c. PROGRAM ELEMENT NUMBER
6. AUTHOR(S)	5d. PROJECT NUMBER
	5e. TASK NUMBER
	5f. WORK UNIT NUMBER
7. PERFORMING ORGANIZATION NAME(S) AND ADDRESS(ES) **Naval Surface Warfare Center CD Code 2230 - Design Integration Tower Bldg 192 Room 128 9500 MacArthur Blvd Bethesda, MD 20817-5700**	8. PERFORMING ORGANIZATION REPORT NUMBER
9. SPONSORING/MONITORING AGENCY NAME(S) AND ADDRESS(ES)	10. SPONSOR/MONITOR'S ACRONYM(S)
	11. SPONSOR/MONITOR'S REPORT NUMBER(S)

12. DISTRIBUTION/AVAILABILITY STATEMENT
Approved for public release, distribution unlimited

13. SUPPLEMENTARY NOTES

14. ABSTRACT

15. SUBJECT TERMS

16. SECURITY CLASSIFICATION OF:			17. LIMITATION OF ABSTRACT	18. NUMBER OF PAGES	19a. NAME OF RESPONSIBLE PERSON
a. REPORT	b. ABSTRACT	c. THIS PAGE			
unclassified	**unclassified**	**unclassified**	**SAR**	**130**	

DISCLAIMER

These reports were prepared as an account of government-sponsored work. Neither the United States, nor the United States Navy, nor any person acting on behalf of the United States Navy (A) makes any warranty or representation, expressed or implied, with respect to the accuracy, completeness or usefulness of the information contained in this report/manual, or that the use of any information, apparatus, method, or process disclosed in this report may not infringe privately owned rights; or (B) assumes any liabilities with respect to the use of or for damages resulting from the use of any information apparatus, method, or process disclosed in the report. As used in the above, "Persons acting on behalf of the United States Navy" includes any employee, contractor, or subcontractor to the contractor of the United States Navy to the extent that such employee, contractor, or subcontractor to the contractor prepares, handles, or distributes, or provides access to any information pursuant to his employment or contract or subcontract to the contractor with the United States Navy. ANY POSSIBLE IMPLIED WARRANTIES OF MERCHANTABILITY AND/OR FITNESS FOR PURPOSE ARE SPECIFICALLY DISCLAIMED.

ADVANCED CUTTING TECHNOLOGY

FOR THIN ALUMINUM AND STEEL PLATES

A PROJECT OF THE NATIONAL

SHIPBUILDING RESEARCH PROGRAM

FOR

THE SOCIETY OF NAVAL ARCHITECTS AND MARINE ENGINEERS

SHIP PRODUCTION COMMITTEE

WELDING PANEL SP-7

JANUARY 14, 1994

Projectt Coordinated By:

R. W. McClellan

Russ W. McClellan cy ojd
Welding Engineer
Ingalls Shipbuilding, Inc.

Report Prepared By:

O.J. Davis
Welding Engineer
Ingalls Shipbuilding, Inc.

ACKNOWLEDGEMENTS :

This project report for SP-7 task #07-89-02 was funded under USN Contract #OO167-90H-O057. The project was performed by the Welding Engineering Department of Ingalls Shipbuilding, Inc. , Pascagoula, MS under subcontract with Peterson Builders, Inc. , Sturgeon Bay, WI, under the NSRP Program Management of James Rogness and Doug Diedrick. Lee Kvidahl served as SP-7 Panel Chairman and Manager of Ingalls Welding Engineering; Administrative leadership was provided by Dale Rome, Naval Surface Warfare Center, Carderock, MD. Appreciation is expressed to O.J. Davis for the evaluation and interpretation of the data and preparation of the project report.

Russ McClellan
Project Coordinator

EXECUTIVE SUMMARY

SUMMARY

Four processes, plasma arc, oxyacetylene, laser, and water jet, were compared for cutting thin aluminum and steel plates. The objective was to determine which process would provide high productivity and cost effectiveness while minimizing distortion. Control of distortion is a major problem in lightweight, welded ship structures.

A unique and innovative application of photogrammetry for measurement of out-of-plane distortion was demonstrated in the project. Photogrammetry, because of its unique ability to produce a large amount of digital data with close tolerance, non-contact measurements, was used to measure the magnitude of distortion on the cut pieces of aluminum and steel. This is believed to be the first use of photogrammetry for measurement of small values of out-of-plane distortion. Quality impact of the processes on the cut edges and base metals was measured by metallography. This included metallurgical effects and hardness adjacent to the cuts. Scanning electron microscopy was used to determine roughness of the cut edges.

CONCLUSIONS

(l)Except for the extreme distortion produced in steel by oxyacetylene, none of the cutting processes were found to cause excessive damage to either aluminum or steel.

(2)Evaluation of the data concluded that Plasma cutting was the fastest and most cost effective method of cutting 3 mm (0.118 in.) aluminum and steel plates with acceptable low levels of distortion.

(3)Photogrammetry can be used where high density data is needed for measurement of out-of-plane contours as small as 0.25 mm (0.01 in.).

RECOMMENDATIONS

The plasma process is recommended for any start-up operation for production cutting of thin aluminum and steel plates. Compared to plasma, laser and water jet were found not to be cost effective for high productivity cutting.

Research should be encouraged to develop real time computer processing of photogrammetric data for use in shipbuilding as a tool in prevention and correction of distortion in structures and as a mechanism for control of robots used in production.

TABLE OF CONTENTS

TABLE OF CONTENTS (Continued)

TABLE OF CONTENTS (Continued)

TABLE OF CONTENTS (Continued)

LIST OF FIGURES

LIST OF FIGURES (Continued)

LIST OF FIGURES (Continued)

LIST OF FIGURES (Continued)

* Welding Handbook, 8th Ed., Vol 2, American Welding Society, Miami, Fl, 1991

** Operators Manual for C-3000 Laser Turret Punch Press, Publication #9202-107-100, Murata Wiedeman Inc. Charlotte, NC

APPENDIX A

APPENDIX A (Continued)

*Note : Conversion factor for English to metric on figures:
1.0 in. = 25.4 mm
1 ft = 304.8 mm

ADVANCED CUTTING TECHNOLOGY FOR THIN ALUMINUM AND STEEL PLATES

BACKGROUND

Reductions in plate and beam thicknesses in shipbuilding to reduce weight and increase payload have been made possible by the availability of plate with improvements in strength, toughness, and quality. Reduced thickness of sections offers production advantages by reducing the amount of welding required in construction, however, with these advantages come the pervasive problem in lightweight ship construction of control of distortion. As plate thicknesses are reduced, distortion problems increase and with that some added problems in fit-up for welding, and in many cases , additional welding. A number of studies of approaches to control and correction of distortion have been made in recent years in attempts to reduce the impact of distortion on cost to fabricate ships using light weight materials. The purpose of this task is to add to the understanding and control of distortion by increasing the base of information available on the relative effects “on distortion of several industrial plate cutting processes. The processes included in the scope of this study are oxyacetylene, plasma, laser and water jet cutting technology applied to 3mm thick aluminum and steel plates. A secondary objective is to evaluate the applicability of photogrammetry to measurement of distortion in plates.

I. INTRODUCTION

Four practical methods of cutting thin plates for lightweight ship structures were compared for advantages in shipbuilding. Plates of 3 mm thickness aluminum and steel were cut for comparative data. The primary objective of the project was to measure the out-of-plane distortion caused by the four processes used - plasma arc cutting (PAC), water jet cutting (WJC), laser cutting, and oxyacetylene (OA) cutting. As a secondary objective an evaluation was made of the use of photogrammetric contour plotting as a tool for distortion control. In addition to out-of-plane distortion, other attributes of the processes were assessed including cut edge quality and heat affected zone (HAZ) changes to the base metal. The potential for practical and cost effective implementation in lightweight shipbuilding was a major factor in the selection of the processes tested.

Photogrammetry, because of its unique ability to acquire and digitize a large amount of dimensional data without separate physical measurements was selected as the most efficient method of analysis of distortion produced by cutting. Parallel stereo photo pairs and computerized stereoplotter instrumentation were used to develop photogrammetric data. Optical microscopy, scanning electron microscopy, 100X metallography and microhardness were used to evaluate the quality of the cut edges and heat affected zones.

II. TECHNICAL APPROACH TO EVALUATION OF THIN PLATE CUTTING PROCESSES

This report will discuss the methods of cutting, the methods of evaluation, and the comparative results of cutting with respect to distortion and quality. The services of four widely recognized companies with appropriate apparatus and special expertise in their respective fields of cutting technology were contracted to meet the requirements of the statements of work for the project. Collaborative efforts were made with a shipyard and cutting equipment supply companies for performing the test cuts. A photogrammetric engineering service company and a materials testing laboratory were contracted to perform the distortion analysis and to evaluate quality effects of cutting.

A. Pattern For Cutting Tests

The statements of work for cutting include a design template (Figure 1) which was based on features of an actual ship bulkhead pattern typical of those fabricated for an 1100 ton corvette, a lightweight surface combat ship under construction at the time of this project. This pattern, selected for cutting, was similar to bulkhead details located adjacent to the turn-of-the-bilge strake. An increase in complexity of the cut was added by including the details of a manway access hole, a pipe penetration hole and a cut out for a longitudinal stiffener beam.

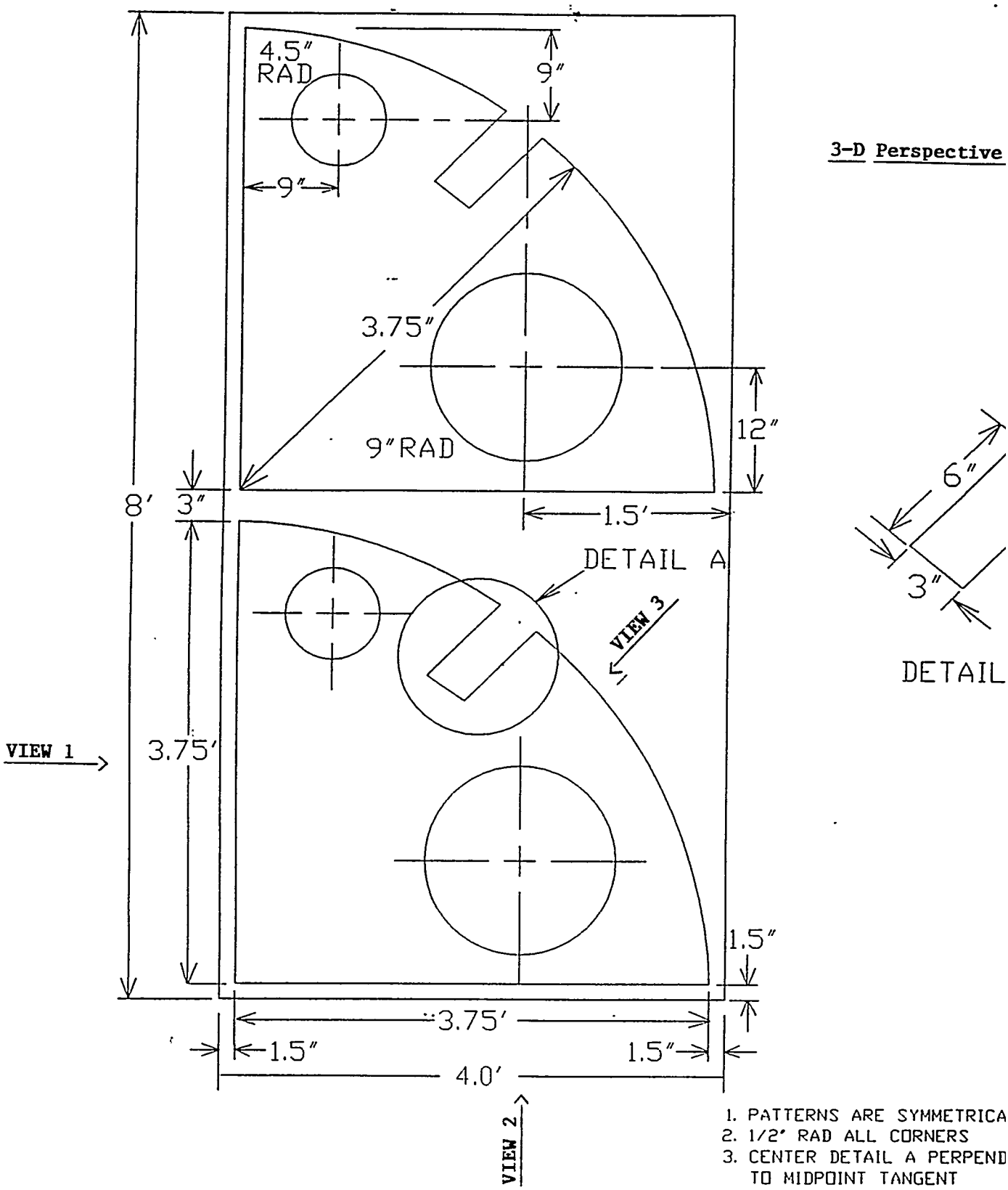

Fig.1 - Test Pattern Used to Compare Oxyacetylene, Plasma, Laser and Water Jet Cutting of Aluminum and Steel Plates.

B. Materials for Cutting Tests

The materials tested were 3mm thick aluminum and steel plates, typical of those required to be cut in construction of the corvette. The aluminum alloy used was ASTM B209/grade 5456, the steel plates were ASTM A715/grade 80. The alloys were also typical of ship specification requirements. To provide for two full size samples of the Figure 1 pattern, 1.23 m X 2.46 m (4 ft X 8 ft) plates were cut into 1.23 m X 1.23 m (4 ft X 4 ft) pieces. Multiple samples for each process provided a basis for estimating the consistency of the processes and results.

Plates as nearly identical as possible were needed to preserve comparability of samples and the results of cutting with the different processes. To meet this need, plates were purchased from the shipyard from the same sourcing which supplied materials for the light weight ship under construction. These plates were shipped to the subcontractors laboratories or shops for cutting by the various processes. One set of samples, those used for the water jet cutting, were cut from nominal 1/8 in. (3.2 mm) plate. This deviation in magnitude from the other sets of 3mm thickness was not considered great enough to adversely affect the validity of the comparison testing.

C. Technical Support for Cutting Processes and Analytical Data

The providers of cutting, metallographic, and photogrammetric services were :

* Water Jet cutting - Flow International Corp. , Kent, WA
* Plasma and oxyacetylene cutting - L-TeC Corp, Florence, SC

* Laser cutting - Murata-Wiedeman Corp. - Charlotte, NC
* Metallography - Materials Evaluation Laboratory, Baton Rouge, LA
* Photogrammetry - Aerometric Engineering Inc., Sheboygan, WI

D. Technical Approach to Cutting of Samples

In all cases the test plates were placed on flat platens in the suppliers laboratory or shop. Supplementary material for preliminary cuts was supplied to enable setting of parameters prior to the test cuts. The cutting heads and cutting tables were equipped with automatic control mechanisms and the ability to program the shape of the pattern to be cut. Where feasible, the cutting path instruction was further adjusted to compensate for the expected width of kerf to preserve the desired part dimension and to allow the kerf to fall on the scrap side of the cut.

E. Technical Approach to Metallography

Materials Evaluation Laboratory received randomly selected pieces of the aluminum and steel plates which were cut from the pattern after all photogrammetric photos were completed. Metallographic testing included macrophotos of the edge profiles at 30X, Scanning Electron Microscope (SEM) photos at 30X of the as-cut surfaces, micrographs at 100X of polished and etched samples transverse and longitudinal to the experimental cuts, and Vickers microhardness tests at intervals perpendicular to the cuts. The metallographic report is reproduced in Appendix A.

F. Technical Approach to Photogrammetric Measurements

Photogrammetry as applied to this project involves the production of stereo pairs of photographs which are used in a stereo plotter to create a three dimensional digital model and then further processed by digital computer for final presentation of graphical and numerical results.

In order to perform the photogrammetric analyses, the plate samples were photographed in place on the horizontal platform on which they were to be cut. The photogrammetric camera used was a Zeiss Jena UMK 10/1318. The camera was equipped with a 100 mm focal length lens which can be varied in 0.4 mm increments and provides focus from 1.4M to infinity. The film was Kodak 2405 B and W aerial negative film. On site processing was done in field developing tanks.

Parallel photographic stereo-pairs were produced for the photogrammetric measurements before and after cutting. The object was to enable “subtraction” of the pre-existing out-of-plane distortion from the after cut distortion and to produce resultant maps showing changes in the surface contours which resulted from the cutting. Parallel stereo pairs rather than convergent photography (camera lenses not parallel) was selected because the short distances to the plates provided limited depth of field even with the smallest obtainable lens apertures. For photogrammetric measurements of accuracy and out-of-plane distortion steps prior to and after cutting included the following.

Prior to cutting:

1. Mapped the upper surface of the plates in position for cutting.
2. Generated maps with data points at intersections of grid lines on 50 mm (2 in.) centers.
3. Produced maps relative to a plane fit to the upper surface of the work platen.

After Cutting:

1. Mapped the upper surfaces of plates in the cut position using fiducial marks as references for measurements.
2. Produced maps using data at intersections of 50 mm (2 in.) centered grid lines established prior to cutting.
3. Produced maps showing location of actual cut edges relative to the test pattern.
4. Produced contour maps of distortion before and after cutting and resultant contour maps of distortion caused by cutting.
5. Marked the magnitudes of distortion of the predominant contour features on the edge plots and contour maps.
6. Produced a 3 dimensional depiction of the distortion data from 3 angles of view. (It will be seen in the 3D contour plots that the scale of the vertical displacements on the 3D perspective diagrams were greatly exaggerated to enable clear presentation of the type and shape of the distortion resulting from the cutting processes.)

Maps of the location and deviation of the cut holes and edges relative to the test patterns were included. The vectors along the edge of the figures, which will be shown for each cutting process, show the direction and magnitude of the deviation of the actual cut from the pattern. Edge Plots, contour maps and 3-D plots are included in this report.

III . OXYACETYLENE (OA) CUTTING OF 3mm STEEL PLATES

A. General Principles of OA Cutting

Oxyacetylene cutting has for many years been a widely used method of thermal cutting of metals. In this process the metal is severed by heating it to an elevated temperature, then providing a jet of pure Oxygen to the heated metal. The metal is melted and oxides are formed by the heat of the chemical reaction of Iron with Oxygen and the velocity of the gas. A typical cutting torch configuration is shown in Figure 2.

Removal of metal and oxides from the kerf is aided by the high velocity of gas in the jet produced by the cutting tip. The kerf, Figure 3, is the gap produced by the cutting action.

Gasses other than acetylene are used in oxyfuel cutting, however, the principle of the Oxygen reaction is the same. Acetylene is the most popular choice of fuel gas because of its higher temperature and relatively low Oxygen requirements. Natural gas has a slightlty lower Oxygen requirement, but also has a lower flame temperature, 4600 F (2540 C) compared to 5600 F (3100 C) for acetylene.

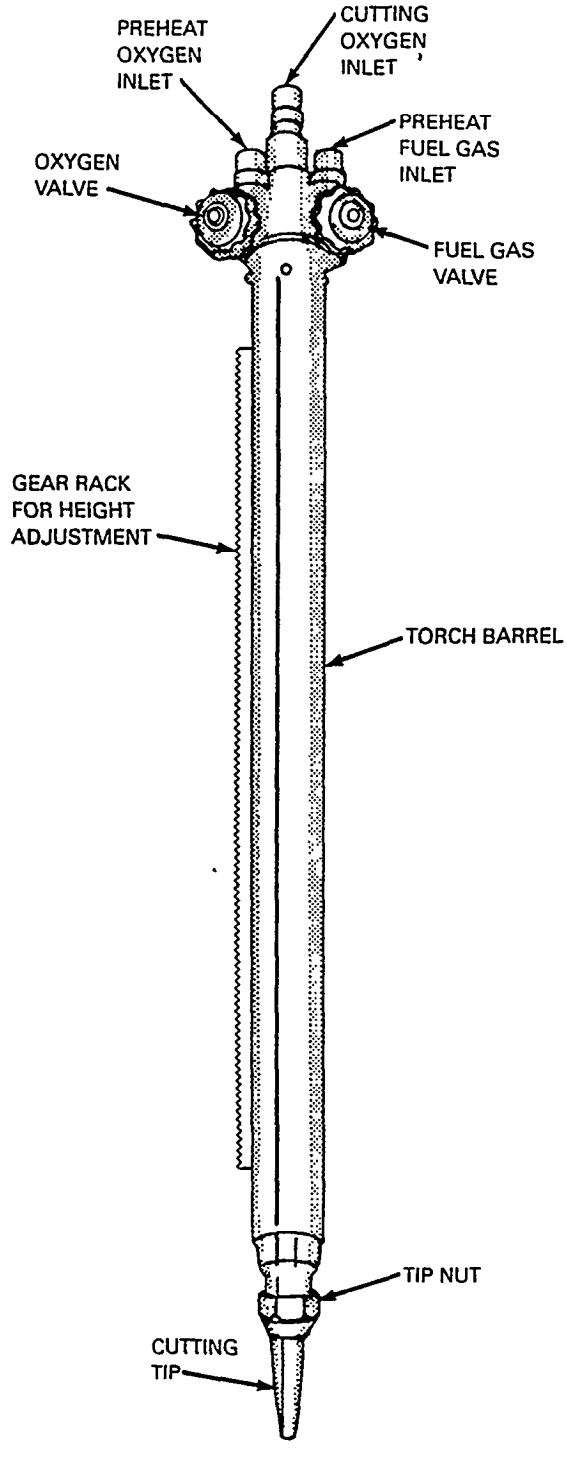

Fig.2 - Typical Configuration of Cross Section of an Oxyacetylene Cutting Torch.

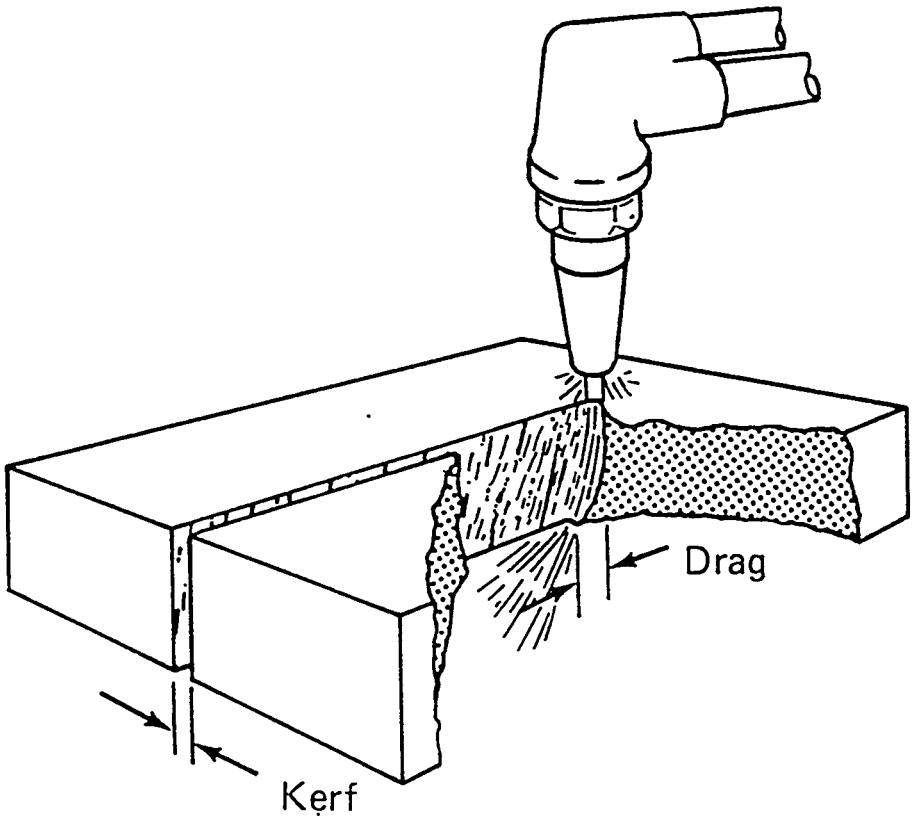

Fig.3 - Illustration of Kerf and Drag in OA Cutting

In this project the evaluation of OA cutting was limited to steel plates because the process is rarely used for aluminum plate. Aluminum very rapidly produces a refractory oxide coating in an Oxygen rich flame which prevents the Oxygen-base metal reaction needed for normal OA cutting.

B. Advantages and Disadvantages of OA Cutting

Some of the disadvantages of OA cutting compared to other processes are: The process is not adaptable to cutting of composites, rubber and textile materials when compared to water jet cutting . It can be used for aluminum but is not as clean as plasma, laser and water jet. Preheat flames and the hot metal are expelled from the kerf and present fire and burn hazards to equipment and personnel. Hardenable steels such as HY/80 and HY/100 which are widely used in ship construction require special control of heat input to prevent adverse metallurgical effects to the HAZ. Acetylene is explosive and presents potential problems in handling and transporting the supply.

Some of the advantages of OA Cutting are: Steel can be cut faster by OA than by machining. OA cutting is adaptable to mechanized travel of the cutting heads for cutting complex shapes. Cutting direction can be changed rapidly on a small radius. Large plates can be cut rapidly by computer numerical controlled movement of the cutting torch rather than by moving the plate. OA cutting is a cost effective method of preparation of steel for welding in shipbuilding and other heavy industry and can readily be used in the field.

C. Equipment Used for OA Cutting of Test Plates

The machine used for OA cutting is capable of handling plates up to 1.8 m X 3.9 m (6 ft X 13 ft) and is also adaptable to plasma cutting, water jet cutting or mechanical routing. Some materials were available for trial cutting to establish cutting parameters, however, it will be seen that more material could have been well used to calibrate the system to cut closer to the dimensions of the trial pattern.

The cutting head was mounted on a power track driven gantry with rack and pinion drive. The cutting head, parameters, and gantry movements were controlled by an L-TeC series 810 numerical control computer. The 810 CNC also controls the associated process equipment.

The CNC program for cutting the test pattern was installed in the computer. The option was taken to attempt to maintain the inside of the kerf along the outer edge of the cutting pattern so that all of the kerf opening would fall on the scrap side of the cut .

D. Preparation of Samples and Equipment for Photogrammetry and OA Cutting

The plates to be used for OA cutting were identified as samples LT 715-2A and 2B. With the first sample, LT 715-2A placed on the cutting table, primer was applied to the surface in an irregular pattern. The primed surfaces were speckled with a random pattern by splattering the surfaces with a mixture of lime chalk and water. This technique provided texture and variation to an otherwise monotone photographic image. These variations in the

images provided for correlation of corresponding points on the sample surfaces while generating digital data in the stereo plotter for photogrammetric analysis.

Reference baselines with known dimensional values for photographic measurements were established by adhesively securing reference targets (fiducials) to the work surface near the corners and mid-sides of the plates. The target positions were measured and recorded by the cutting machine.

A sample installed on the cutting table was photographed by placing the camera directly above the plate at each of two pre-determined positions. The camera was suspended by cantilevering the vertical mount unit from the top of a platform. The elevation of the camera above the surface of the plates was 1.8m (5.9ft). The distance between camera positions for the stereo pair photography was 1.2 m (4 ft). According to the photogrammetric engineers this configuration was expected to provide an estimated measuring accuracy of 0.2 mm (0.008 in.)

E. Cutting the Test Pattern by the OA Process

After all steps needed for photogrammetry prior to cutting were complete the first OA sample, LT 715-2A was cut. Gas parameters used were 0.69 bar (10 psi) for acetylene, 1.7 bar (25 psi) for preheat oxygen, 2.4 bar 35 psi) for cutting oxygen. Travel speed was 0.56 m/min. (22 in./min.).

All of the steps described above were repeated for the second OA test plate, LT 715-2B. After development of the photographs to assure that the needed exposures were achieved, the sample plates

were sectioned for metallographic evaluation. Results of the testing and analysis of data from OA cutting provided by the metallographic and photogrammetric services follow.

F. Results of Metallographic Evaluation of OA Cut Plates

As noted above only steel was cut for the OA tests. Evaluation of edge quality and heat affected zone effects were performed on random sections cut from steel plate sample identified in Appendix A as #WE-lD-A715A.

The macro view at 30X of the profile of the cut shows that the OA process had produced a kerf with a rounded cut with a radius of 5.6 mm (0.25 in.), as seen in Figure 25 of Appendix A. This view also shows the heat affected zone at a magnification of 30x. The heat affected zone is between 25 and 40 roils deep.

The high depth of field afforded by the scanning electron microscope is evident in Figure 26 of Appendix A. The SEM view of the face of the cut at 30X does not reveal the cutting lines but does show the presence of adherent oxide as scale and clumps.

Optical microscopy examination was made on a transverse and a longitudinal Section of an OA cut plate, Figure 27 and 28 of Appendix A. The resulting photomicrographs at 100X with the samples etched with nitric acid show that OA cutting produced a grain coarsened heat affected zone in the A715 plate greater than 10 roils thick. The longitudinal view of the OA cut, Figure 28, Appendix A, shows a relatively smooth surface. The surface appeared to be suitable for fitup for conventional welding with some clean up of the oxides required.

The microhardness traverse of the HAZ of the OA cut plate was performed with a 500 gram primary load on a Vickers hardness indenter. The first reading was at 4 roils from the cut edge, followed by readings at each 6 mil to a depth of 34 roils. The resulting hardness values are: 197, 238, 223, 214, 174, and 166.

G. Photogrammetric Measurements of Oxyacetylene Cut Plates

As described in the technical approach to photogrammetry, the plates were set up on the cutting platens and photographed prior to and after cutting. The before and after stereo photographs were digitized in the stereo plotter/computer system at Aerometric Engineering and the data used to generate analytical edge plots, contour plots and 3D models of distortion resulting from cutting.

Reproduction of the stereo pair photos of OA cut sample LT715-2A after cutting are shown in Figures 4 and 5. The small square patches of tape along the edges contain the reference fiducial marks.

Although the stereo photos appear quite similar, they were taken with a camera parallax of four feet. All of the data resulting from the parallax is present in the two figures which can be viewed as a stereo image with suitable optics.

The stereo photos were analyzed on a precision stereo plotter and the resulting dimensional and distortion data are presented in the figures which follow.

1.0 Plots of Cut Edges of OA Cut 3mm Steel Plates

The edge plots show the perpendicular distance of the actual

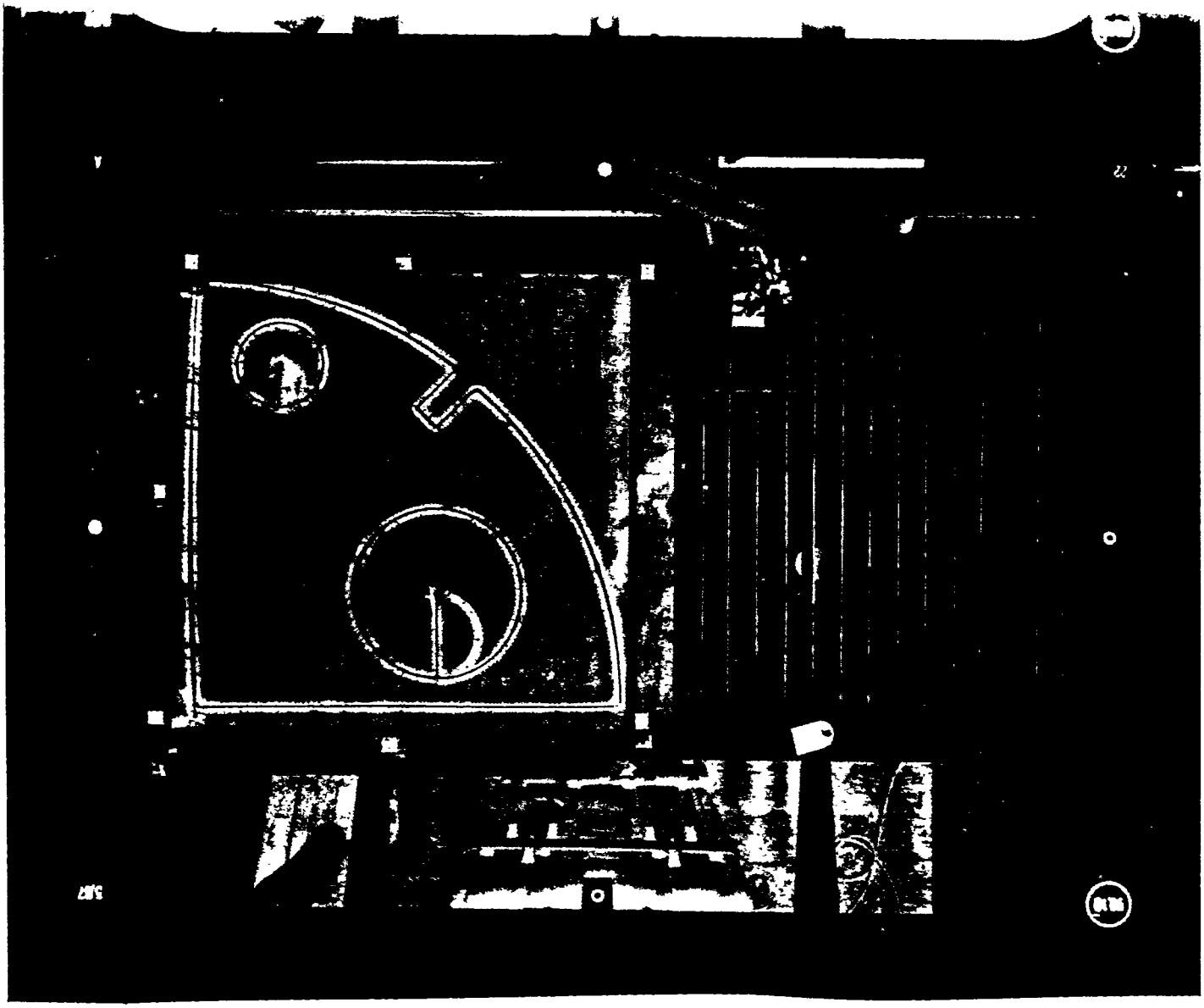

Fig.4 - Right Hand Photo of Stereo Pair of Plate Sample LT 715-2A after Oxy-acetylene Cutting. Photo Shows Actual Cut-out Pattern

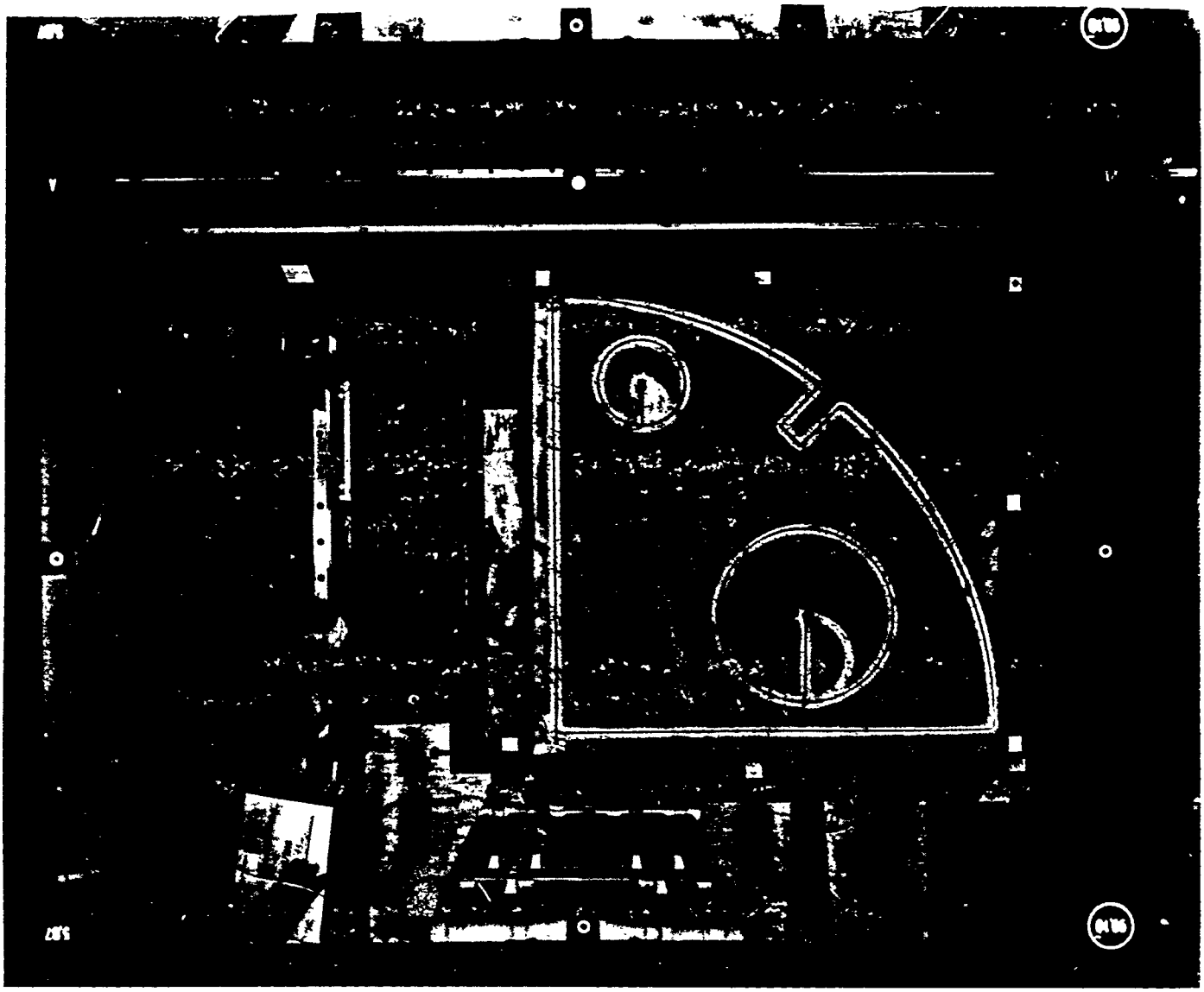

Fig.5 - Left Hand Photo of Stereo Pair of Plate Sample LT715-1 after OA Cutting

cut from the “true” value of the cutting pattern as vectors. The ends of each vector not on the line is the actual cut edge location. The design template is plotted at a scale of 1:8 with the vector deviations at a scale of 1:1.

It is readily seen from Figures 6 and 7 that the stiffener slot cut in sample LT 715-2A and 2B were programmed and cut approximately 12 mm (0.50 in.) out of place relative to the test pattern. The other vectors along the edge of the part show the cut to range from no deviation at the lower right corner to 11 mm (0.43 in.) short near the stiffener slot on sample 2A. The large circular cut on LT715-2A had a nearly optimum circularity but with a displacement of 2.5 mm to 2.8 mm (0.10 in. to 0.11 in.) from nominal on one diameter. The smaller circular cut, suitable for a 20 cm (8 in.) pipeway shows the circle to be out of round by approximately 1.5 mm (0.06 in.) but is otherwise nearly perfectly centered.

On sample LT715-2A, Figure 6 shows the deviation from the pattern was O to 9 mm (0.35 in.) short of the target value for the curved edge. It also shows a displacement of 1.8 mm to 3.3 mm (0.07 in. to 0.13 in.) on one diametral line of the large circular cut . On sample LT 715-2B the pipeway is nearly circular but shows the center to be off by 1.8 mm to 2.8 mm (0.07 in. to 0.11 in.).

2.0 Contour Plots of Out-of-Plane Distortion for OA Cut Steel

On the contour plots elevations on the uncut surface were determined relative to the reference plane at zero elevation. The data was transported to an engineering design computer which formed

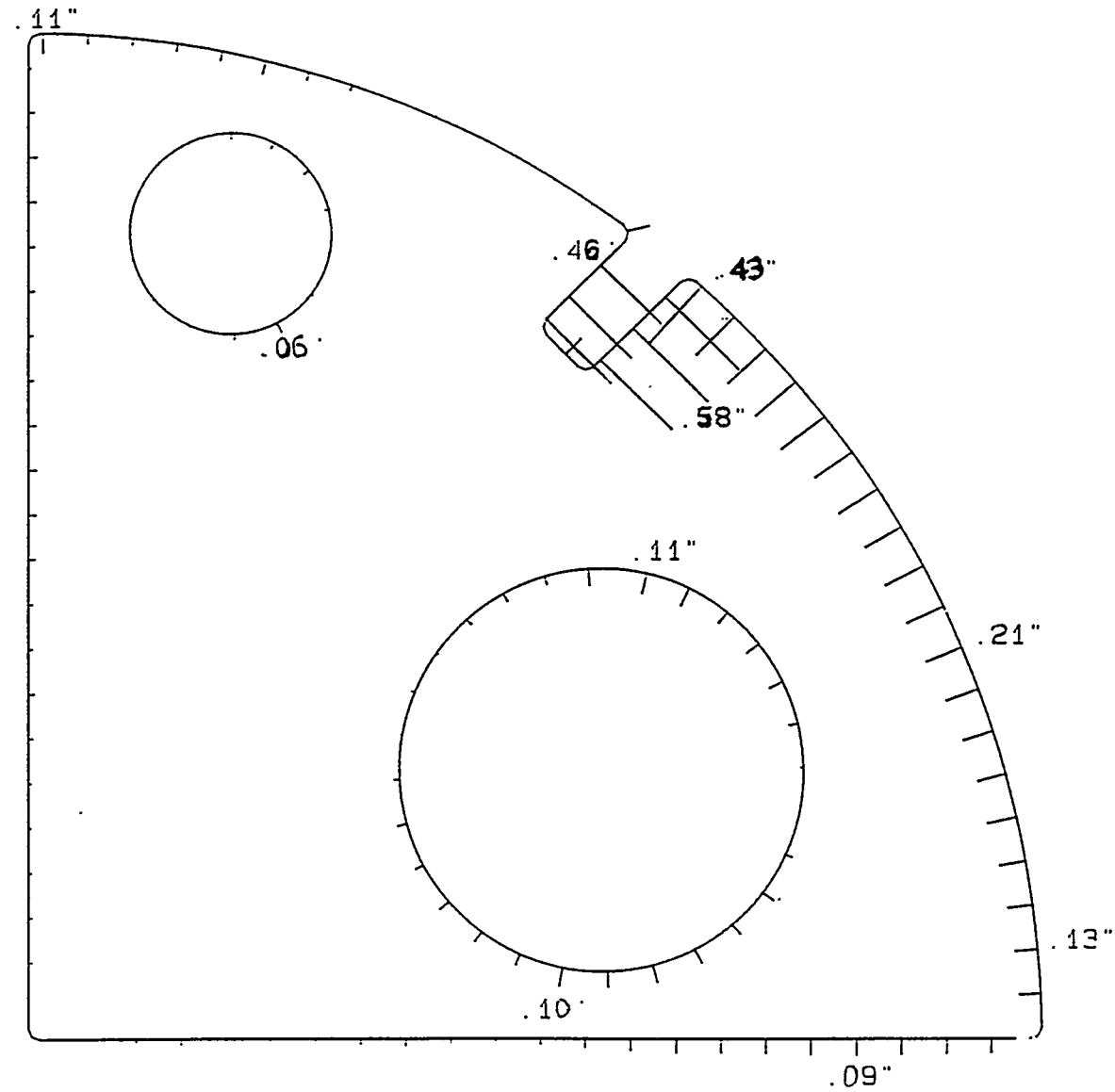

LT715-2A
Cut edge versus design template
Scale. 1"=8"
Vector scale. 1"=1"

Fig.6 - Edge Plot of Oxyacetylene Sample, LT 715-2A; Vectors along Edge Indicate Distance of Cut Edge from Test Pattern Design

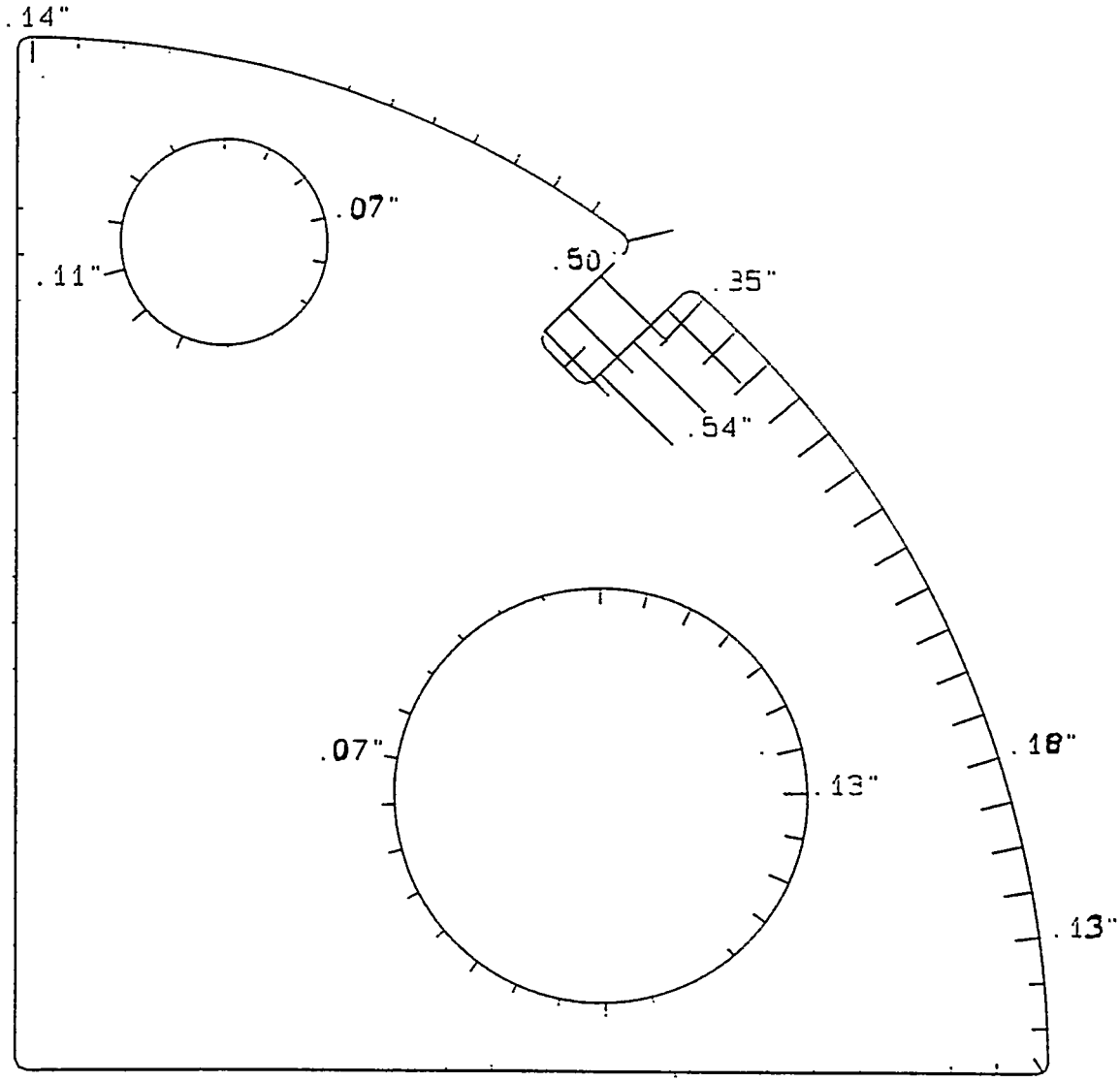

LT715-2B
Cut edge versus design template
Scale. 1"=8"
Vector scale. 1"=1"

Fig.7 - Edge Plot of Oxyacetylene Cut Sample LT 715-2B

a digital elevation model from the plotter digitized data. The contour plot for sample LT 715-2A prior to cutting is shown in Figure 8. The contour lines for LT 715-2A and 2B are plotted at 2.5 mm (0.10 in.) intervals because the magnitude of distortion produced by OA cutting made the intended intervals of 0.25 mm (0.01 in.) too close together to be readable. Also, because of the greater than expected distortion of the plates which resulted from OA cutting, the after cut stereo photographs were delayed for over 20 minutes to allow the plates to cool down and stabilize.

The sequence of photography and stereo plotting as described above was repeated to produce contour plots of the distortion after cutting. The contours of Sample LT715-2A after cutting are shown in Figure 9. The before and after contour plots for the second steel sample are not shown, however, the resultant contour plots are given for both samples.

The actual out-of-plane distortion which can be ascribed to the process of oxyacetylene cutting of the test pattern from steel plates LT 715-2A and LT 715-2B are shown in the resultant plots, Figures 10 and 11. Complete processing of all the digitized data produced these resultant plots by computer “subtraction” of the values of plot 1, distortion in the uncut plate, from plot 2, distortion in the plate after cutting, and printing out the results as plot 3. If no distortion had resulted from the cutting, all values on plot 3, the resultant plots, would be zero. Figure 10 shows that LT 715-2A bowed 38 mm (1.5 in.) in the most extreme contour line on the surface and this elevation continued to the left edge of the plate from the camera perspective.

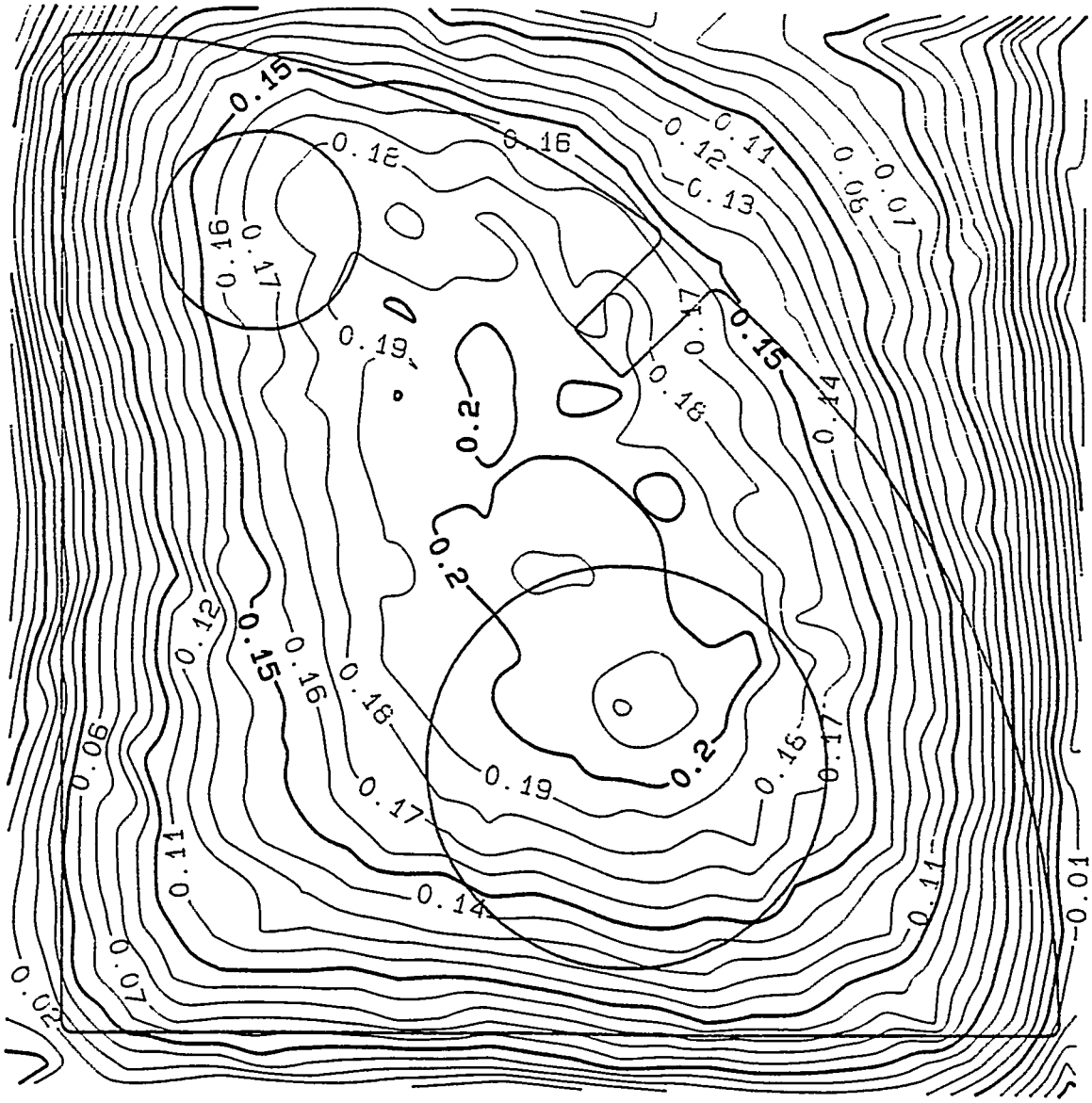

LT715-2A
Plot 1
Scale. 1"=6"
CI: 01"

Fig.8 - Contour Plot of 3mm Steel Plate - Sample LT 715-2A prior tc OA Cutting

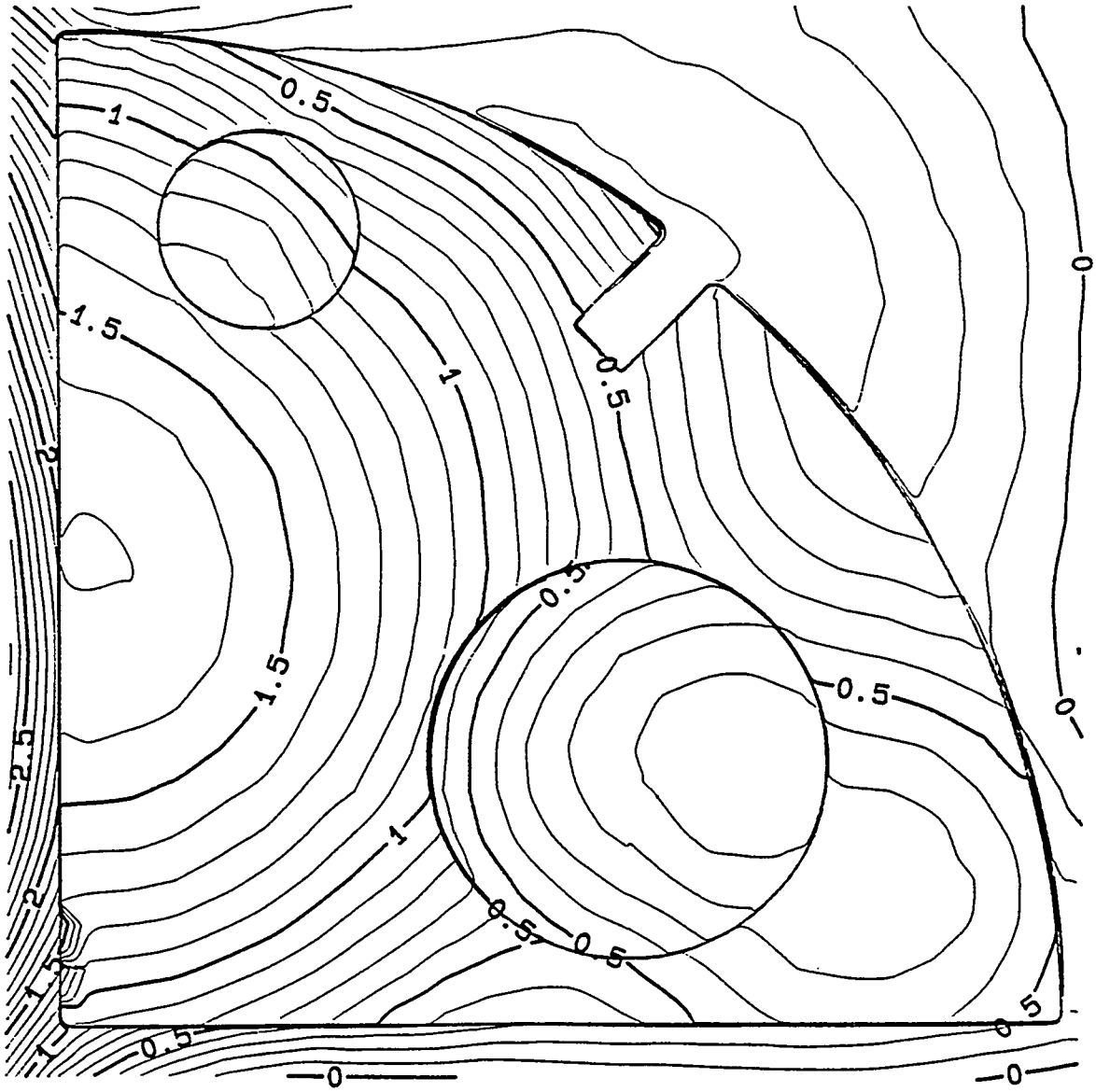

LT715-2A
Plot 2
Scale. 1"=8"
CI: 10"

Fig.9 - Contour Plot of 3mm Steel Plate - Sample LT 715-2A after Oxyacetylene Cutting.

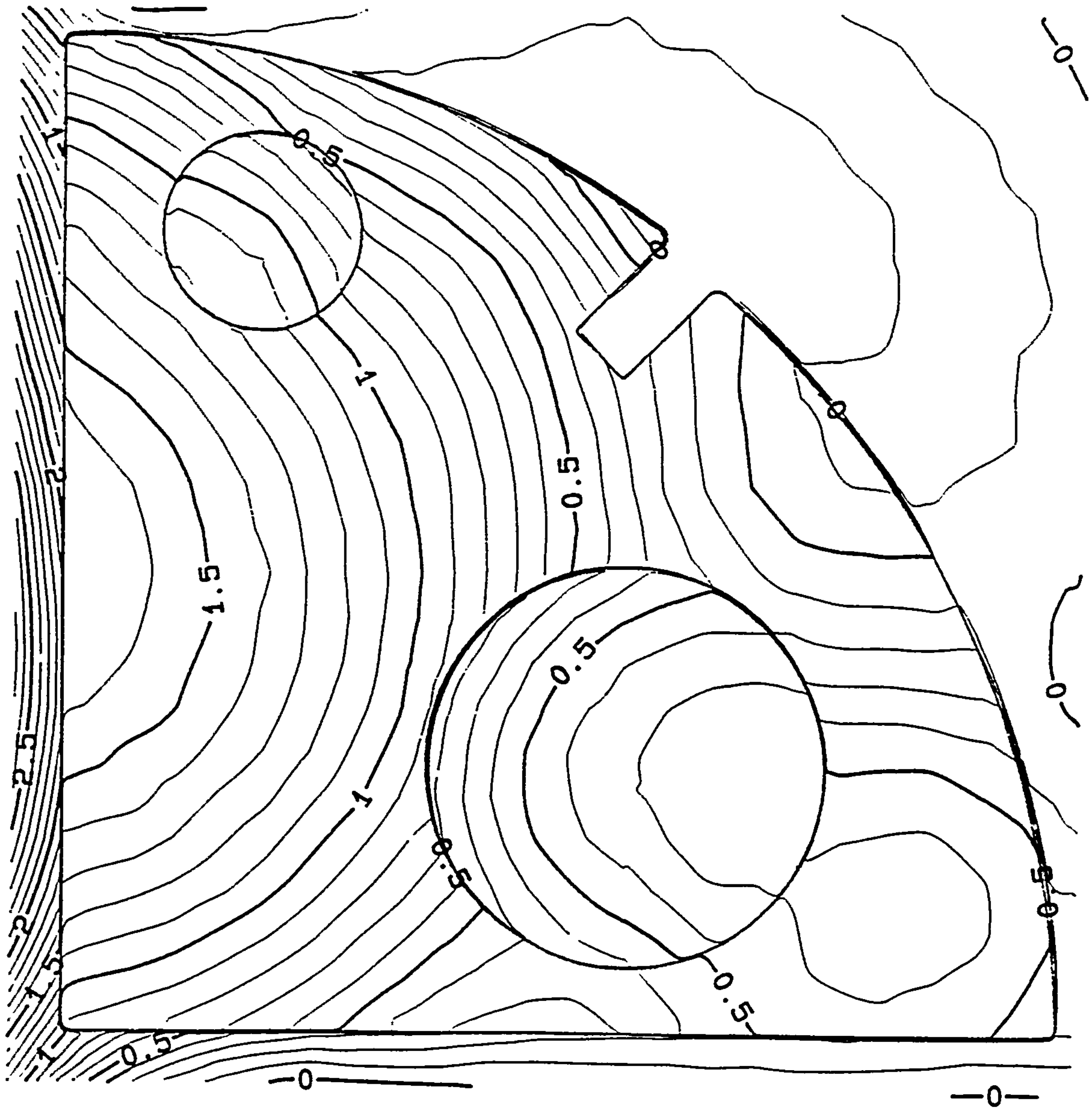

LT715-2A
Plot 3
Scale: 1"=8"
CI: .10"

Fig.10 - Resultant Contour Plot of Distortion Produced by Oxyacetylene Cutting of 3mm Steel Plate Sample LT 715-2A

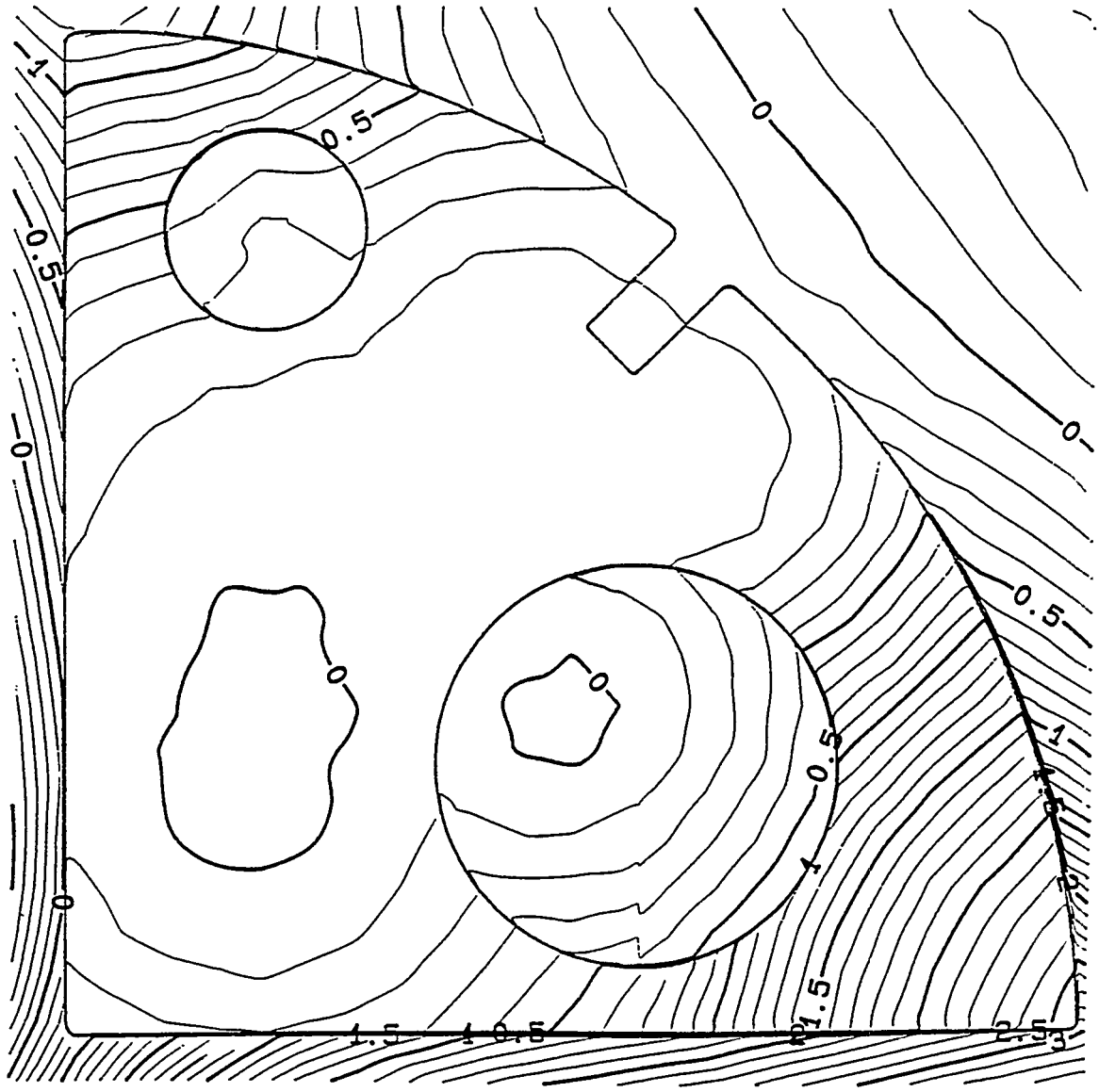

LT715-2B
Plot 3
Scale. 1"=8"
CI: 10"

Fig.11 - Resultant Contour Plot of Distortion Produced by OA Cutting of 3mm Steel Plate Sample LT 715-2B

The distortion in the second OA cut was approximately the same in magnitude as the first cut. Figure 11 , the resultant plot shows that the location of the 38 mm (1.5 in.) line of elevation is in an altogether different place relative to the manway hole and the 200 mm (8 in.) pipe penetration.

3.0 3-D Perspective Plots of Distortion Produced in OA cut Steel plates

The software used to produce the contour plots of the photogrammetric data of the steel plates was PLUS 3 TERRAMODEL. This software package had the capability of generating “perspective " 3D views of the digitized data from any angle of view. Figures 12 and 13 are 3D perspective plots of resultant distortion data (corrected for pre-cut distortion) from the angle of view 3 in Figure 1 for samples LT 715-2A and 2B after cutting. View 3 places the large manway hole of the pattern to the left and the rectangular cut out for the stiffener on the curved edge in the foreground.

The perspective views depict changes in elevation of the surface as curves and displacements of the grid lines. The stereo contour plots give specific elevations for each contour line but the 3D plots do not have a uniform scale and do not lend themselves to specific dimensional measurement because the angle of perspective makes the scale of the grid lines not constant. However, presenting the data in this format eliminates the need to interpret the numbers and lines on the contour maps qualitatively to visualize the distortion relative to the geometric features of the cut piece.

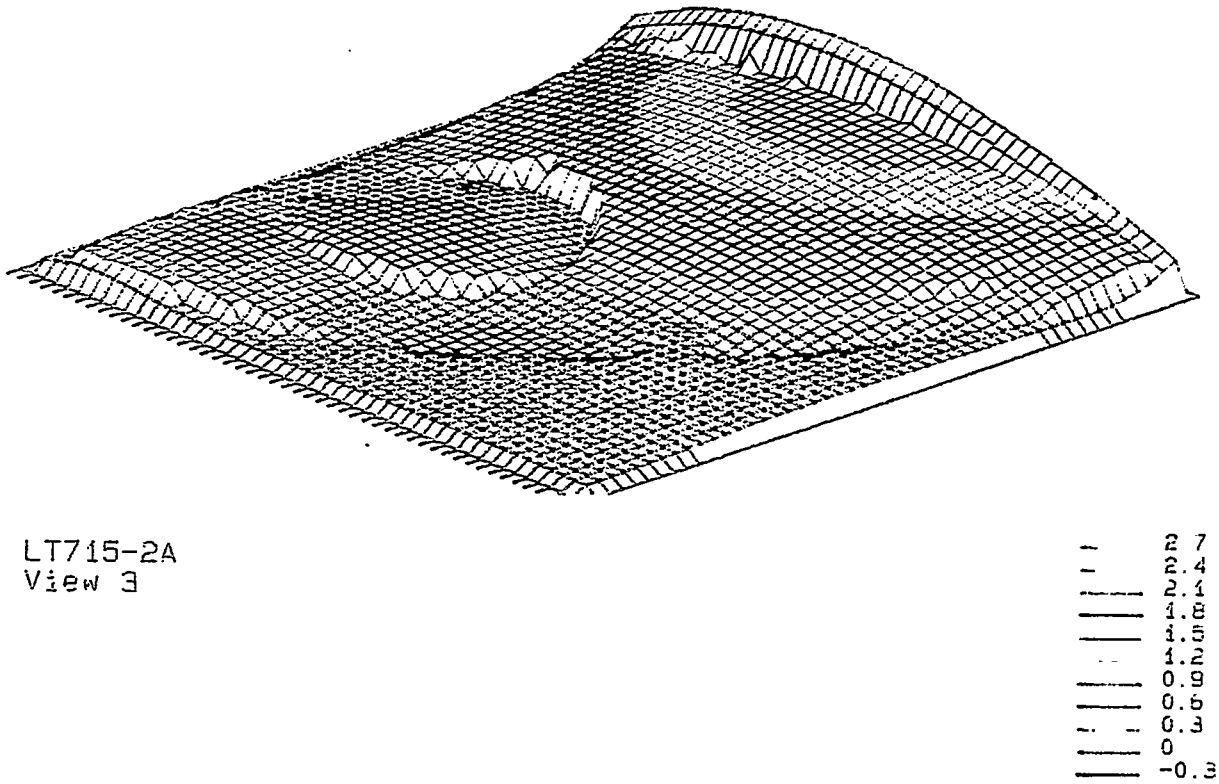

Fig.12 - 3D Perspective Plot of Distortion in OA Cut 3mm Steel Plate Sample A715-2A. The large Manway Hole is on the Left.

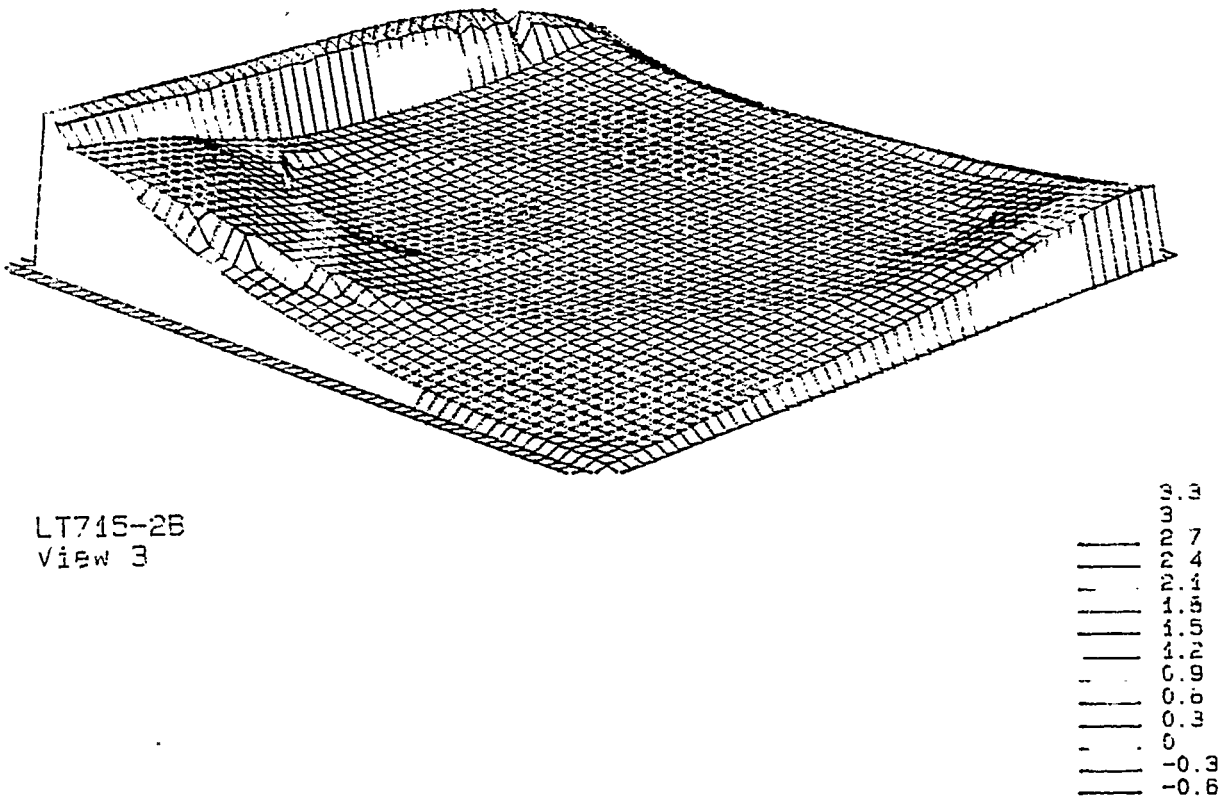

Fig.13 - 3D Perspective Plot of Distortion in OA Cut 3mm Steel Plate Sample A715-2B.

IV. PLASMA ARC CUTTING (PAC) OF 3mm ALUMINUM AND STEEL PLATES

A. General Principles of Plasma Arc Cutting

Plasma arc cutting severs metal with the heat produced by a constricted arc generated between a nonconsumable Tungsten electrode and a workpiece. This process has the advantage of being able to cut most metals. Figure 14 illustrates a typical plasma torch design and Figure *15* shows the basic plasma arc cutting circuitry.

Many plasma cutting systems use compressed air to form the plasma gas cutting arc. Relatively large volumes of gas may be,used in routine plasma cutting operations. Compressed air is widely used to hold down the cost of the plasma forming gas.

The process operates on direct current, straight polarity. The orifice directs the plasma stream from the electrode toward the workpiece. When the arc melts the workpiece, the high-velocity jet blows away the molten metal to form the kerf. The cutting arc attaches to or transfers to the workpiece, and is referred to as a transferred arc.

B. Advantages and Disadvantages of PAC

Some of the advantages and disadvantages of PAC compared to other processes include its cost effectiveness because of rapid travel speeds and its relative ease of use, which reduces necessary operator training time. Air plasma arc cutting is a continuous process which eliminates the time consuming start and stop procedures typical of OA cutting.

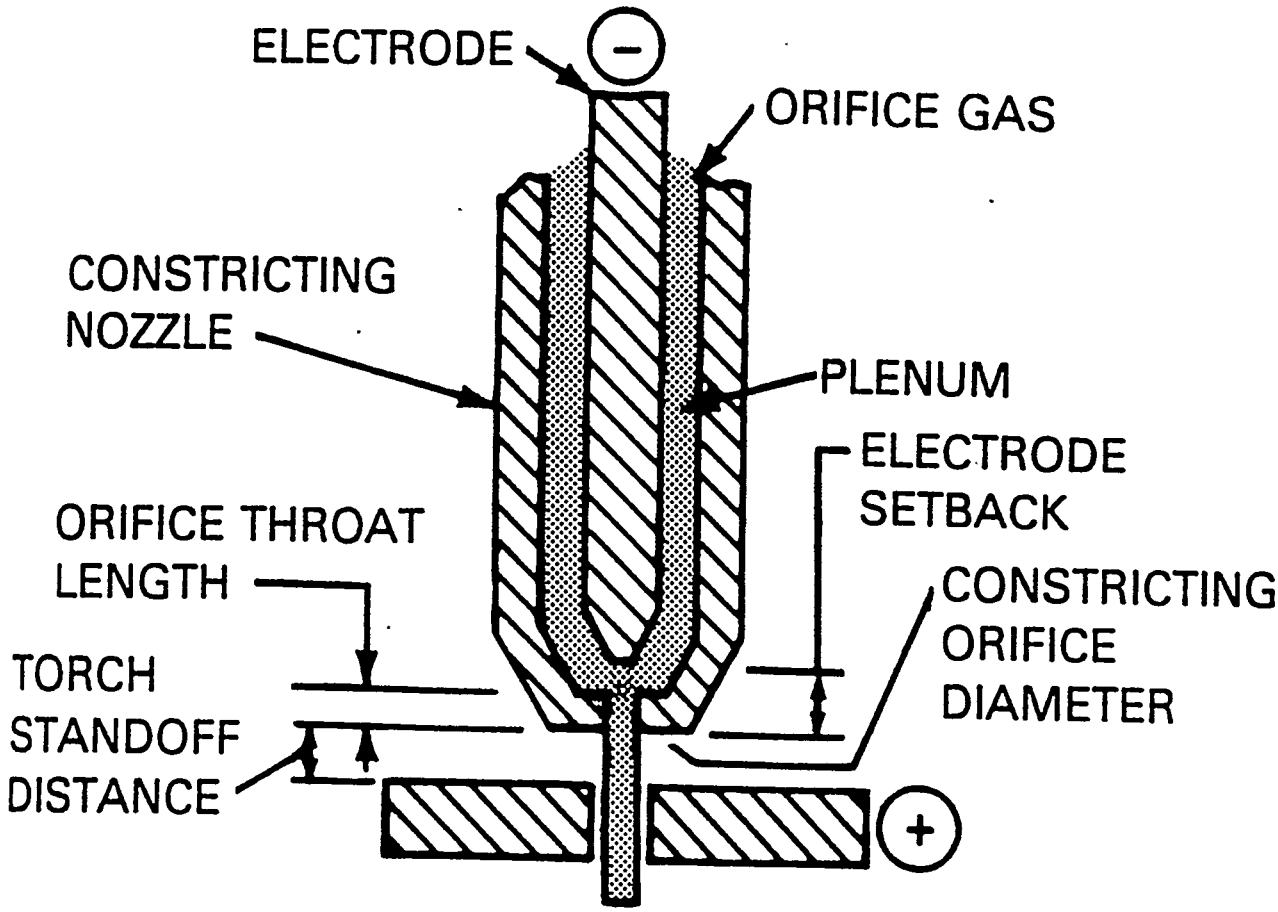

Fig.14 Typical Plasma Cutting Torch Configuration

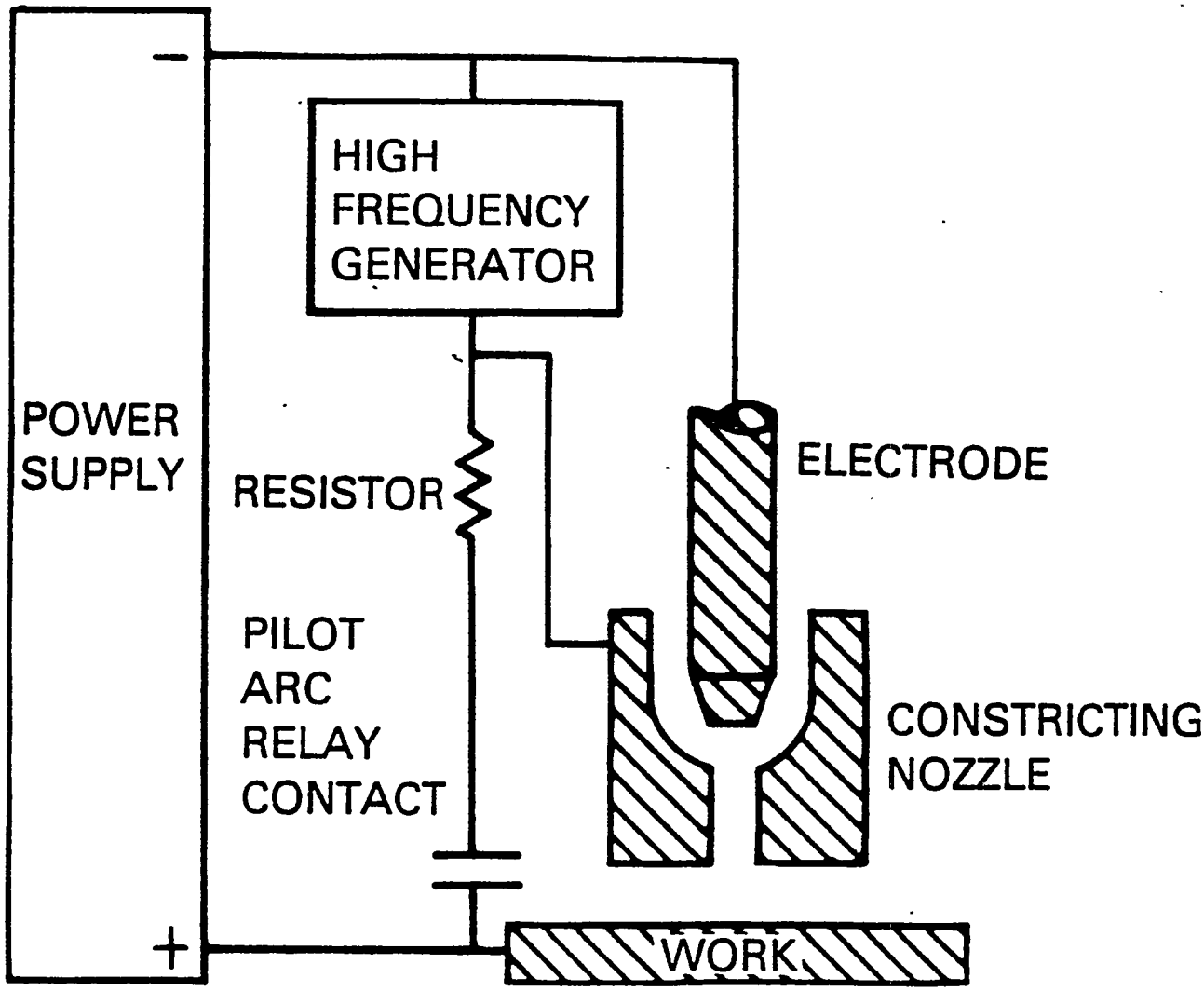

Fig. 15 - Typical Block Diagram for Plasma Arc Cutting Circuitry (from AWS Welding Handbook, Vol. 2, American Welding Society, 1991)

PAC involves the use of high intensity arcs and extremely high velocity ionized gasses. Such high intensity arcs and gas velocities generate conditions which require eye and ear protection for personnel.

C. Description of Plasma Cutting Equipment

L-TeC, of Florence, SC, performed the plasma cutting for this project and cut the specified patterns. The L-Tee PT-17A plasma cutting torch with a L-Tee PCM-1OO Plasma Cutting Power Supply were used with the same table and control equipment used for OA cutting. The CNC program was also the same as that for OA cutting.

D. Preparation of Samples for Plasma Cutting

The preparation of samples for plasma cutting included essentially all of the same steps previously described for the OA cutting including alignment of plates on the table, attachment of targets for photo measurements and shooting of pre-cutting stereo pair photographs.

E. Cutting the Test Pattern by the Plasma Process

Air was used for both the shielding and the cutting gas during performance of the plasma cuts for both aluminum and steel. Pressure was set at 6.9 Bar (100 psi). Travel speed for the aluminum plates was programmed to be 4.6 m/min. (180 in./min.), the current was set at 70 amperes, and the arc height was set for 6.4 mm (0.25 in.). The same parameters were used for cutting the steel, except travel speed was set at 4.1 m/min. (160 in./min.) .

F. Laboratory Evaluation of Plasma Cut Aluminum

The metallography photos of the plasma arc cut 5456 aluminum plate are included in Appendix A. The samples labled WE-lA-B209A are aluminum. Figure 5 of Appendix A, the profile of the plasma cut at 30X, shows a slightly rounded edge with an included angle of approximately 35 degrees with the widest opening at the top of the cut

The scanning electron microscope face-on-view of the plasma cut at 30X, Figure 6, Appendix A, shows roughness and formation of several roils of oxide scale. Poorly defined lines of waviness with crest spacing of 10 roils are visible. The lines were parallel but had a 50 mm (2 in.) radius of curvature across the face.

Longitudinal and transverse photomicrographs of mounted, polished and etched samples were made at 100X (Figures 7 and 8, Appendix A). In the transverse views, a crust of aluminum oxides can be seen adhering to the surface. The crests seen in the face-on SEM view are also seen in the 100X longitudinal view. Very little microstructural change is seen in the HAZ.

The microhardness readings transverse to the cut surface were taken with a 200 gram load on a Vickers type indenter. Starting at 4 roils from the cut edge with indentations at 6 mil intervals, the hardness readings are 85.4, 86.2, 93.4, 90.8, 98.4, and 102.

G. Laboratory Evaluation of Plasma Cut Steel Plate

The plasma cut steel sample for lab test was labled WE-lA-A715A. The macroscopic evaluation at 30X showed an included angle caused by the cut of approximately 45 degrees with the widest

opening at the top. The HAZ on the cut face is 8-10 roils thick (Figure 1, Appendix A).

The SEM study showed a relatively smooth cut surface with very little debris. There are parallel lines on the surface which have a spacing of approximately 10 roils. The upper half of the lines are straight, while the lower half curved on a 2.5 cm radius (1.0 in.) radius (Figure 2, Appendix A) .

The transverse view of the 100X microscopic examination shows a thin layer of adherent oxide scale and a HAZ approximately 10 roils deep (Figure 3, Appendix A). The longitudinal view (Figure 4, Appendix A) also shows some grain coarsening in a 10 to 12 mil HAZ and a 2 to 4 mil thick oxide scale. The cut edge is smooth (Figure 4, Appendix A).

The microhardness measurements made on the steel sample with the Vickers indenter loaded at 500 grams start at 4 mils from the cut edge with impressions taken at 6 mil intervals. The hardness values are 320, 231, 189, 177, 164, and 161.

H. Photogrammetric Measurements of Plasma Cut Plates

Pre-cut and post-cut stereo photographs were processed by the photogrammetric engineers to produce the digital data and plots needed to evaluate accuracy and distortion of plasma cutting of 3mm aluminum and steel plates. The same sequence of data processing as was used for OA was followed for plasma cut samples to develop edge and contour plots.

1.0 Photogrammetric Plots of Plasma Cut Edges of Aluminum Plates

The accuracy of the plasma cuts of aluminum relative to the Figure 1 test pattern can be seen in Figures 16 and 17. It is noted that the cut out in the upper right of the curved edge has essentially the same magnitude of error as the cut out for OA cut steel. The deviation of the slot in the sample by 13 mm (0.5 in.) is attributed to an error in the CNC programming and not related to the cutting process.

The edge plot figures for plasma cut aluminum show the large holes and the 20 mm (8 in.) pipe penetration holes to be slightly out of round on one diameter. The pipe hole deviates by +2.3 mm to -1.5 mm (+.09 in. to -0.06 in.) on one sample and approximately 3.8 mm (0.15 in.) on the other. The large hole is out of round by approximately 2.8 mm (0.11 in.) on one and 3.0 mm (0.12 in.) on the other. The deviation of the cut edge from the target values of Figure 1 for plasma cutting is 1.3 mm (0.05 in.) to 6.8 mm (0.27 in.) on the “A” sample and 0.8 mm (0.03 in.) to 6.8 mm (0.27 in.) on “B” on the curved edges. The deviations are consistent and could probably be significantly reduced in a repetitive production situation.

2.0 Contour Plots of Out-of-Plane Distortion in Plasma Cut Aluminum

The resultant contour plots for the two aluminum plates are shown in Figures 18 and 19. The after-cutting stereo photo pairs were made with the “scrap” still in place and the plots show the outline of the cut pattern. These plots were made with lines of elevation differing by only 0.2 mm (0.01 in.) .

The distortion along the outsides of the cut pattern and on the

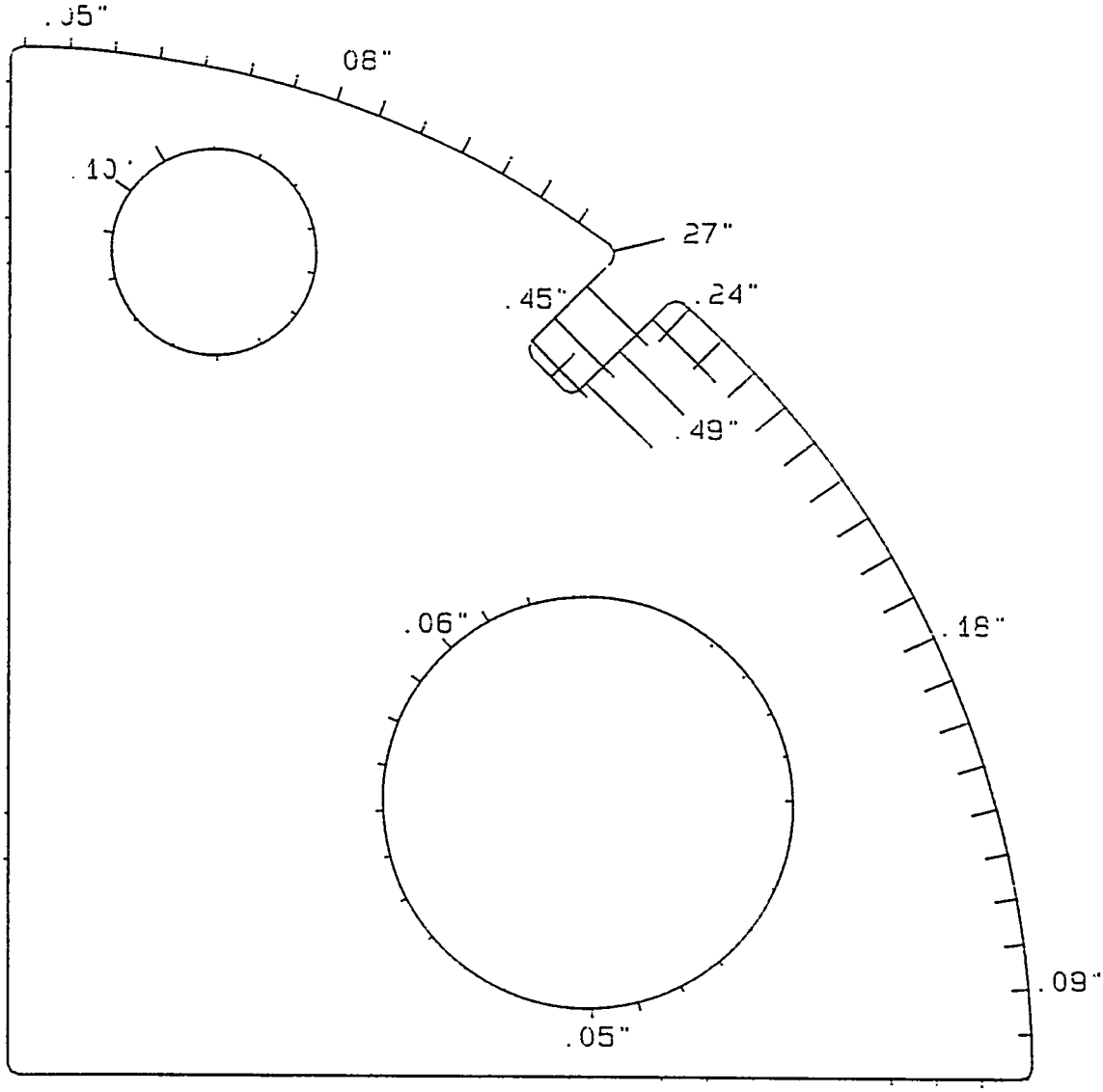

LT209A
Cut edge versus design template
Scale. 1"=6"
Vector scale. 1"=1"

Fig.16 - Edge Plot of Plasma Cut Aluminum Plate, Sample LT209A
Ends of Vectors Show Location of Cut Relative to the Test Pattern.

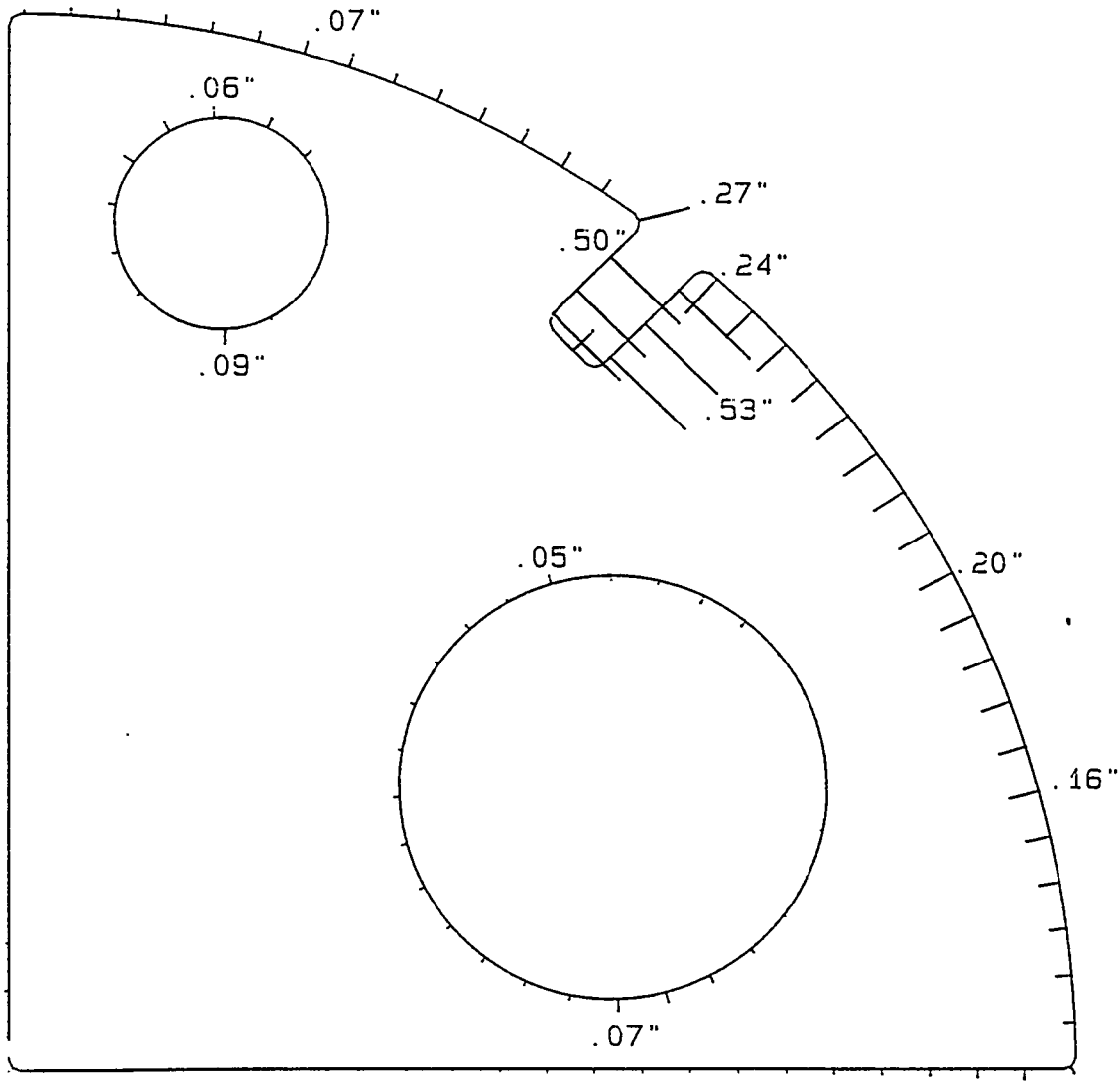

LT209B
Cut edge versus design template
Scale: 1"=8"
Vector scale. 1"=1"

Fig.17 - Edge Plot of Plasma Cut Aluminum Plate, Sample LT20
Ends of Vectors Show Location of Cut Relative to the Test Pattern

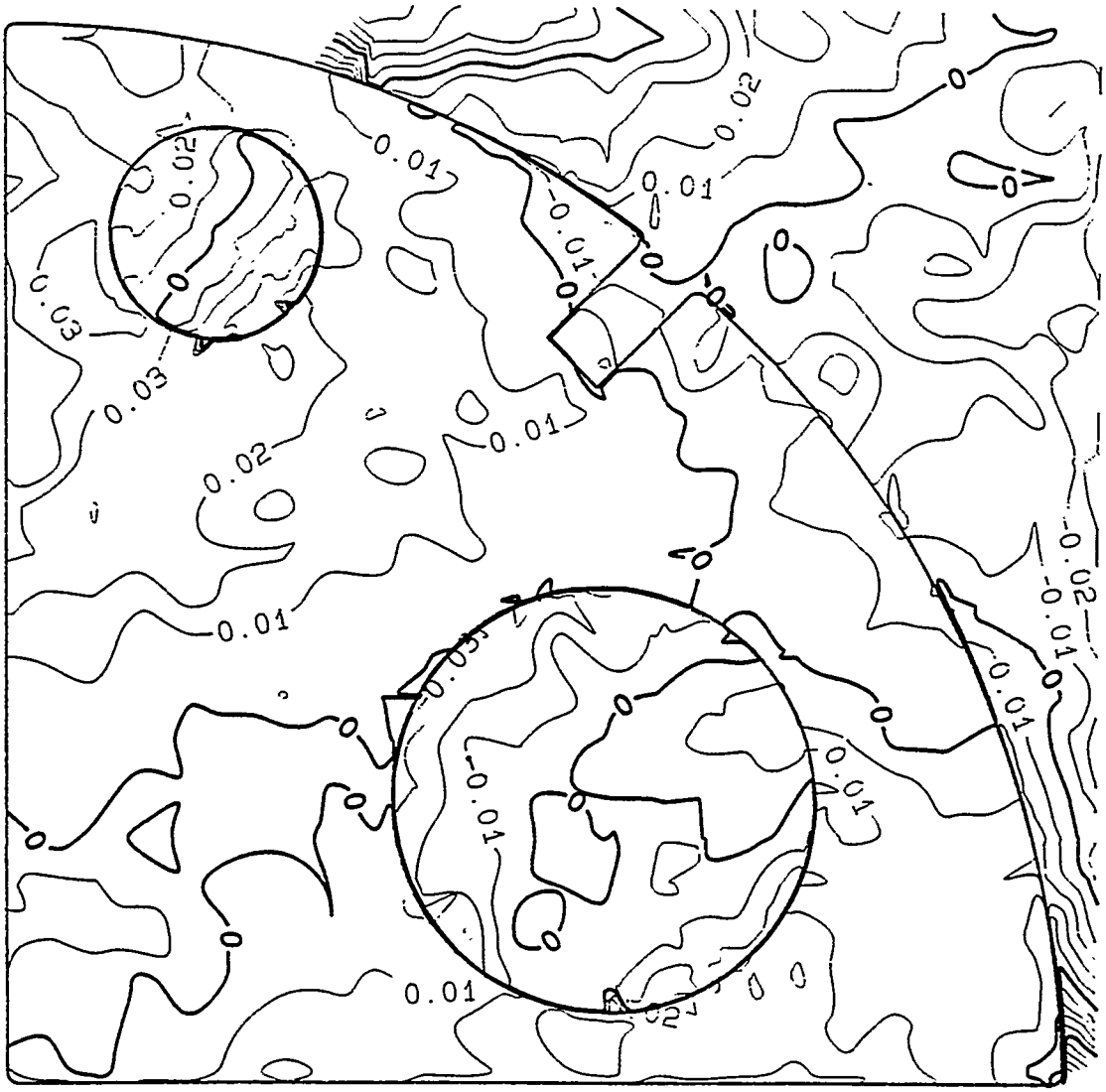

LT209A
Plot 3
Scale: 1"=8"
CI: 01"

Fig.18 - Resultant Contour Plot of Distortion Produced by Plasma Arc Cutting of 3 mm Aluminum Plate Sample LT 209A

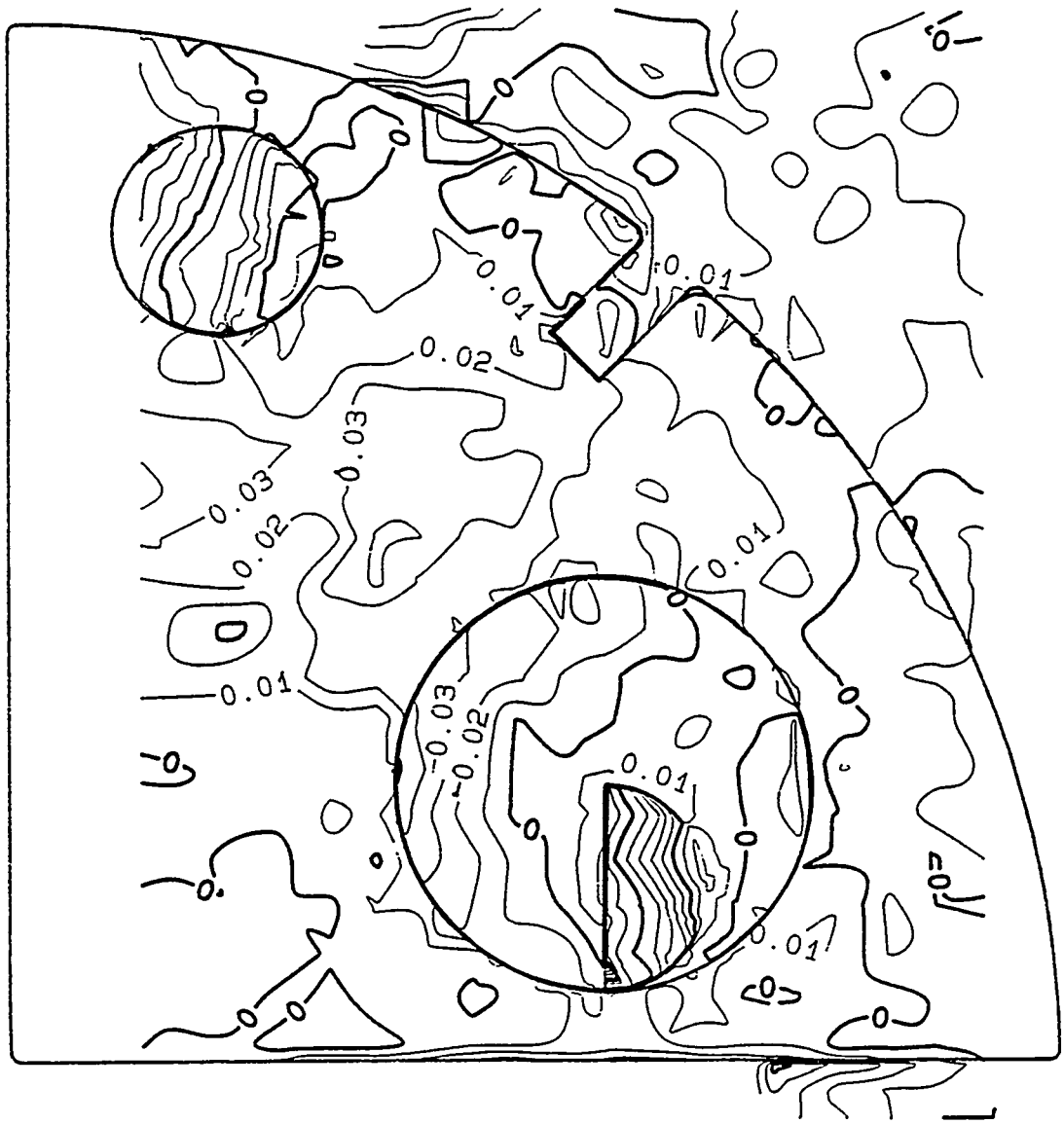

LT209B
Plot 3
Scale: 1"=8"
CI: 01"

Fig.19 - Resultant Contour Plot of Distortion Produced by Plasma Arc Cutting of 3 mm Aluminum Sample, LT209B.

edges of the holes was between 0.0 and 0.8 mm (0.03 in.) for both samples. These small amounts of distortion present very little or no problems in conventional shipfitting practices.

3.0 3-D Perspective Plots of Distortion in Plasma Cut Aluminum Plates

The software and sequence followed in producing 3D perspective images of the distortion produced by plasma cutting is the same as that described under OA cutting. The 3D plots defined by Figure 1 as view 3 of the two plasma cut aluminum plates are shown in Figures 20 and 21.

4.0 Photogrammetric Plots of Plasma Cut Edges of Steel Plates

The deviation from accuracy of the location of cut part lines relative to Figure 1 for both of the plasma cut steel plate samples are similar in magnitude and direction to those of the plasma cut aluminum. It is noted that both of the above were cut on the same table with the same program and torch path controls as were used for aluminum. The edge plots for steel samples LT-715-lA and LT-715-lB are shown in Figures 22 and 23. The maximum deviation of the cut holes from the test pattern as 0 to 2.5 mm (0.10 in.) on one diameter on the large hole on LT715-lA. The deviation on the curved edge of LT715-lA was from slightly oversize to -7.4 mm (-0.29 in.). The other sample was similar with a maximum of 6.9 mm (-0.27 in.) on the outer edge.

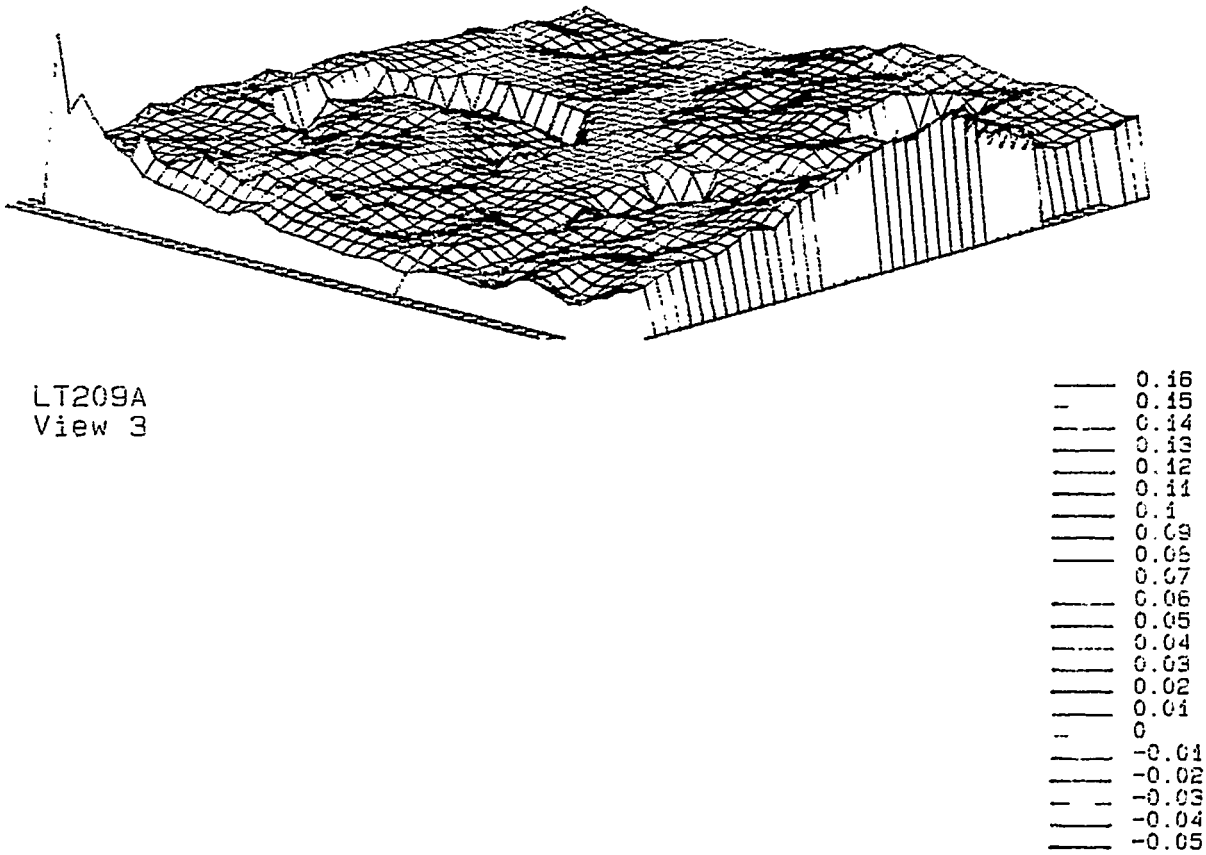

Fig.20 - 3D Perspective Plot of Plasma Cut Aluminum Plate Sample LT 209A Showing Resultant Contours Relative to the Uncut Surface

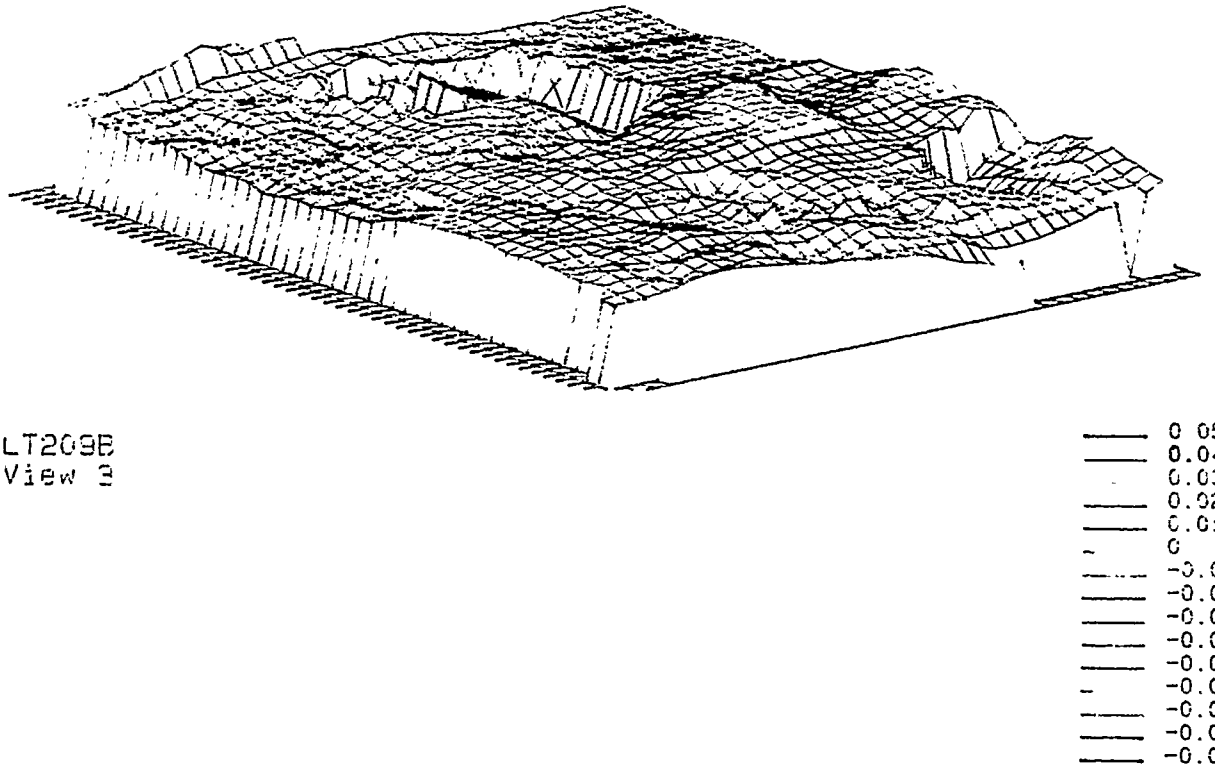

Fig.21 - 3D Perspective Plot of Plasma Cut Aluminum Plate Sample LT 209B Showing Resultant Contours Relative to the Uncut Surface.

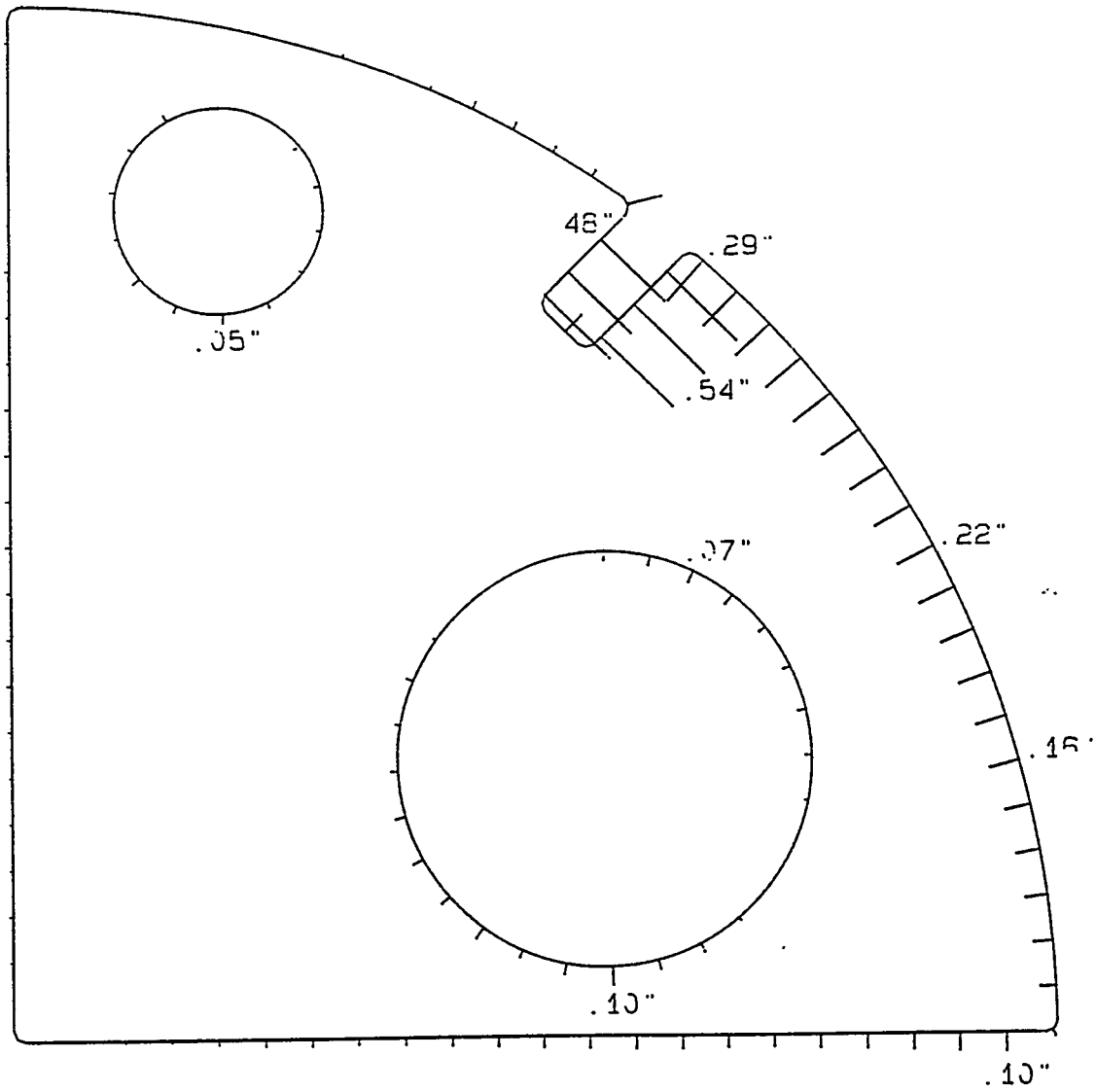

LT715-1A
Cut edge versus design template
Scale: 1"=3"
Vector scale: 1"=1"

Fig.22 - Edge Plot of Plasma Cut Steel Plate LT 715-1A - End of Vectors not Touching Template Show Deviation of Cut from Nominal.

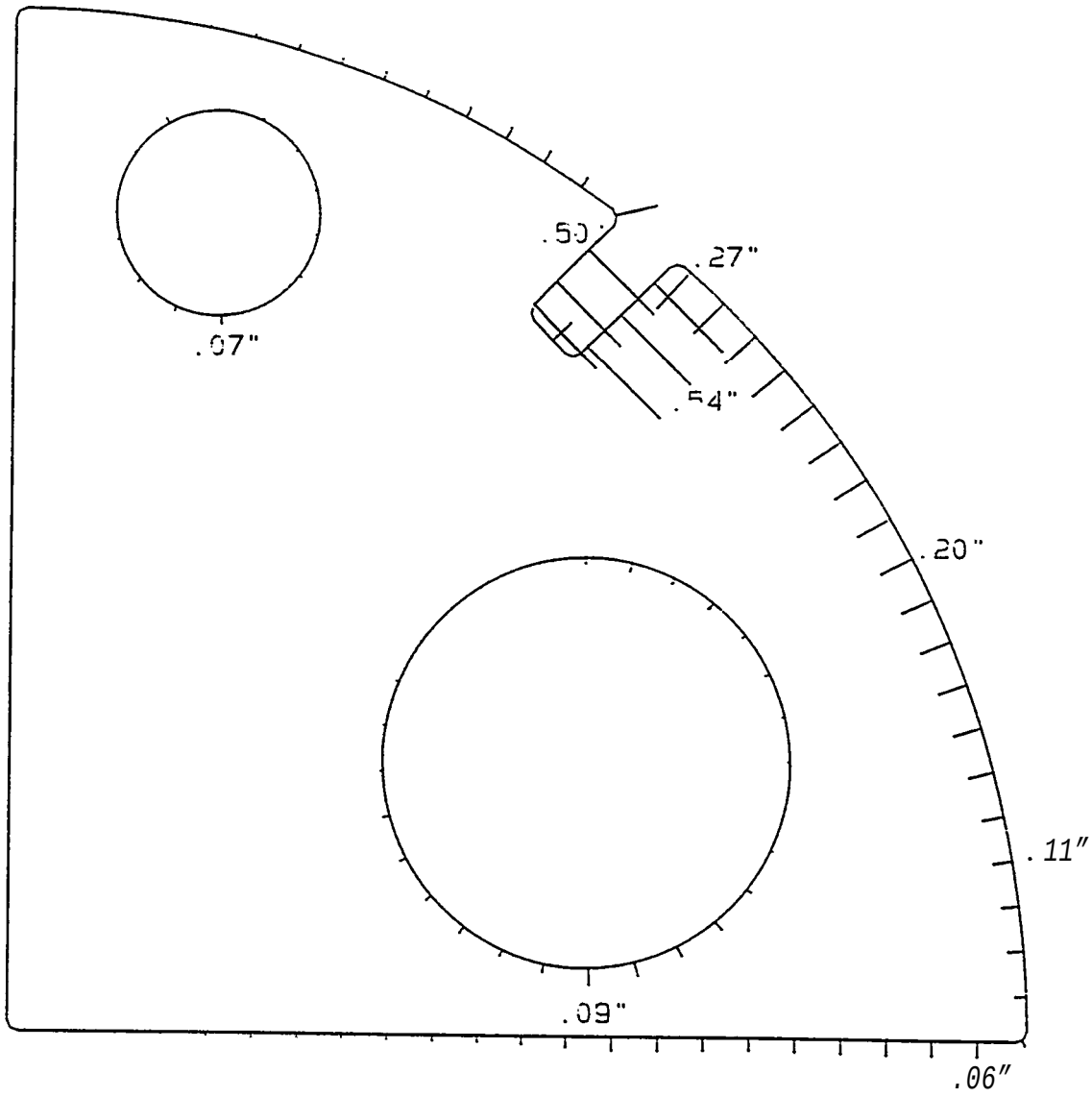

LT715-1B
Cut edge versus design template
Scale: 1"=6"
Vector scale: 1"=1"

Fig. 23 - Edge Plot of Plasma Cut Steel Plate LT 715-lB -End of Vectors not Touching Template Show Deviation of Cut from Nominal

5.0 Contour Plots of Out-of-Plane Distortion of Plasma Cut Steel Plates

Figures 24 and 25 are the resultant contour plots for the two steel plates cut by plasma arc to the Figure 1 pattern. The resultant plot of sample LT715-lA, (Figure 24) shows distortion ranging from -0.8mm (-0.03 in.) to +O.5mm (+0.02 in.). Figure 25 shows distortion in sample LT715-lB from -2.5 mm to +2.5 mm (-0.10 in. to +0.10 in.). In both cases distortion was greatest in the lower right area of the pattern as shown in the figures.

6.0 3-D Perspective Plots of PAC Steel Plates

The digitized resultant contour data for the two Plasma cut steel plates are depicted in the 3D perspective plots shown in Figures 26 and 27. The angle of perspective is view 3 as defined in Figure 1. The vertical displacement is not to scale and is exaggerated for ease of interpretation.

V. LASER BEAM CUTTING OF 3MM ALUMINUM AND STEEL PLATES

A. General Principles of Laser Beam Cutting

Laser beam cutting of metals is basically a thermal cutting process in which the metal is severed by melting or vaporizing it with a laser beam. “Laser” is the acronym for light amplification by stimulated emission of radiation. Light is emitted from atoms or molecules when the electron energy state is raised above normal. Light emitted by atoms in an object heated to incandescence has a wide spectrum of frequencies and the photon emissions are totally random relative to other photon emissions.

The two fundamental types of lasers are solid state lasers such

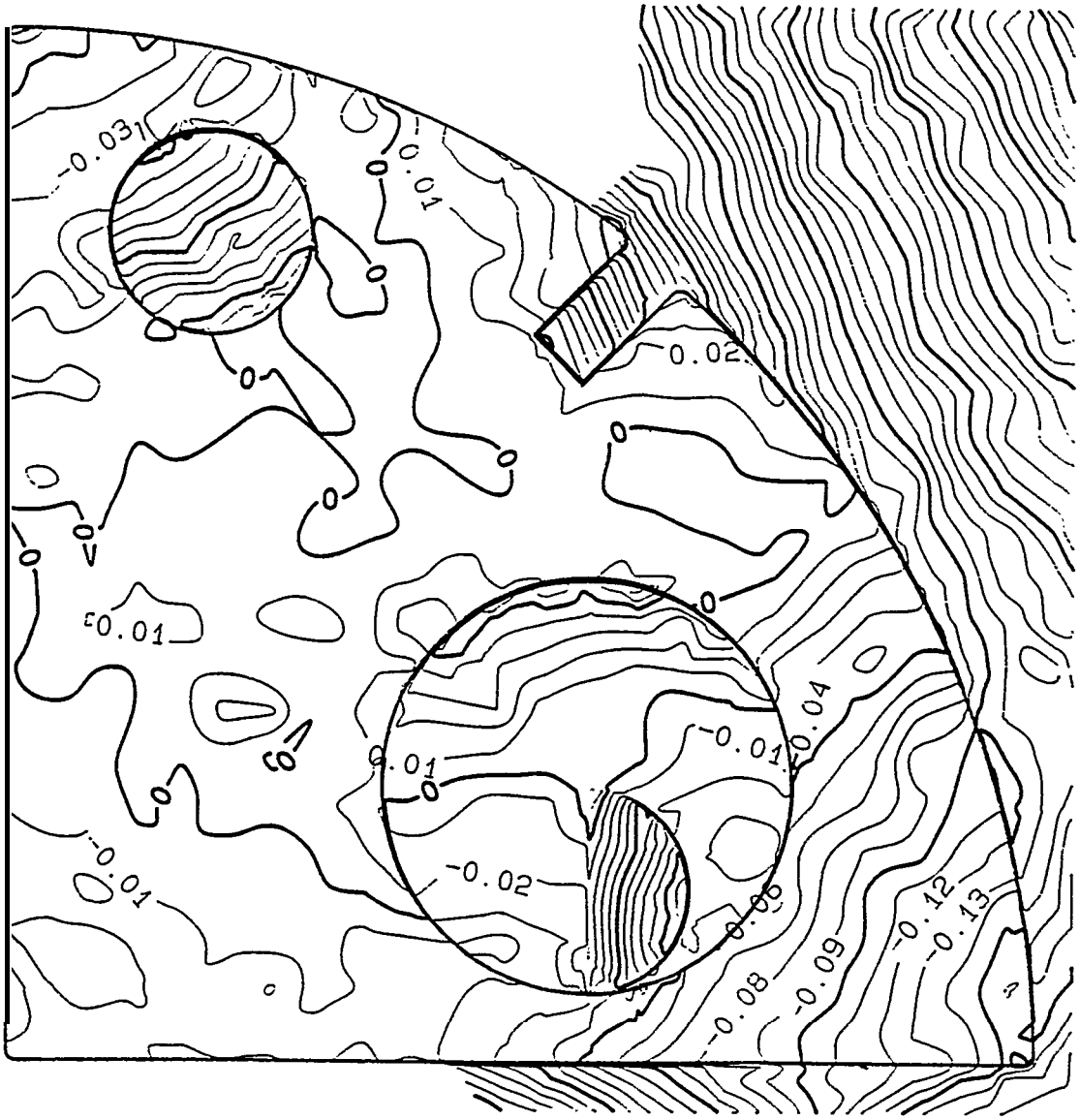

LT715-1A
Plot 3
Scale. 1“=8”
CI: 01”

Fig.24 - Resultant Contour Plot of Distortion Produced by Plasma Arc Cutting of 3mm Steel Plate Sample LT 715-1A.

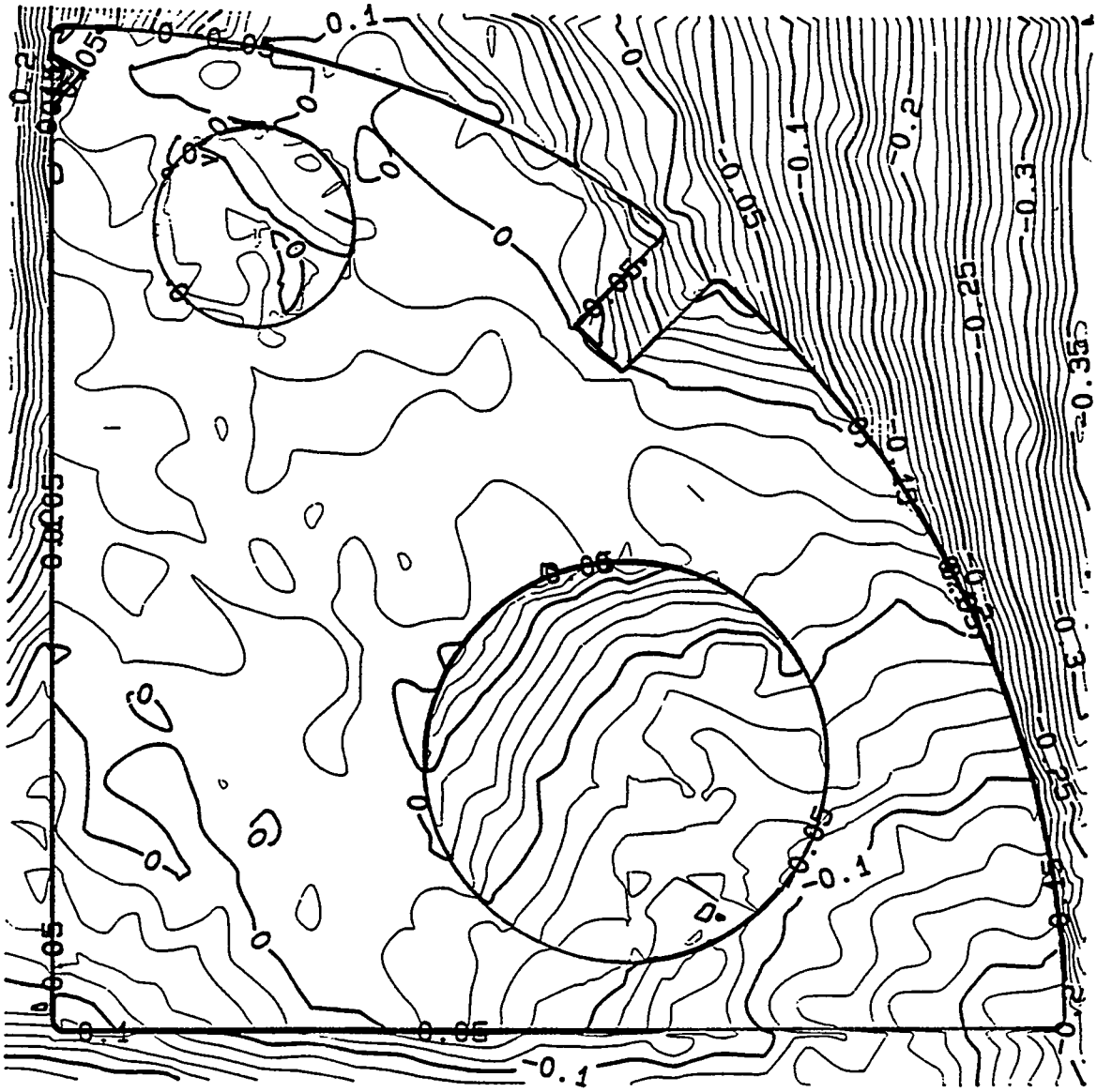

LT715-1B
Plot 3
Scale: l″=8"
CI: 01″

Fig.25 - Resultant Contour Plot of Distortion Produced by Plasma Arc cutting of 3mm Steel Plate Sample LT 715-lB

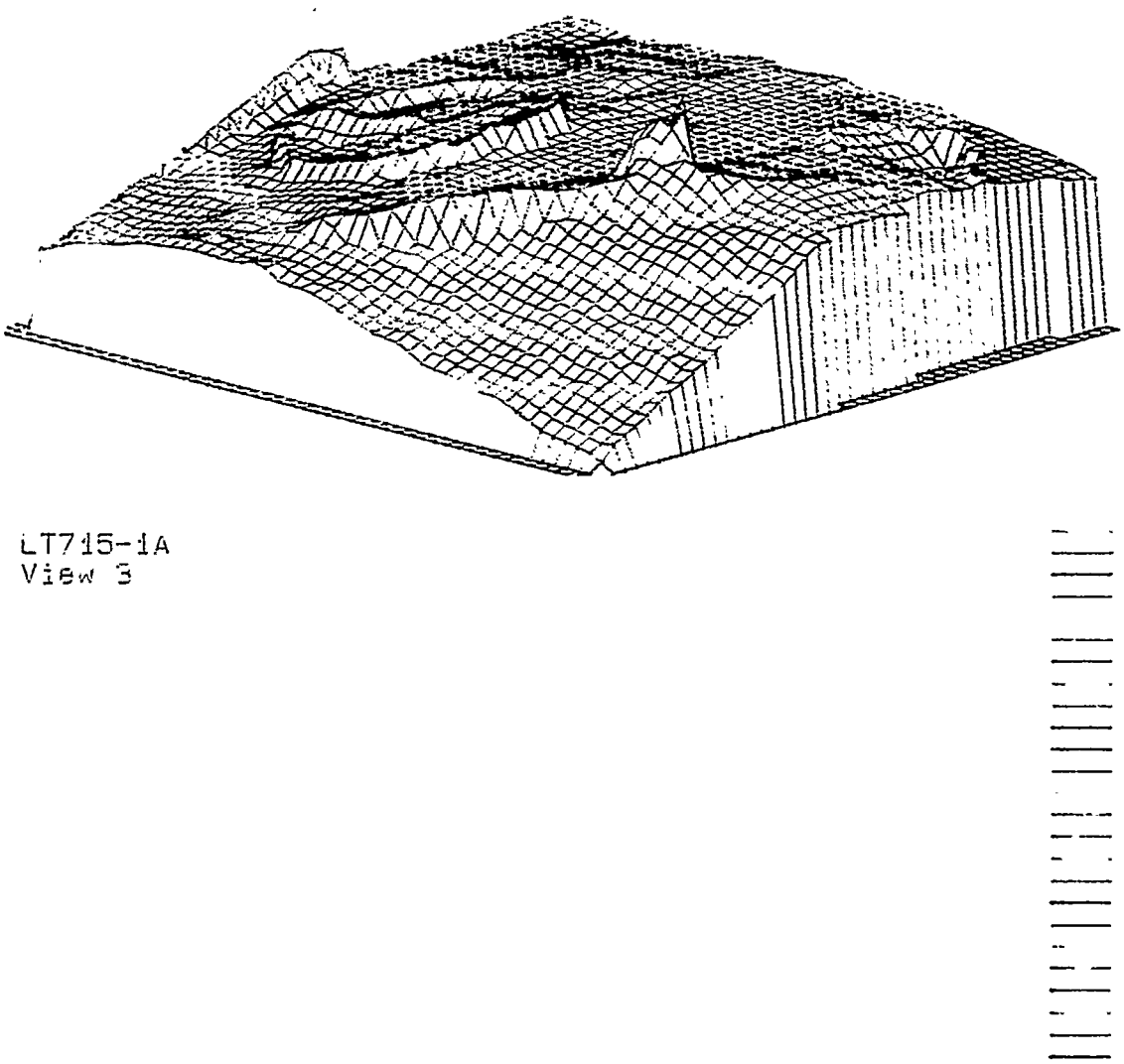

Fig.26 - 3D Perspective Plot of Plasma Cut 3MM Steel Plate Sample LT 715-1A.

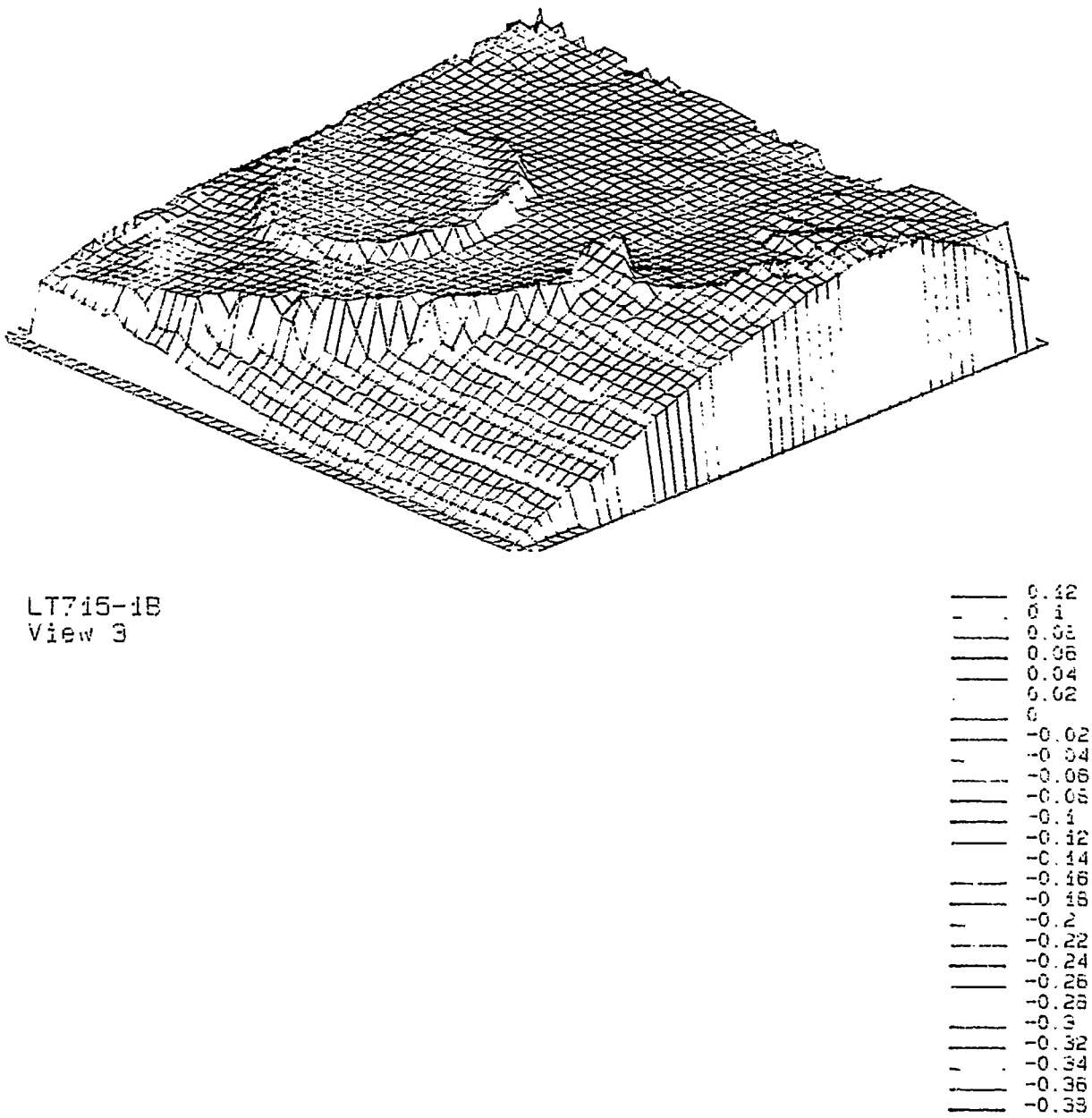

Fig.27 - Plasma Cut Steel Plate Sample LT715-1B - 3D Perspective Showing Contours After Cutting Relative to the Uncut Surface

as Nd:YAG (Neodymium:Yttrium Aluminum Garnet) and gas lasers such as carbon dioxide. The energy state of electrons in the material can be raised by incident light energy as in solid state lasers or by electromagnetic induction as in carbon dioxide gas lasers.

In a laser, the active atoms or molecules are raised to higher than normal energy levels by absorbed energy. A condition referred to as an inversion is produced by reflecting part of the emitted light back through the medium with mirrors on the ends. One of the mirrors is partially reflective to allow the laser beam to transmit. In the inversion condition a very large number the atoms of the laser active element are “pumped up" and coherent light of uniform wave length and frequency, characteristic of the activated element, is transmitted from the laser in phase and collimated in a non-divergent beam along the axis of the rod or gas tube. The coherent light beam which is emitted can be focused with conventional transmission optics (lenses) or with spherical or parabolic metal coated mirrors.

Focusing a laser beam to a small diameter can produce an area of extremely high energy density - sufficient to vaporize or melt metal. When used for cutting metals, laser cutting systems use an assist gas such as nitrogen, oxygen or air to aid in ejection of molten metal from the kerf. The mechanism of laser cutting is illustrated in Figure 28. The curved line of the cut in the figure is common to plasma, oxyacetylene and laser cutting and is seen in the metallographic photos of the faces of the cuts in Appendix A.

The primary limitation of Nd:YAG systems is in the relative low power output available compared to carbon dioxide lasers. It is

more difficult to remove excess heat from the crystal rods than from a gas laser. Nd:YAG lasers are available with up to 2.4 kilowatts output which is quite useful in low energy applications such as welding and cutting thin sections. In fact, cutting of ship components has been demonstrated with a Nd:YAG laser and the results reported in a National Shipbuilding Research Program project report, (NSRP 0363, Cutting of Structural Members with a High Powered Nd:YAG Laser.) In that project, conducted at Penn State, a 2.5 KW Nd:YAG with the laser output coupled to an optical fiber and manipulated by a robot was used and the system is available commercially. The project report also included results of cutting structural beams using a carbon dioxide laser.

Carbon dioxide lasers with power output up to 25 KW are commercially available. For such high powered lasers the problem of removal of excess heat and replenishment of carbon dioxide is accomplished with transverse flow of gas across the optical axis. Lower energy gas lasers may employ axial flow which is simpler and less costly. Figure 29 illustrates a typical transverse flow laser schematic and shows the geometry of the electrodes which pump up the molecules of carbon dioxide to the inversion state with high energy electr ical discharge in the gas mixture. Although carbon dioxide is. the smallest percentage of gas in the laser, it is the laser active material in the gas mix which includes helium and nitrogen. In the laser process, carbon dioxide is ionized to CO + 0, is recirculated through a heat exchanger, cooled, replenished and returned to the laser column. A carbon dioxide laser was used in this project.

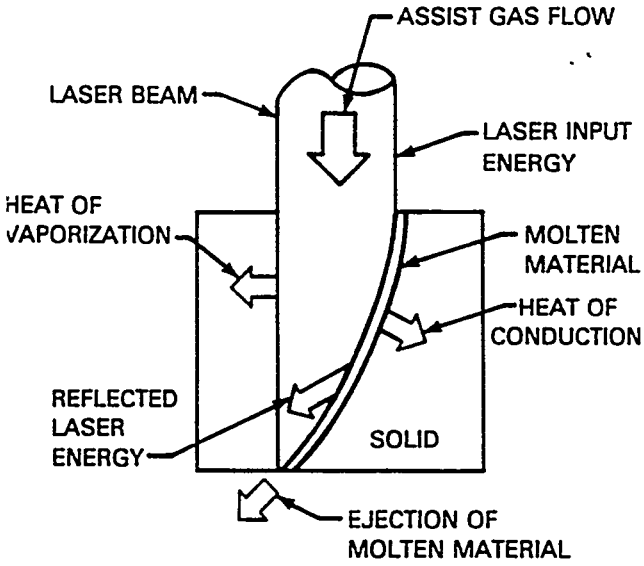

Fig.28 - Mechanism of Laser Cutting of Metal using Assist Gas to Remove Molten Metal from Kerf (from AWS Welding Handbook, Vol 2, American Welding Society, 1991)

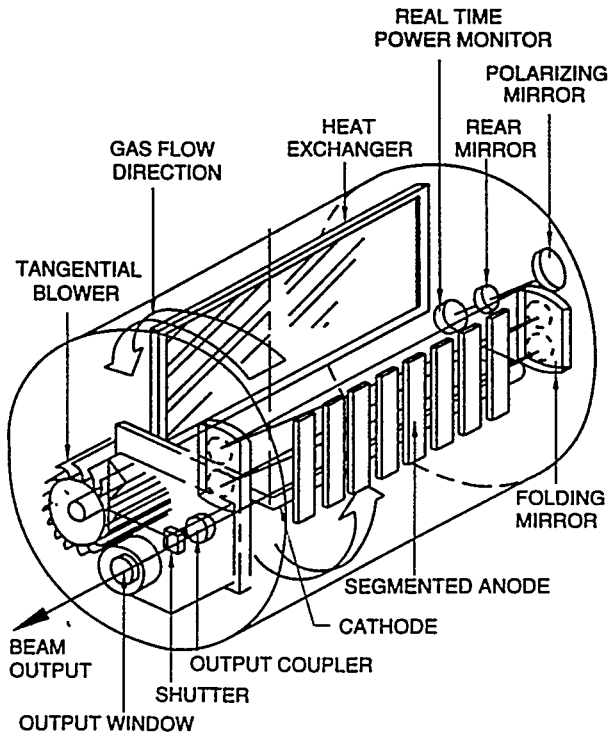

Fig.29 - Typical Arrangement of Components of a Transverse Flow Carbon Dioxide Laser from AWS Welding Handbook, Vol 2, American Welding Society, 1991

B. Advantages and Disadvantages of Laser Cutting

One of the distinctive productivity advantages of laser cutting of thin metal sections is its high cutting rate with low energy input to the adjacent base metal. Low heat input to the base metal minimizes thermal distortion. Kerf widths, narrower than either OA or PAC, are usually possible and the edges of the cuts are clean with only slight oxidation. Fume levels are minimal.

On the minus side, laser systems are more costly to install than plasma and oxyacetylene systems. Power requirements for energizing and cooling are high compared to power output. Special precautions are needed to protect personnel from potential injury from electrical equipment and from the laser beam itself.

C. Description of Laser Cutting Equipment

The equipment used in this project to cut 3 mm thick aluminum and steel plates was the 33 ton C-3000 Hybrid, CNC combination Laser/Turret punch system located at Murata Wiedeman, Inc. in Charlotte, North Carolina. The laser is a Fanuc fast axial flow type carbon dioxide gas laser, activated by 2 megahertz radio frequency discharge from a solid state oscillator power supply.

The cutting table afforded 150 cm by 200 cm (60 in. X 80 in.) travel at 38 m/min. (1500 in./min.) with AC servo controls. Figure 30 shows the arrangement of equipment used for the laser cutting.

D. Preparation of Samples for Laser Cutting

The steps necessary to provide for photography preparatory to

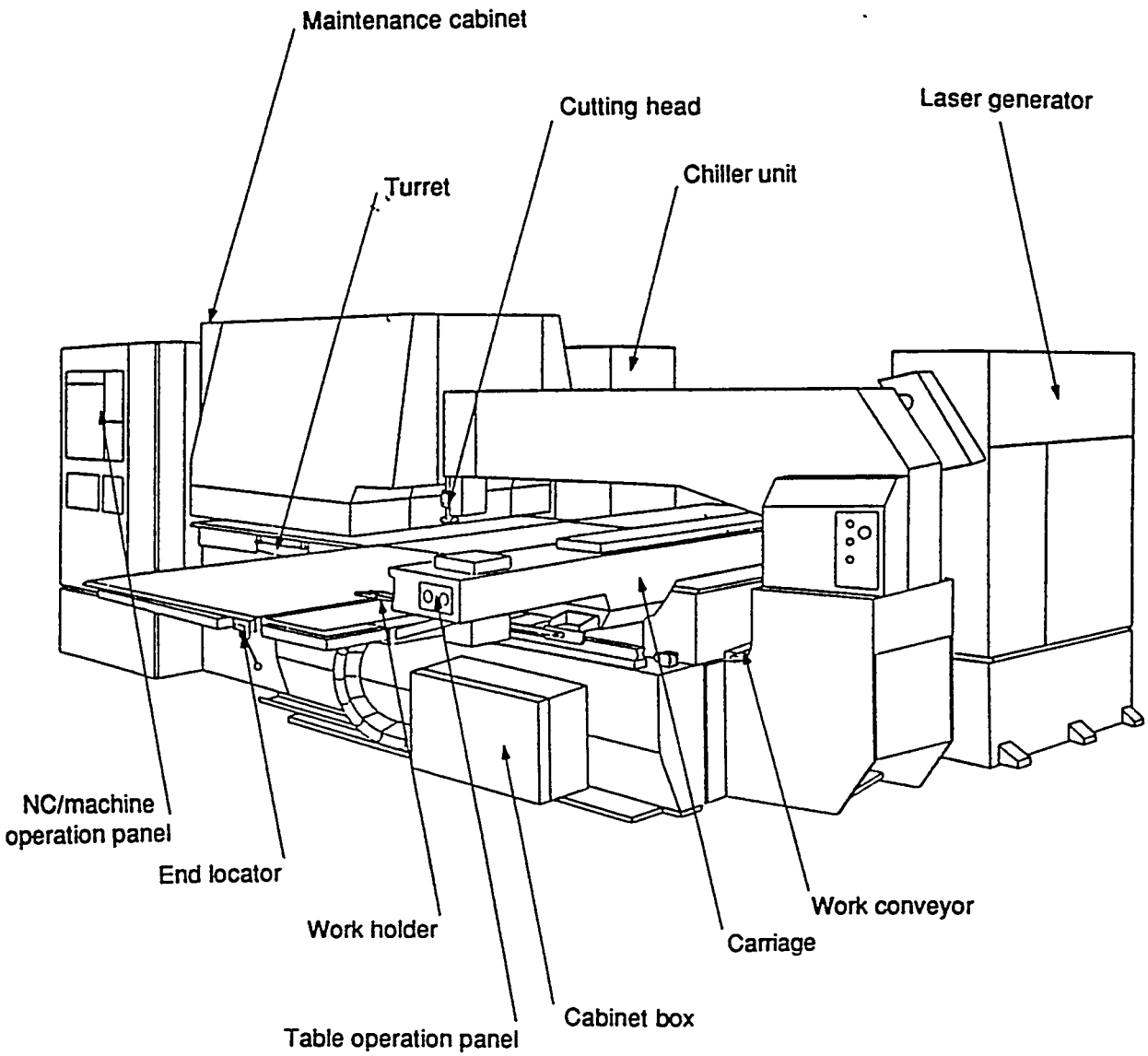

Fig.30 - Arrangement of Laser Equipment used to Cut 3mm Aluminum and Steel Plates

laser cutting were essentially the same as those described above for OA and plasma cutting. The CNC controller was programmed to move the platen under the cutting head to cut the template pattern out of the aluminum and steel plates. Stereo pair photos with fiducial marks in place were taken before and after cutting.

E. Cutting the Pattern by the Laser Cutting Process

The laser cutting of the aluminum plates was done at 150 cm/min. (60 in./min.) using assist gas at 1.25 bar (18 psi) pressure. The power level used was 1500 watts continuous beam. Cutting time for the complete test pattern was 7 minutes 37 seconds. Focal point of the beam was 1 mm (0.040 in.) below the surface of the plate.

F. Laboratory Evaluation of Laser Cut Aluminum

The metallographic photos of the laser cut aluminum in Appendix A are labled WE lC-B209B. The profile view at 30X" (Figure 21, Appendix A), shows a very straight, clean cut. The cut shows very little bevel angle relative to the plate surface and only slight rounding at the edges to a radius of approximately 70 roils.

The SEM micrograph at 30X (Figure 22, Appendix A), shows the texture of the cut surface with wavy lines approximately 5 roils apart. Only slight debris is adherent on the cut surface.

The longitudinal and transverse samples were mounted, polished and etched with hydrofluoric acid. The Optical microscopy views at lOOX, (Figures 23 and 24, Appendix A) show the cut edges to be clean and straight. No significant microstructural changes are

seen in the HAZ which is barely detectable. The cut edges could be used for welding with only minor mechanical clean-up of the oxides present on the cut surface.

Microhardness travserse of the HAZ starting 4 mils from the cut edge and continuing at 6 mil intervals were taken with a Vickers indenter at 200 grams load. The readings are 76.8, 86.2, 90.8, 96.2, 84.9 and 87.5.

G. Laboratory Evaluation of Laser Cut Steel Plate

The metallographic photos of laser cut steel in Appendix A are marked WE-lC-A715A. The macroscopic photo at 30X (Figure 17, Appendix A) shows the cut edge to be straight and perpendicular to surfaces of the plate (minimal kerf angle). A HAZ 4 to 6 roils thick was produced. This is much less heat effect than either the plasma or OA cut HAZ on steel. The face-on SEM view at 30X shows wavy lines 5 roils apart and a fine network of craze-cracks over part of the surface of the cut face. The craze cracks are superficial and can not be clearly resolved at 100X in the transverse microscopy of the same sample. The transverse section shows a HAZ about 5 roils thick. The slightly coarsened grain of the HAZ is also seen in the longitudinal cut.

A Microhardness traverse across the HAZ starting 4 roils from the edge taken with a 500 gram Vickers test showed 174, 156, 149, 149 and 149. The hardening in the HAZ is much less than in OA or in the plasma arc cutting samples.

H. Photogrammetric Measurements Of Laser Cut Plates

The sequence of photogrammetric reference photos and stereo plotting measurements to determine accuracy and distortion was essentially the same as previously described for OA cutting.

1.0 Photogrammetric Evaluation of Laser Cut Edges of Aluminum Plates

The accuracy of the laser cuts of aluminum relative to the template are seen in Figures 31 and 32. The figures show that the left edge of both aluminum samples were taken as the baseline. The vectors show the curved edge to be 1 mm to 1.5 mm (0.04 in. to 0.06 in.) inches short on sample MW209A and between 1.8 mm and 4.1 mm *(0.07* in.and 0.16 in.) short on sample MW209B. The holes vary from circularity by 1 .3mmto 2.3mm (0.05 in. to 0.09 in.) on both samples.

2.0 Contour Plots of Out-of-Plane Distortion of Laser Cut Aluminum Plates

The contour plots in Figures 33 and 34 are the resultant plots for laser cut of 3mm aluminum plates after subtraction of pre-cut from post -cut distortion. The distortion attributable to the laser cutting is seen on sample MW209A to vary from 0.25 mm to 0.50 mm (0.01 in. to 0.02 in.). On sample MW209B distortion was from -0.25 mm to +0.50 mm (-0.01 in. to +0.02 in.). It is noted that on the cut out part of the large circle, distortion was somewhat greater, 0.00 to lmm (+0.04 inches on one and0.00to0.8mm (0.03 in.)) on the other.

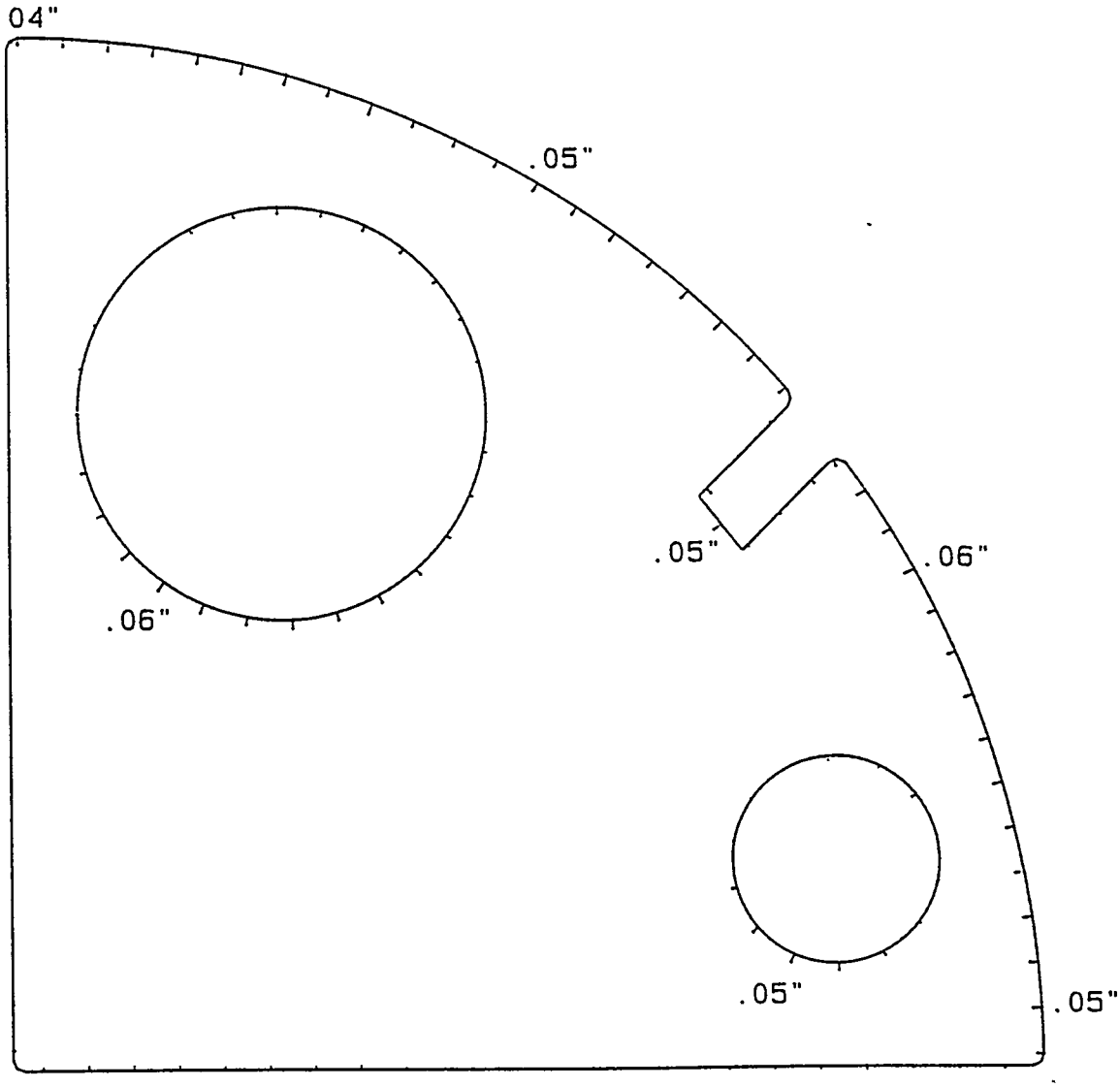

MW209A
Cut edge versus design template
Scale: 1"=8"
Vector scale: 1"=1"

Fig.31 - Cut Edge Versus Design Template for Laser Cut Aluminum Sample MW 209A - Ends of Vectors Show Actual Location of Cut Edge.

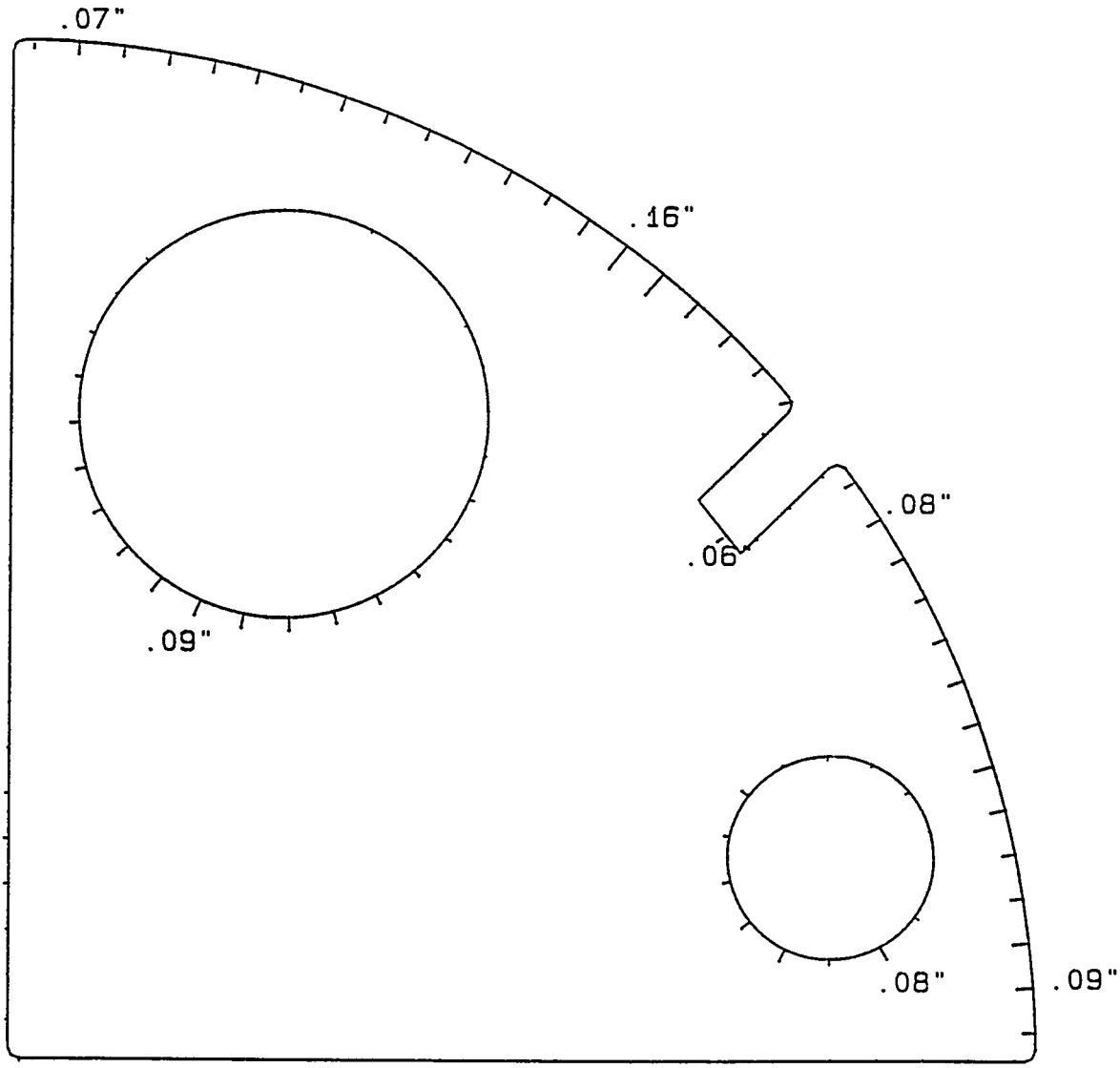

MW209B
Cut edge versus design template
Scale: 1"=8"
Vector scale: 1"=1"

Fig.32 - Cut Edge Versus Design Template for Laser Cut Aluminum Sample MW209B - Ends of Vectors Show Actual Location of Cut Edge

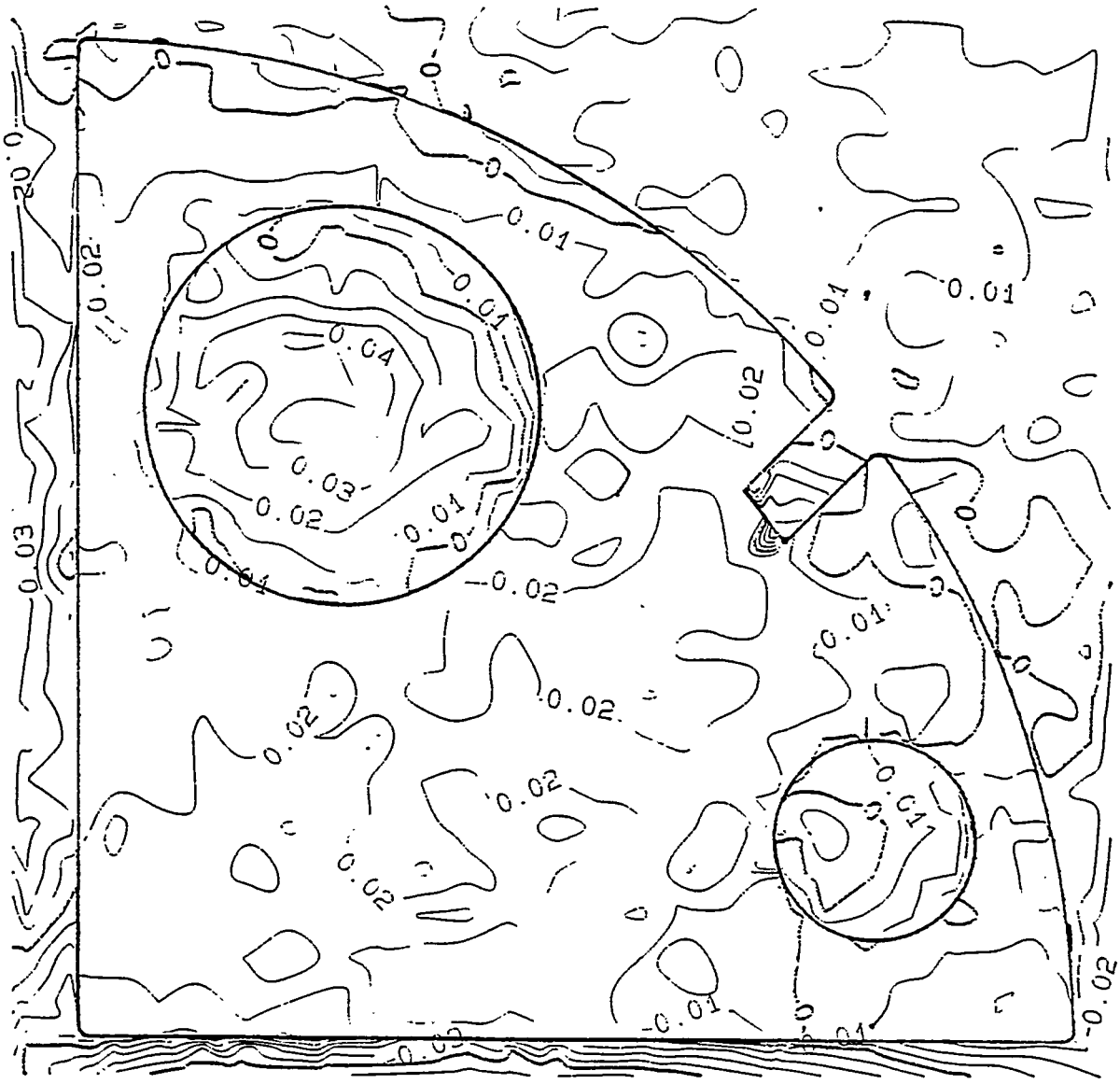

Fig.33 - Resultant Contour Plot of Distortion Resulting from Laser Cut of Aluminum Sample MW209A

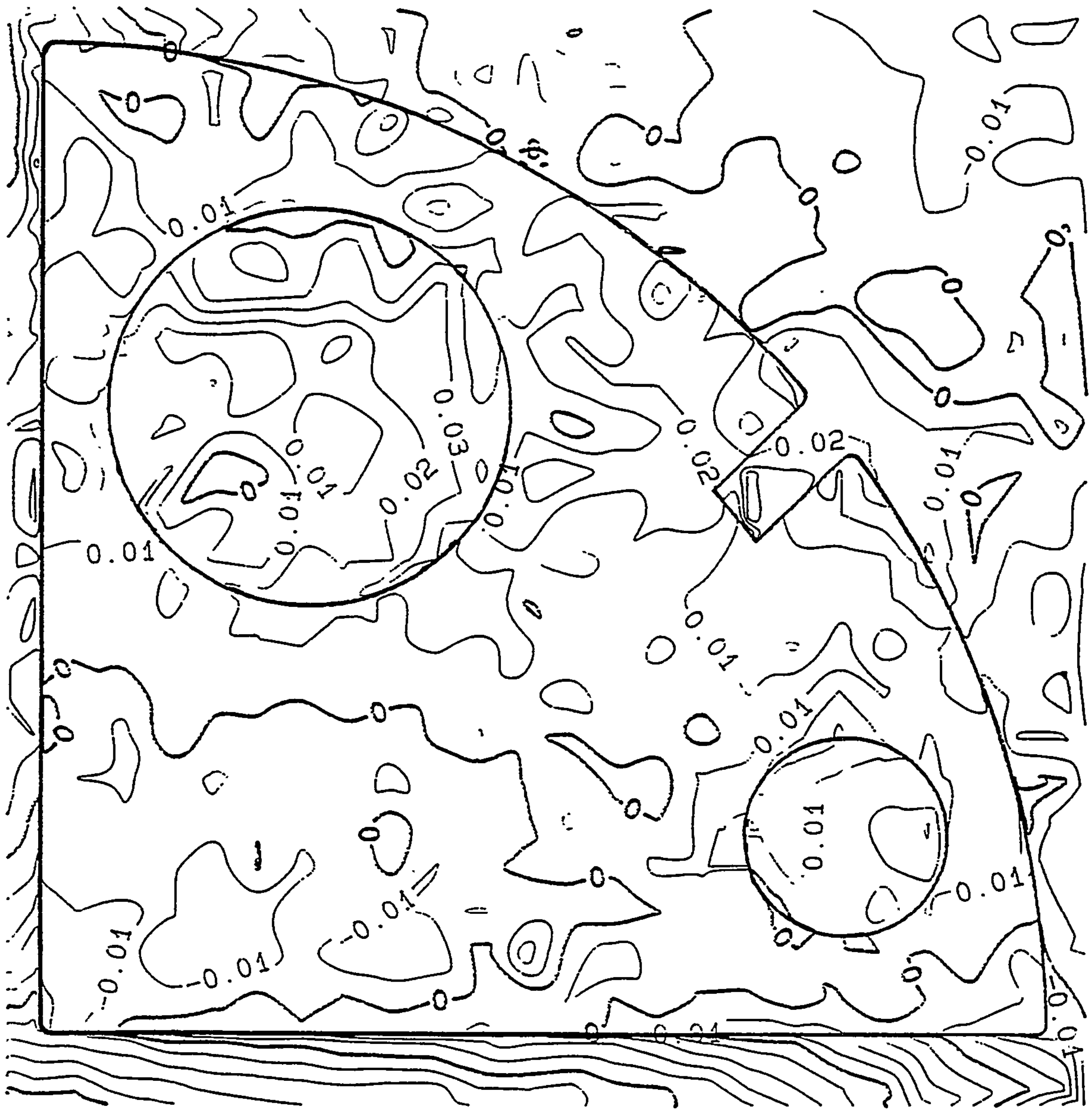

MW209B
Plot 3
Scale. 1"=8″
CI: 01″

Fig.34 - Resultant Contour Plot of Distortion Resulting from Laser Cut of Aluminum Sample MW209B

3.0 3-D Perspective Plots of Distortion in Laser Cut Aluminum

The digitized data from the resultant stereo plots for laser cut aluminum were translated by computer analysis to depict a perspective view from over the curved edge (3 Figure 1, view 3). The 3D plots of samples MW209A and MW209B are shown in Figures 35 and 36.

4.0 Photogrammetric Evaluation of Laser Cut Edges of Steel Plates

The deviation of the laser cut steel plates from nominal values of the template were measured by photogrammetry. As seen in Figures 37 and 38 the left edge is used as a baseline reference. The curved edge is seen in sample MW715A to be cut under the nominal dimension by lmm to 3 mm (0.04 in. to 0.12 in.); MW715B is cut undersize between 0.00 and 2 mm (0.08 in.). The large circular cuts are out of round by 1.5 mm (0.06 in.) in MW715A and by 1 mm (0.04 in.) on the other. The small holes are off on one diameter by 2.8 mm (0.11 in.) on one and 1 mm (0.04 in.) on the other sample.

5.0 Contour Plots of Out-of-Plane Distortion of Laser Cut Steel Plates

The resultant contour plots from subtraction of distortion prior to laser cutting from distortion after cutting 3mm steel plates are given in Figures 39 and 40. The maximum distortion within the outline of the test patterns is 0.5 mm (0.02 in.) as seen on sample MW715B . Sample MW715A had only 0.2 mm (0.01 in.) distortion resulting from the laser cut.

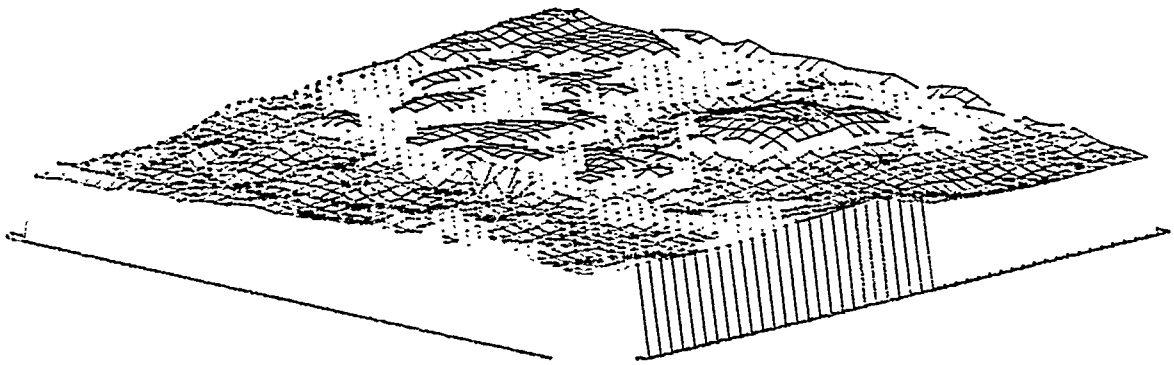

MW209A
View 3

0.044
0.033
0.022
0.011
0
-0.011
-0.022
-0.033
-0.044
-0.055
-0.066
-0.077
-0.088
-0.099
-0.11
-0.121

Fig.35 - 3D Perspective Plot of Laser Cut Aluminum Plate Sample MW209A

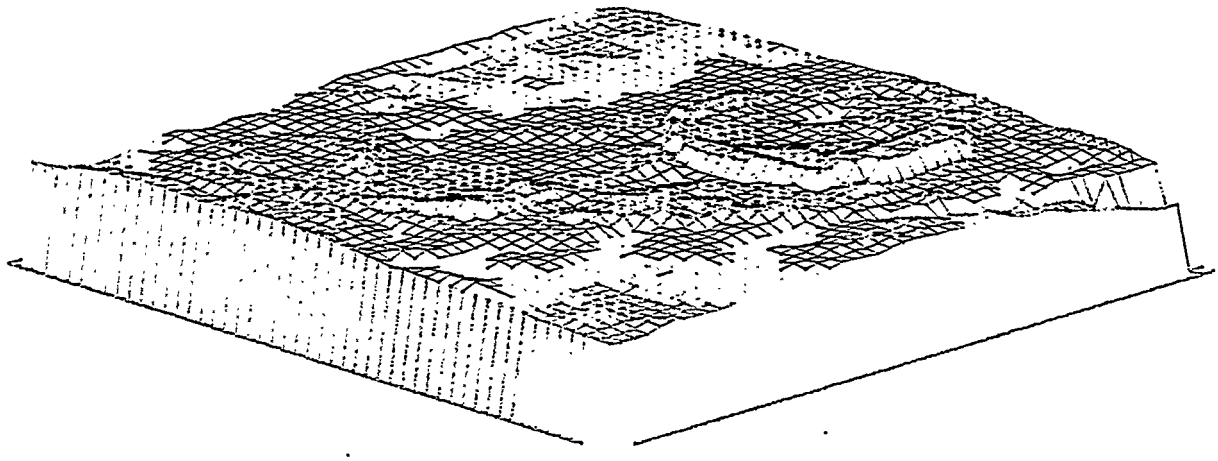

MW209B
View 3

0.06
0.05
0.04
0.03
0.02
0.01
0
-0.01
-0.02
-0.03
-0.04
-0.05
-0.06
-0.07
-0.08
-0.09
-0.1
-0.11
-0.12
-0.13
-0.14
-0.15
-0.16
-0.17
-0.18
-0.19
-0.2
-0.21

Fig.36 - 3D Perspective Plot of Laser Cut Aluminum Plate Sample MW209B

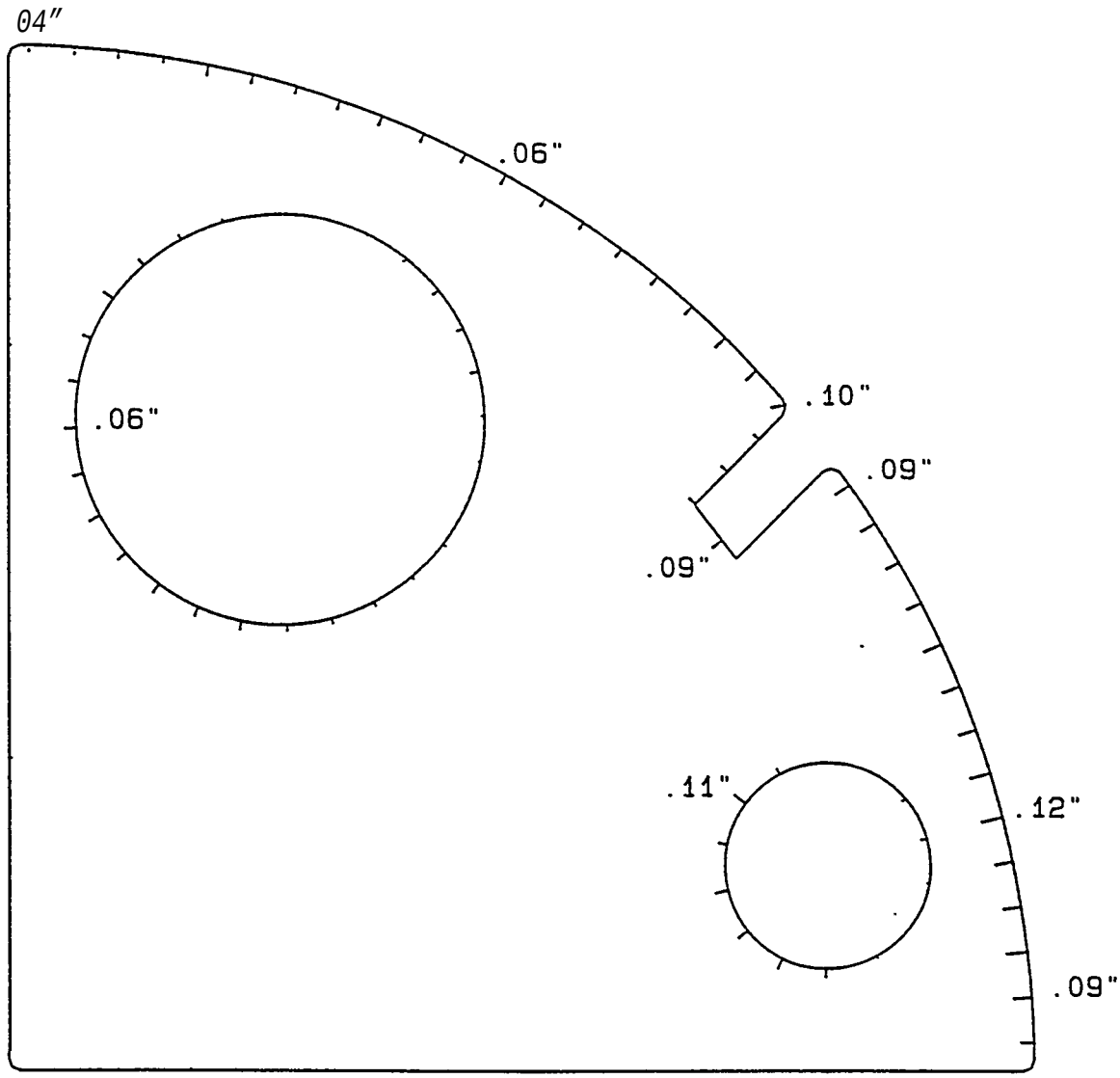

MW715A
Cut edge versus design template
Scale: 1"=8″
Vector scale: *1″=4″*

Fig.37 - Edge Plot of Laser Cut Steel Sample MW715A - Ends of Vectors Show Location of Actual Cut Edge Relative to the Design Template.

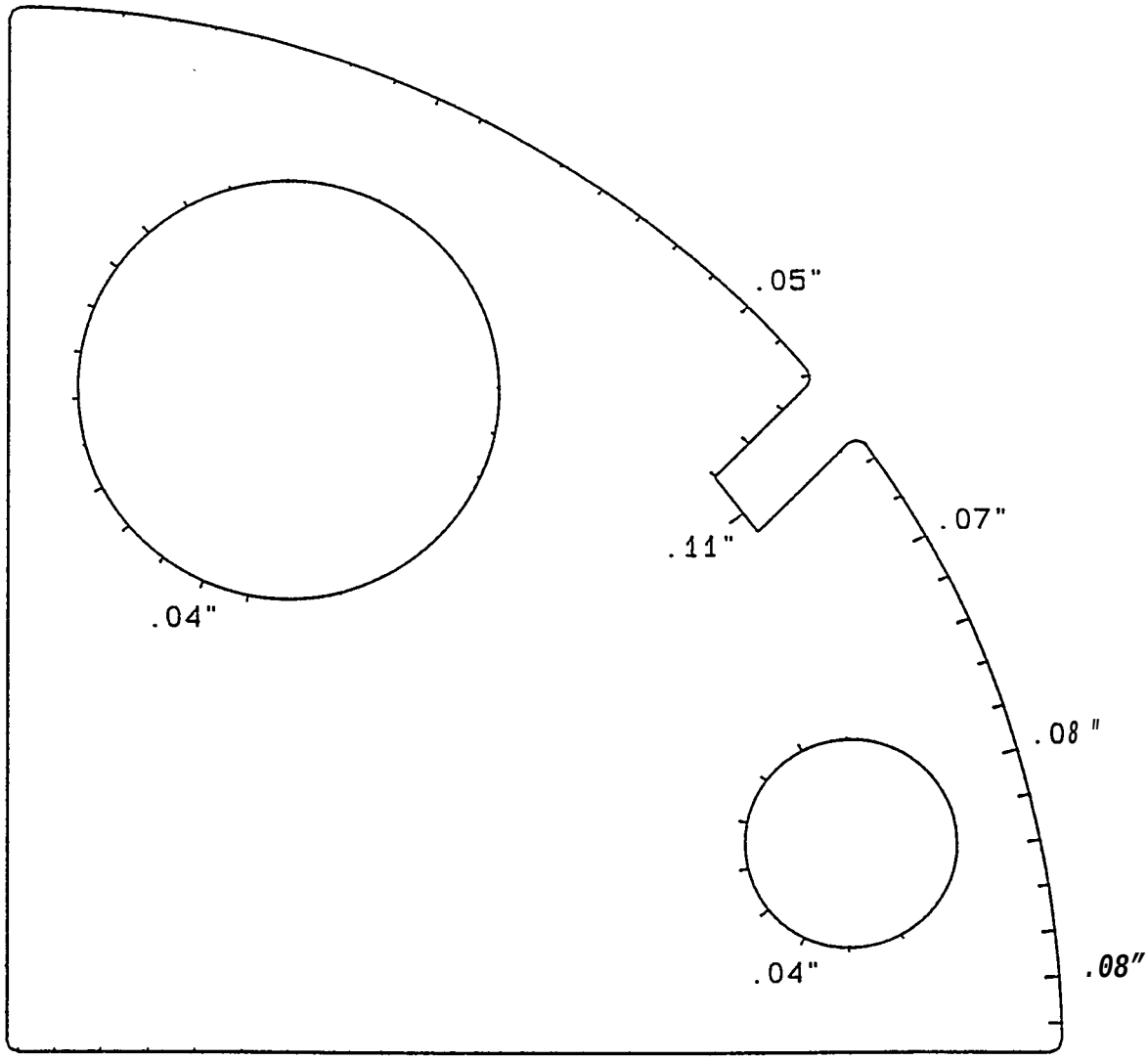

MW715B
Cut edge versus design template
Scale: 1"=8″
Vector scale: 1“=1”

Fig.38 - Edge Plot of Laser Cut Steel Sample MW715B - Ends of Vectors Show Location of Actual Cut Edge Relative to the Design Template

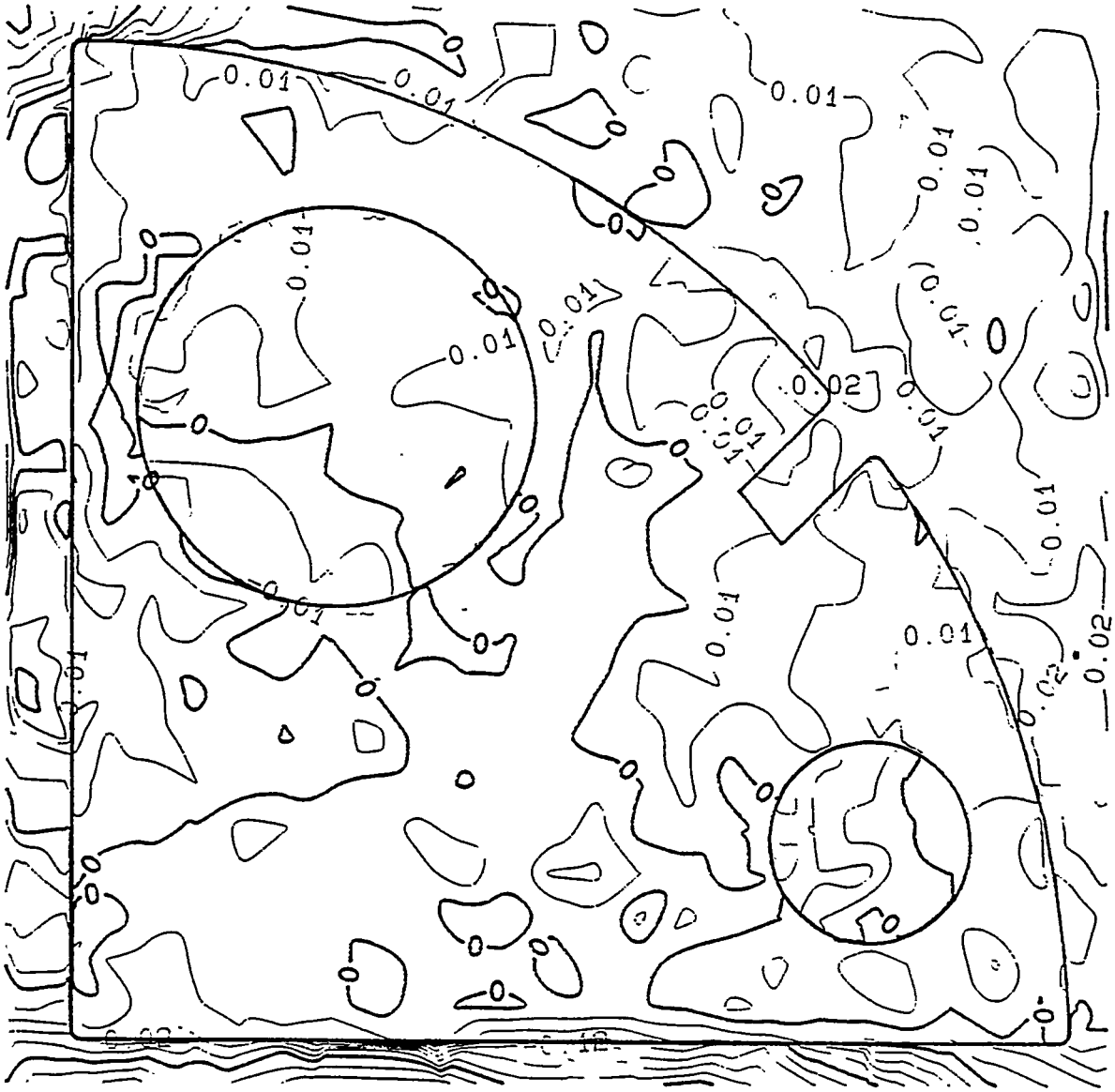

MW715A
Plot 3
Scale 1"=8"
CI: 01"

Fig.39 - Resultant Contour Plot of Laser Cut Steel Plate Sample MW715A Showing Distortion Relatives to the Uncut Plate

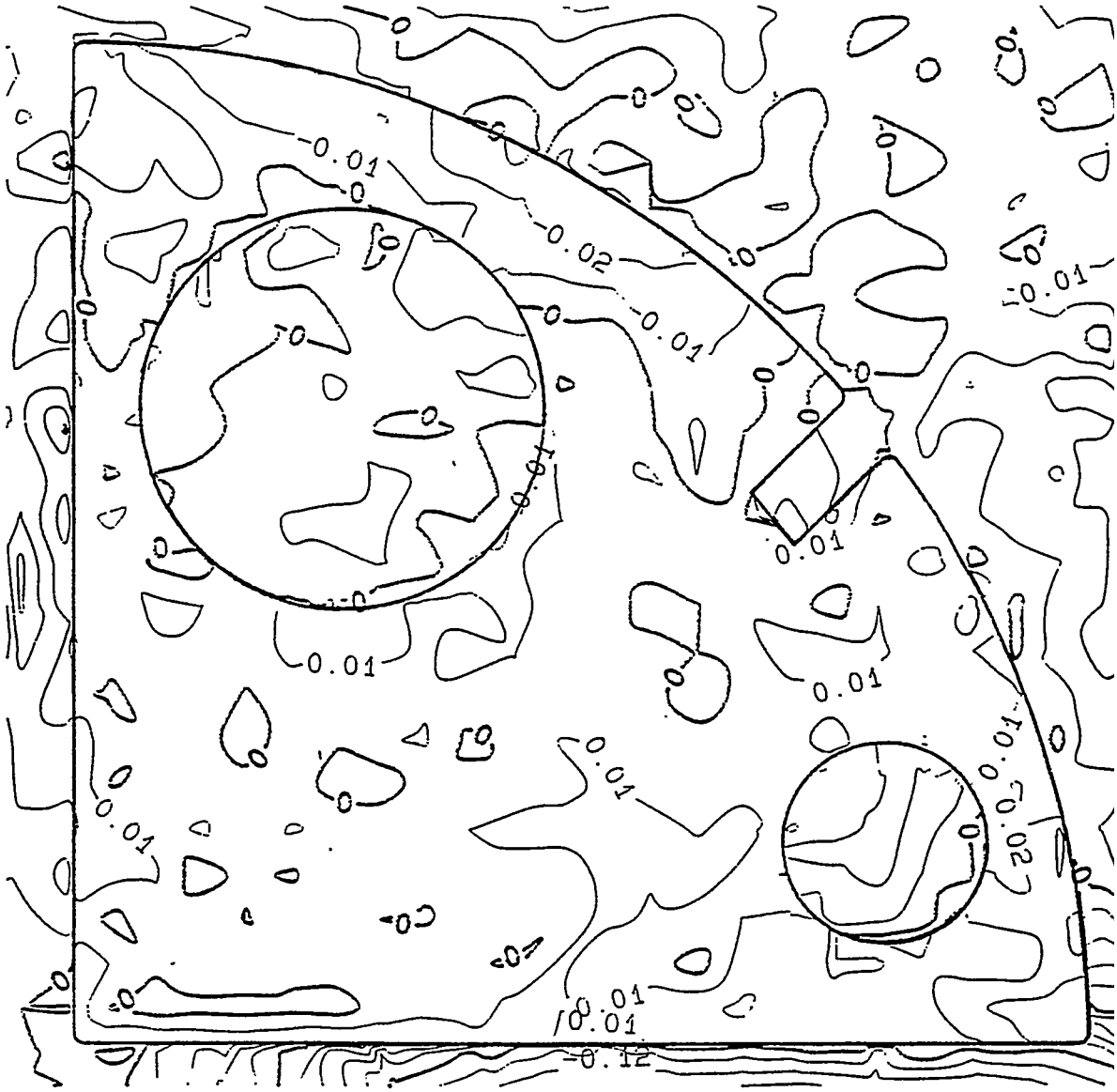

MW715B
Plot 3
Scale. 1"=8"
CI: 01"

Fig.40 - Resultant Contour Plot of Laser Cut Steel Plate Samp
MW715B Showing Distortion Relative to the Uncut Plate

6.0 3D Perspective Plots of Distortion in Laser Cut Steel Plates

The resultant 3D perspective views of the laser cut steel samples are shown in Figures 41 and 42. These depictions readily show the low overall distortion of the plates cut by laser compared to the cuts made by the other two thermal processes.

VI. WATER JET CUTTING OF 3MM ALUMINUM AND STEEL PLATES

A. General Principles of Water Jet Cutting

Water jet cutting as the technology is used today began with the development in the late 1960s of high pressure intensifier pumps capable of pressuring water to over 3800 bar (55,000 psi). For cutting of materials, the ultra high pressure water is jetted through a nozzle orifice with a diameter of as little as 0.1 mm (0.004 in.). The resulting water jet reachs a velocity over Mach 3, well over 3200 km/hr (2000 mph).

The cutting capability of the water jet is greatly enhanced by the introduction into the water stream of abrasive particles usually on the order of 60 to 80 mesh size. Sapphire orifices are generally used for water jet nozzles; harder, more resistant carbide nozzles are used when the abrasives are added to the water. OliVine and garnet are widely used abrasives. Olivine, a magnesium-iron silicate, is softer and about 30% less costly than garnet. Garnet is most often used for metal cutting and in 1993 was less than $0.30 per pound.

Examples of materials cut by water jet include hard and soft metals, composites such as Kevlar as fabric or in resin matrices, stone and glass. Very little material is wasted in water jet

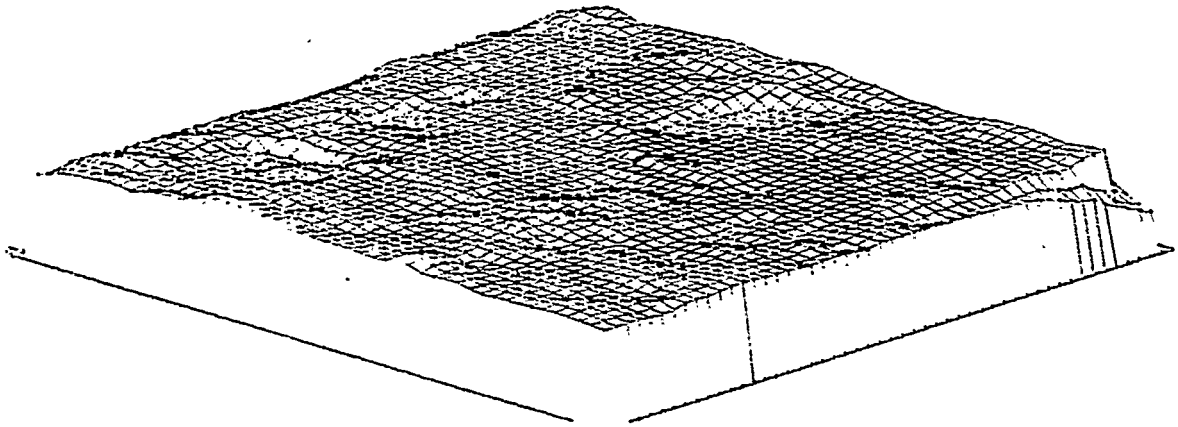

MW715A
View 3

0.03
0.02
0.01
0
-0.01
-0.02
-0.03
-0.04
-0.05
-0.06
-0.07
-0.08
-0.09
-0.1
-0.11
-0.12
-0.13
-0.14
-0.15
-0.16
-0.17
-0.18

Fig.41 - 3D Perspective Plot of Distortion Produced in Steel Plate MW715A by Laser Cutting.

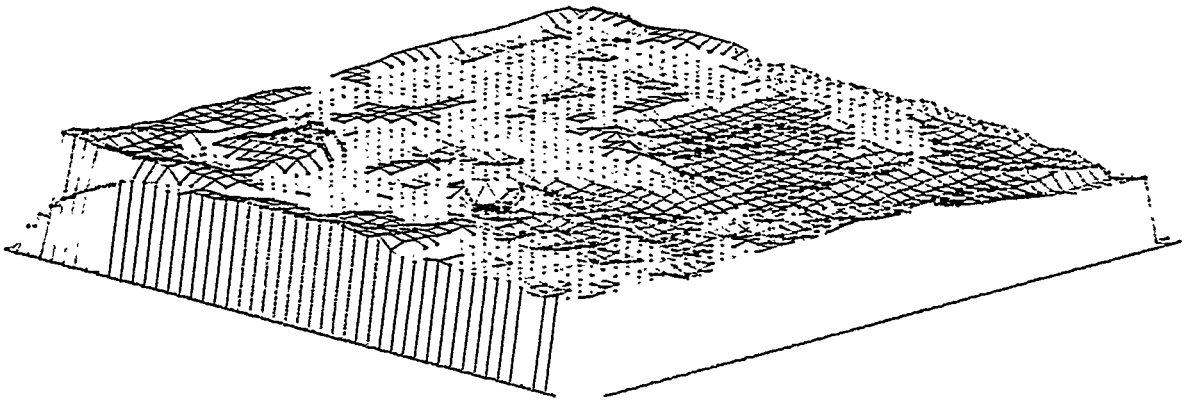

MW715B
View 3

0.033
0.022
0.011
0
-0.011
-0.022
-0.033
-0.044
-0.055
-0.066
-0.077
-0.088
-0.099
-0.11
-0.121
-0.132

Fig.42 - 3D Perspective Plot of Distortion Produced in Steel Plate MW715B by Laser Cutting

cutting because the water stream and the kerf may be only 0.8 mm to 2.5 mm (0.03 in. to 0.10 in.) wide. The cut edges are without thermal effects such as fumes from composites or heat affected zones in metals.

The key items of equipment comprising a water jet cutting system include a high pressurizer intensifier pump and filtration system, a hydraulic piston pump, a nozzle assembly, plumbing and catch tank. A typical configuration of an abrasive water jet cutting system is shown in Figure 43.

B. Advantages and Disadvantages of Water Jet Cutting

One of the advantages of water jet cutting is its versatility compared to thermal processes when cutting composites, rubber and textiles. The absence of a HAZ and minimal thermal distortion is a distinct advantage of WJC. Another plus for water jet is the elimination of need for support gasses and electrical hazards. Distortion is also reduced to a minimum.

Cutting rates for metals are generally slower with water jet than for competitive thermal processes. The high velocity water jet emits noises over 90 decibels intensity and operators need ear protection. Applications in cutting sections over 13 mm (0.5 in.) are limited due to the slow cutting speed relative to laser, plasma and oxy-acetylene.

C. Preparation and Cutting of Aluminum and Steel by Water Jet

Two plates each of 5456 alloy aluminum and ASTM A715 GR 80 HSLA steel were cut with the Flow International system at Kent,

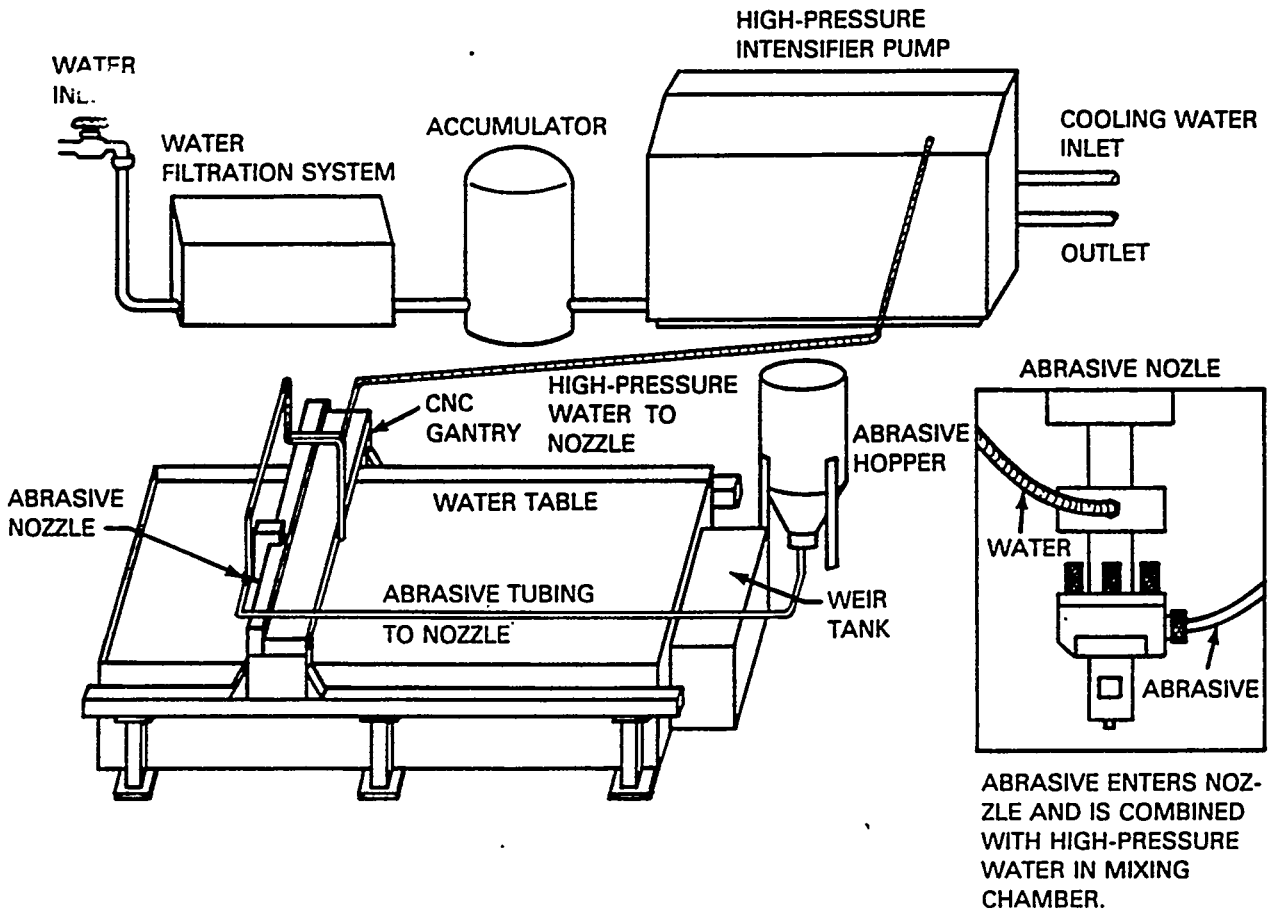

Fig.43 - Configuration of a Typical Water Jet Cutting System (Welding Handbook, Vol 2, American Welding Society, 1991)

Washington. The cutting system is identified by Flow International as the Paser II system. It operates at 3800 bar (50,000 psi) pressure The cutting head is manipulated by an ASI 5 axis gantry mounted robot.

The Figure 1 cutting pattern used for the thermal cutting evaluations was also used for water jet cutting. The cutting head was programmed using Autocad and translated to the robot control language to cut the template.

The Paser system used 80 grit garnet abrasive at 1.25 lbs./min. with an orifice diameter of 0.4 mm (0.016 in.) Stand off distance was 0.2 mm (0.01 in.) and travel speed was 64cm/min. (25 in./min.) .The same parameters were used for both aluminum and steel. All of the photogrammetric procedures described previously were used except as noted below.

D. Metallographic Evaluation of Water Jet Cut Aluminum

The water jet cut aluminum plate samples submitted to Materials Evaluation Laboratory for evaluation of the cut edges are labled WE-lB-B209A. The metallographic photos are included in Appendix A.

The optical macro shot of aluminum at 30X, (Figure 13, Appendix A) shows a slightly rounded shoulder at the top of the cut with a radius of 50 roils but the two faces were straight and free of a noticeable kerf angle. The SEM study showed a slightly roughened texture (Figure 14, Appendix A). The microscopic photos at 100X taken on a cut, transverse to the direction of the waterjet cut, shows a straight and very clean cut and obviously no heat

affected zone. The roughened texture shown in the SEM is clearly seen also in the 100X micrograph in Figure 16 of Appendix A, and the cut surface is free of oxides and debris.

The Vickers microhardness traverse of the water jet cut aluminum alloy plate was taken with a 200 gram load. The readings starting at 4 mils from the edge and at 6 mil intervals were 102, 101, 101, 110, and 102.

E. Metallographic Evaluation of Water Jet Cut Steel

The metallographic photos of the water jet cut plates in Appendix A are Figures 9, 10, 11, and 12 and are marked WE lB-A715A. The profile macro photo at 30X shows the cut to be straight and the kerf edges are essentially parallel. A small burr of deformed metal was formed on the inside of the cut. The scanning electron micrograph at 30X (Figure 10, Appendix A) shows the water jet produced a slightly roughened texture but did not form the wavy lines characteristic of the thermal cutting processes. The uniform grain size and microstructure and the total absence of HAZ are evident in Figures 11 and 12 which are the polished and etched samples at 100X. The slight roughness seen in the SEM is also seen in the 100X longitudinal view.

Vickers microhardness (500 gram) readings at 4 mils from the edge and at 6 mil intervals were 220, 228, 229, 225, 229, and 232.

F. Photogrammetric Evaluation of Water Jet Cut Plates

The sequence for making stereo reference photos for measurement of accuracy of the cut edges and out-of-plane

distortion from water jet cutting was the same in principle as described previously for the thermal cutting processes. It was necessary, however, to develop a procedure to accommodate the fact that the water jet system cuts through not only the test plate but also the support plate on the catch tank. This was not anticipated for the first cut sample which was a steel plate. As a result of this discrepancy and the fact that only two steel plates were available, one set of photogrammetric data was lost for the steel samples.

In order to proceed it was necessary to solve the problem of repositioning the cut pattern and establishing suitable reference points for stereo plotting of the after-cut sample. Quoting from the photogrammetrists report:

> " We solved this problem by photographing the cut tooling plate and defined the orientation and intersection of the long linear cuts as offset by the width of the cut. We then measured the orientation and location of the same edges of cut piece and determined the necessary rotation and translation parameters to transform from one system to the other. The vertical was offset by the thickness of the supporting plate."

1.0 Photogrammetric Evaluation of Water Jet Cut Edges of Aluminum

The accuracy of the fit of the water jet cut edges to the dimensions of the template are shown in Figures 44 and 45. The curved edge is seen to be undersize relative to the straight left edge of the part by 2.3 mm to 3.3 mm (0.09 in. to 0.13 in.) on the

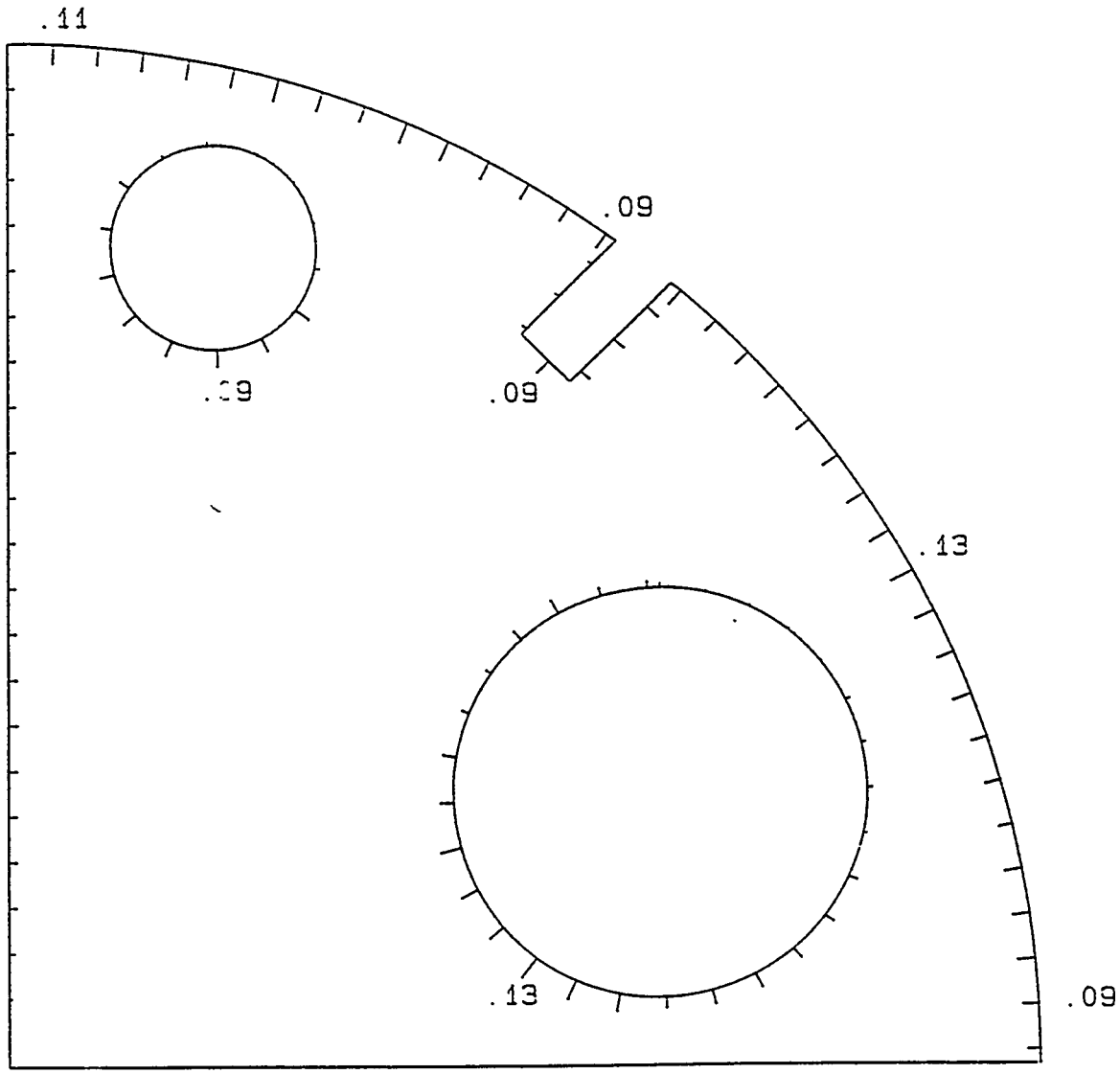

FI209A
Cut edge versus design template
Scale: 1"=8"
Vector scale. 1"=1"

Fig.44 - Edge Plot of Water Jet Cut Aluminum Plate Sample FI209A Vector Ends Show Actual Location of Edge of Cut Relative to th Design Template

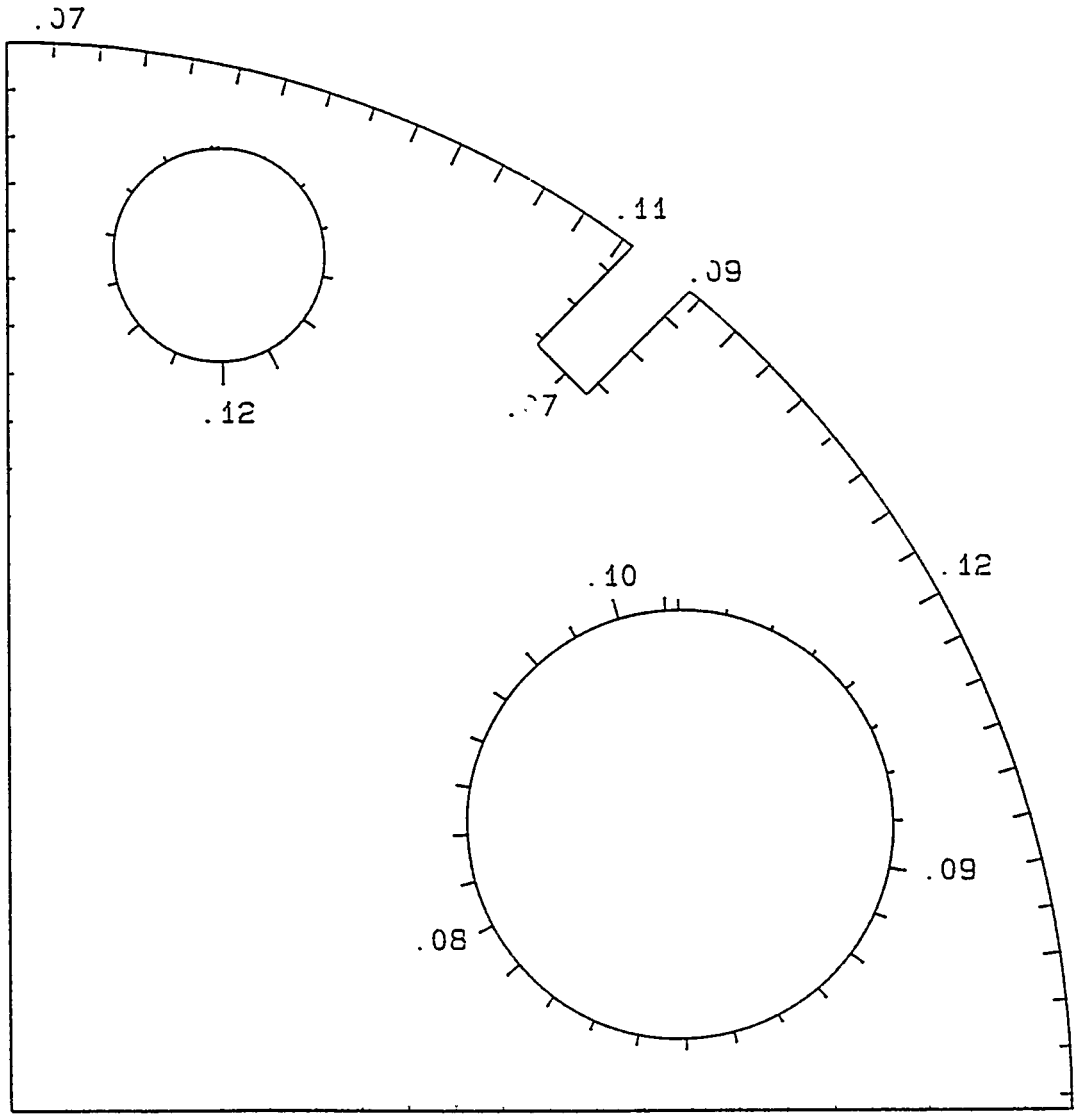

FI209B
Cut edge versus design template
Scale. 1"=8"
Vector scale. 1"=1"

Fig.45 - Edge Plot of Water Jet Cut Aluminum Plate Sample F1209B; Vector Ends Show Actual Location of Cut Edge Relative to the Design Template

"A" sample and about 1.8 mm to 3.0 mm (0.07 in. to 0.12 in.) on the "B" sample. The large holes were over cut by 3.3 mm (0.13 in.) on "A" and 2.5 mm (0.10 in.) on “B”. One of the small pipe way holes was out by 3 mm (0.12 in.) making the hole that much out of round. The discrepancies are considered to be such that, with additional iterations of the cuts as would occur in a production situation, most of the deviations could be corrected by adjusting the CNC guidance program.

2.0 Contour Plots of Out-of-Plane Distortion of Water Jet Cut Aluminum Plates

The resultant contour plots from digital plotting of the stereo photos of water jet cut aluminum are shown in Figures 46 and 47. The figures show the resultant contours after correcting the post cut distortion by “subtracting” the distortion present prior to cutting. Figure 46 indicates that distortion ranged between -1.3 mm to +0.8 mm (-0.05 in. to +0.03 in.) on sample "A" and -0.2 mm to +0.8 mm (-0.01 in. to +0.03 in.) on sample “B”.

3.0 3D Perspective Plots of Water Jet Cut Aluminum

The 3D perspective plots of the water jet cut aluminum are shown below. The angle of perspective is view 3 as defined by Figure 1. Unlike the 3D plots for the thermally cut processes, the baseline grid is visible in the water jet cut samples. This was the result of the discrepancy explained above in the introduction to photogrammetry of the water jet cut samples. The cut out scrap was not re-placed on the platen. The 3D plots for aluminum are shown below in Figures 48 and 49.

FI209A
Plot 3
Scale. 1"=8"
CI: 01"

Fig.46 - Contour Plot of Distortion Produced by Water Jet Cutting of Aluminum Plate, Sample FI209A

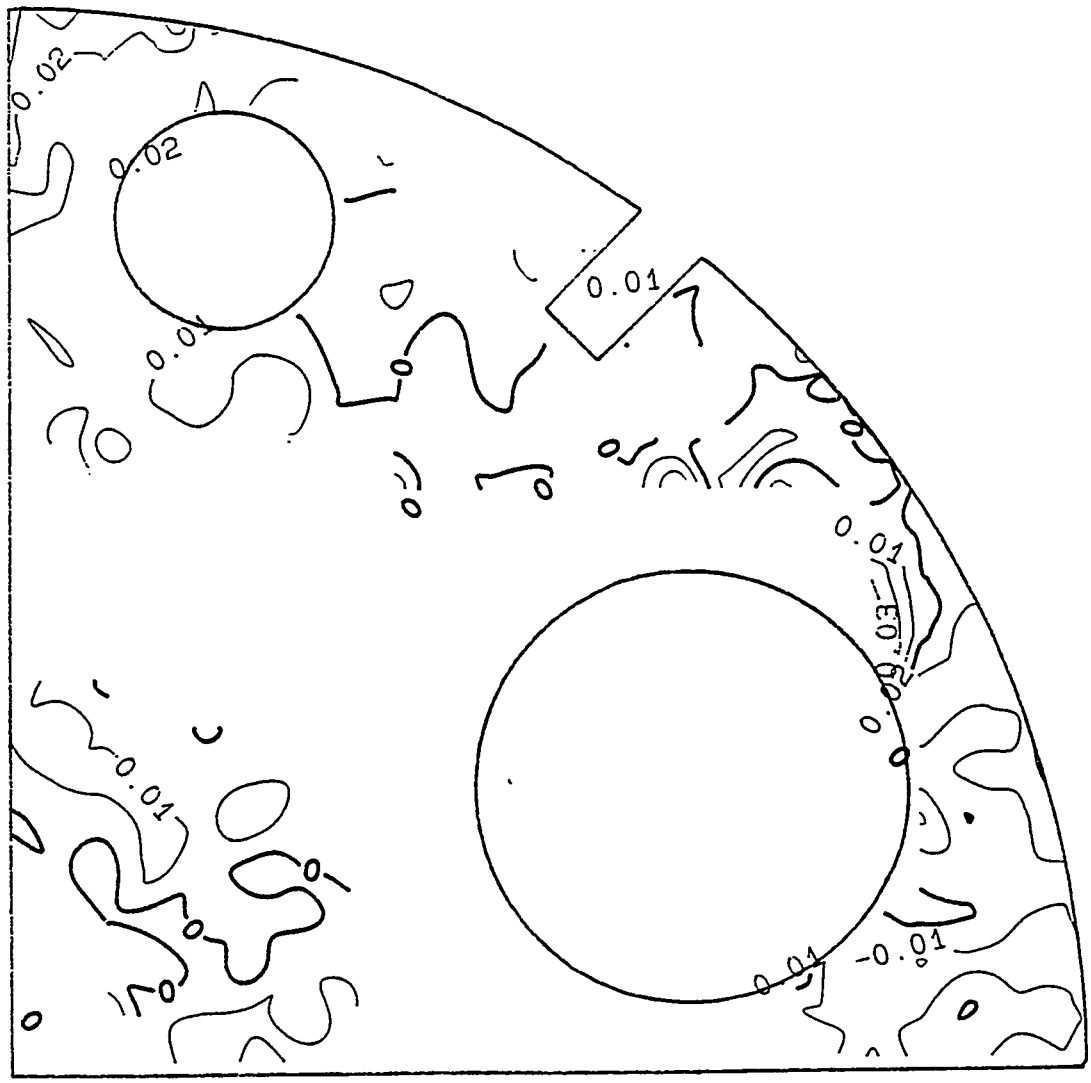

FI209B
Plot 3
Scale. 1"=8"
CI: .01"

Fig.47 - Contour Plot of Distortion Produced by Water Jet Cuttir
of Aluminum Plate, Sample FI209B

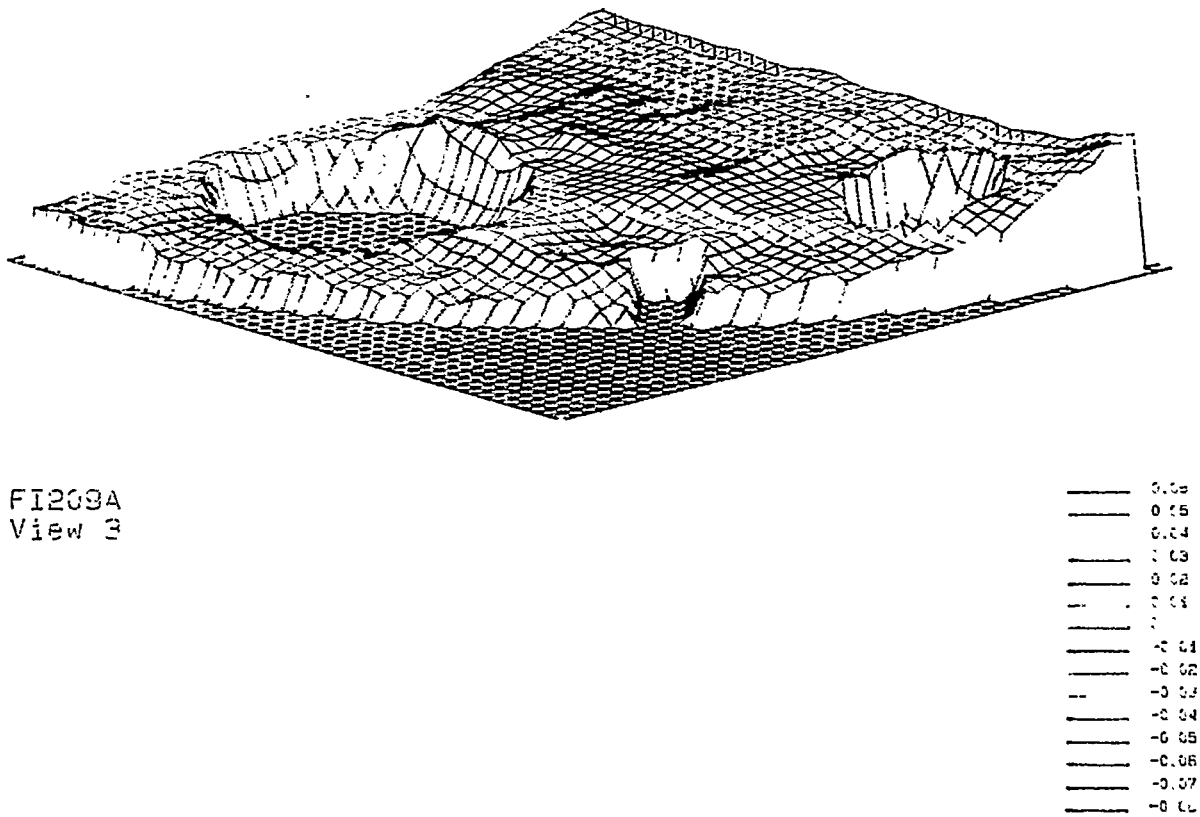

Fig.48 - 3D Perspective Plot of Distortion in Aluminum Sample FI209A

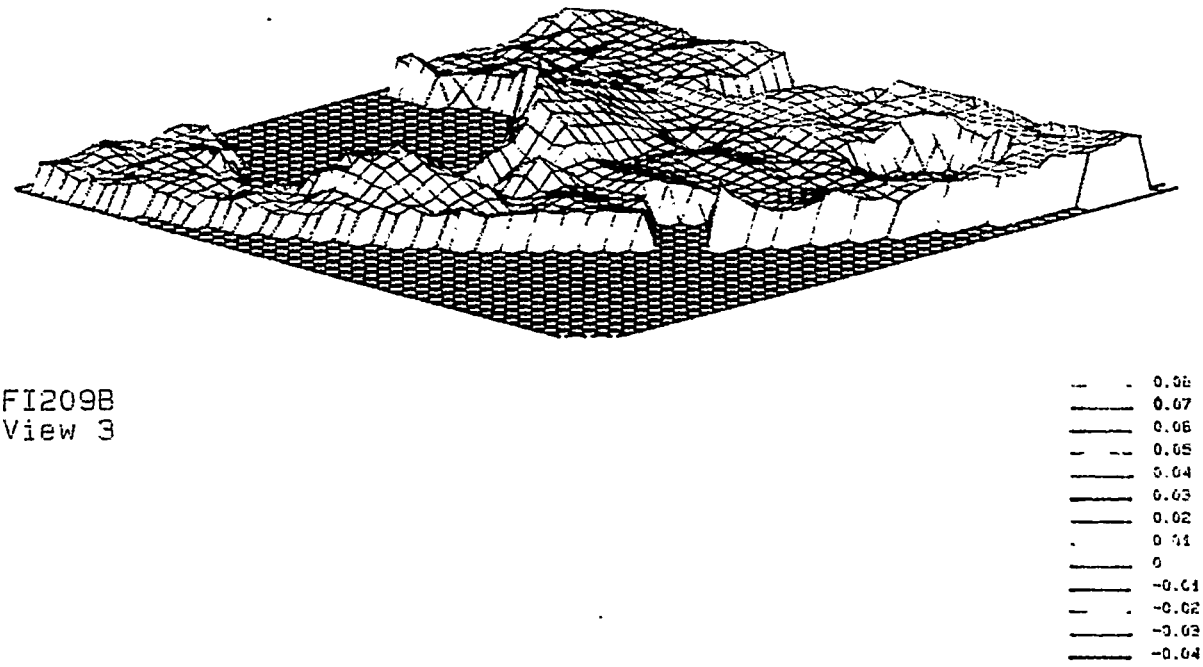

Fig.49 - 3D Perspective Plot of Distortion in Aluminum Sample FI209B

4.0 Photogrammetric plots of Water Jet Cut Steel Plate

Only one set of photogrammetric data was available for making the edge, contour and 3D plots for water jet cutting of steel. The data on the first steel plate was irrecoverably lost when the steel sample dropped out of position in the water jet catch tank and the exact position of the pre-cut fiducial marks were lost. The problem was resolved for the second steel sample and the resultant plots for the steel plate are shown in Figures 50 and 51.

5.0 Edge Plot of Water Jet Cut Steel Plate

The deviation from nominal values of Figure 1 for the water jet cut steel plate, as seen in sample FI-715B Figure 50 are quite similar in magnitude and direction to those of aluminum. On the curved edge the maximum deviation is -3.3 mm (-0.13 in.) The large hole is out of round by 2.8 mm (0.11 in.) and the smaller hole by 2.5 mm (0.10 in.).

6.0 Contour Plot of Out-of-Plane Distortion of Water Jet Cut Steel Plate

The maximum resultant out-of-plane distortion of the water jet cut steel plate, sample F1715B, as seen in Figure 51 is -0.8 mm (-0.03 in.) in the negative direction and 0.2 mm (0.10 in.) in the positive direction.

7.0 3D Perspective Plot of Steel Plate Cut by Water Jet

The resultant distortion in the water jet cut steel plate is show in 3D perspective in Figure 52.

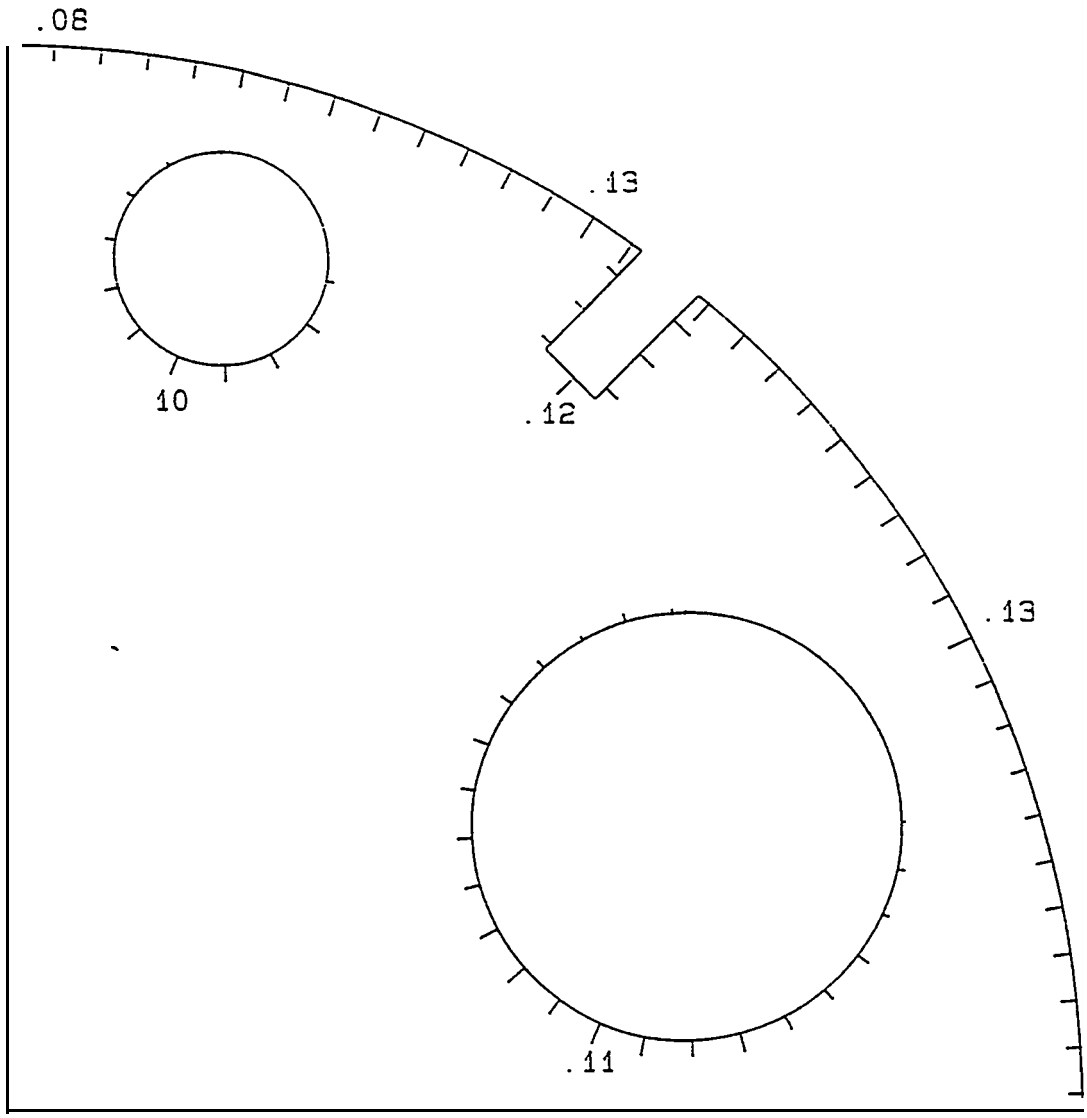

FI715B
Cut edge versus design template
Scale. 1"=8"
Vector scale. 1"=1"

Fig.50 - Edge Plot of Water Jet Cut Steel Plate Sample FI-715B

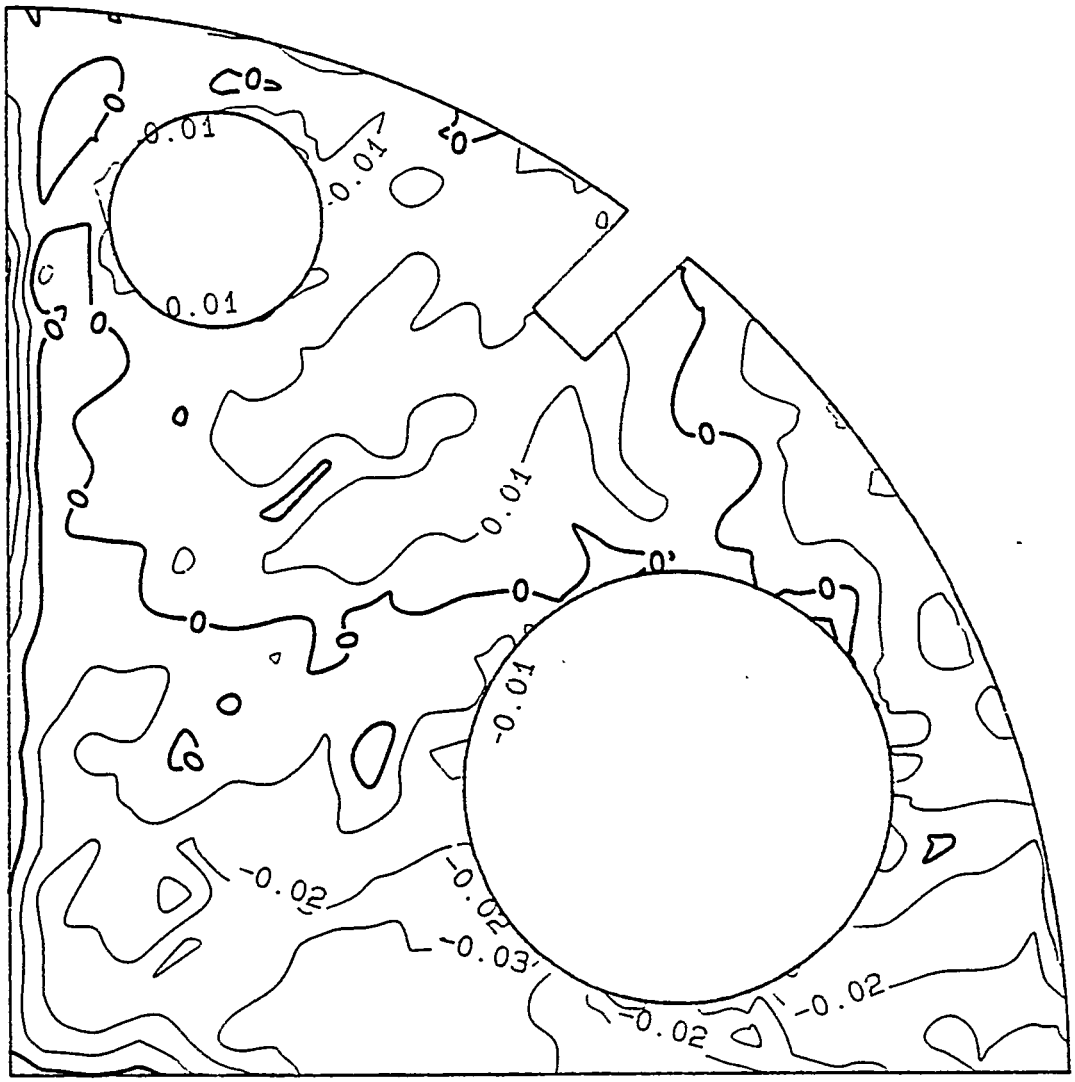

FI715B
Plot 3
Scale: 1"=8"
CI: .01"

Fig.51 - Resultant Out-of-plane Distortion of the Water Jet Cut Steel Plate FI-715B

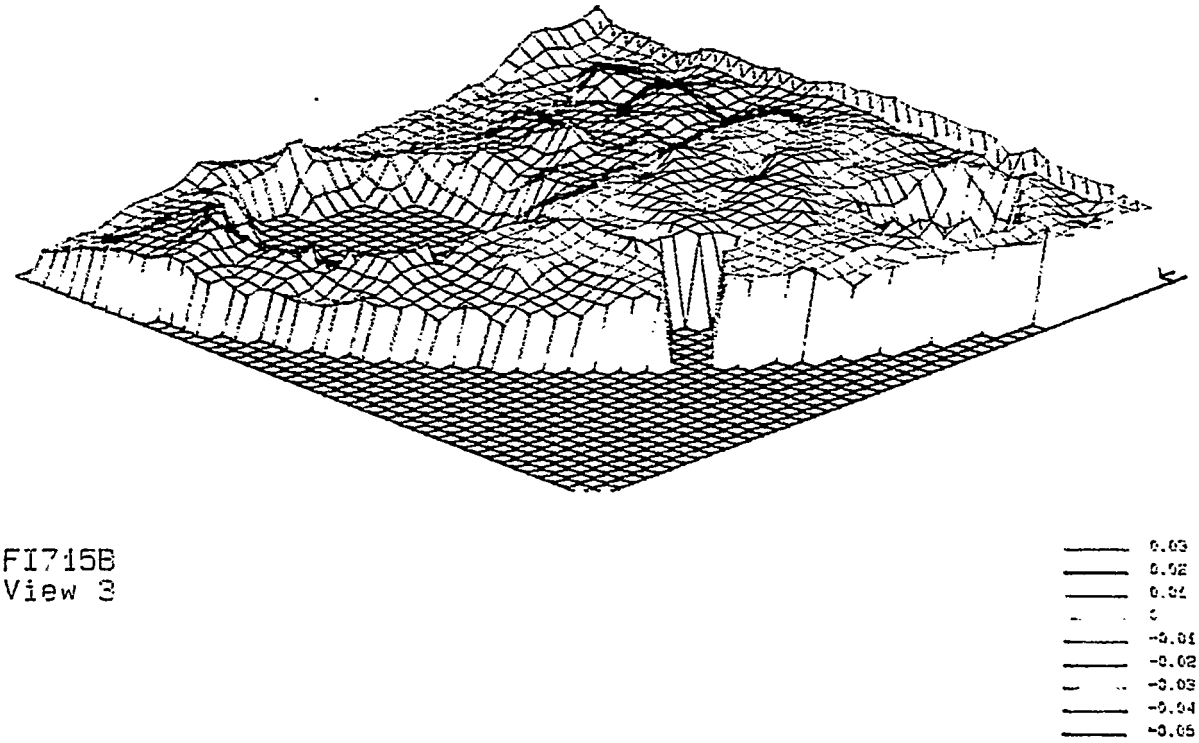

Fig.52 - 3D Perspective Plot of Resultant Distortion in Water Jet Cut Steel Plate FI-715B

VII. SUMMARY, CONCLUSIONS AND DISCUSSION

A. SUMMARY OF DATA

Comparative cutting rates, measurements of out-of-plane distortion, and edge hardness resulting from cutting 3 mm (0.118 in.) aluminum and steel using oxyacetylene, plasma, laser and water jet processes are shown in Graphs 1 and 2 and are summarized below.

Rate of Cutting Aluminum:

Oxyacetylene	not used
Plasma	457 cm/min. (180 in./min.)
Laser	152 cm/min. (60 in./min.)
Water Jet	63.5 cm/min. (25 in./min.)

Out-of-plane Distortion of Aluminum:

Plasma	0.8 mm (0.03 in.)
Laser	1.0 mm (0.04 in.)
Water Jet	-1.3 to +0.8 mm (-0.05 to +0.03 in.)

Rate of Cutting Steel:

Oxyacetylene	55.9 cm/min. (22 in./min.)
Plasma	406 cm/min. (160 in./min.)
Laser	152 cm/min. (60 in./min.)
Water Jet	63.5 cm/min. (25 in./min.)

OUT OF PLANE DISTORTION
UNIT OF MEASUREMENT - mm

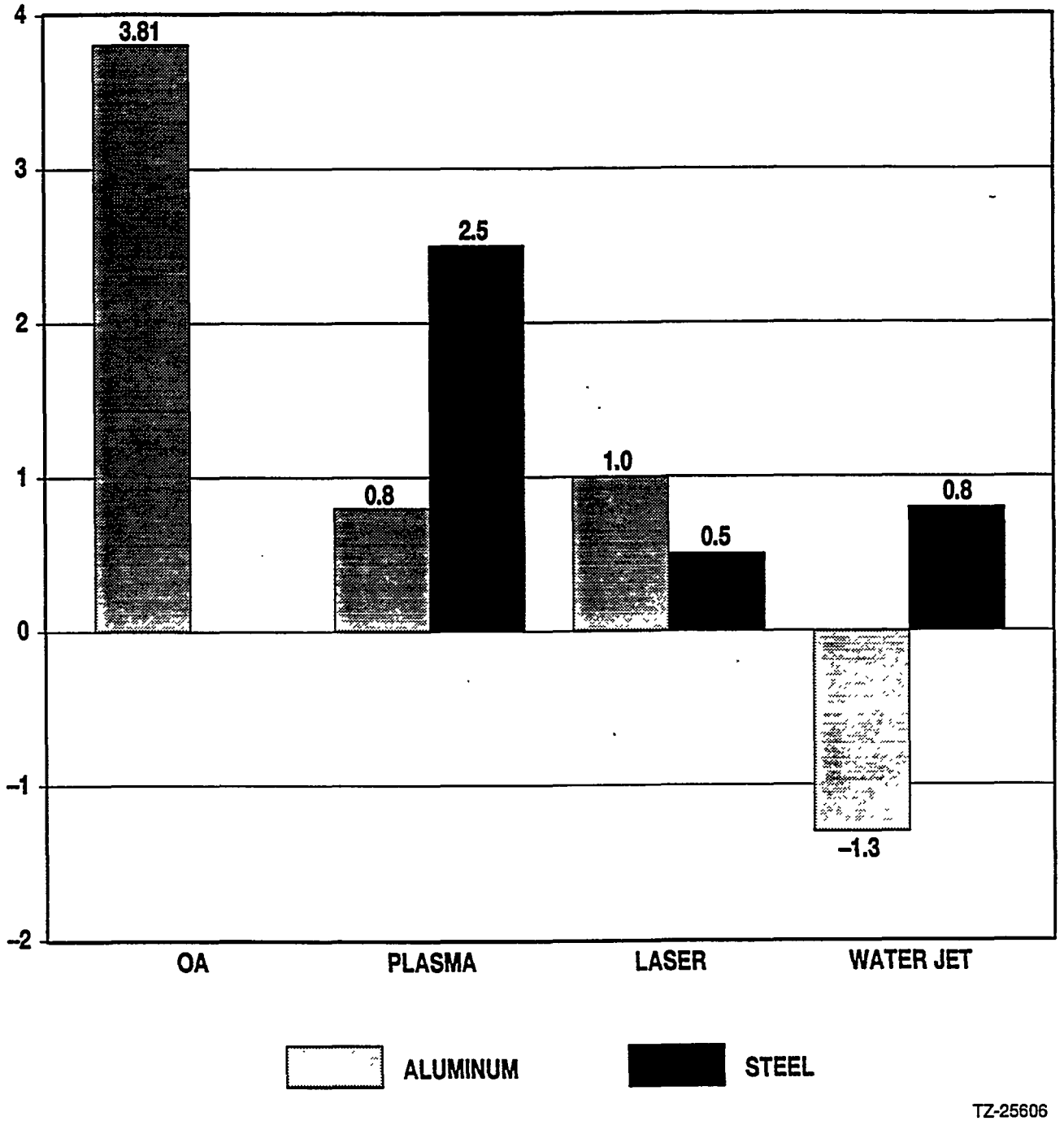

TZ-25606

GRAPH 1

RATE OF CUTTING
CM/MINUTE

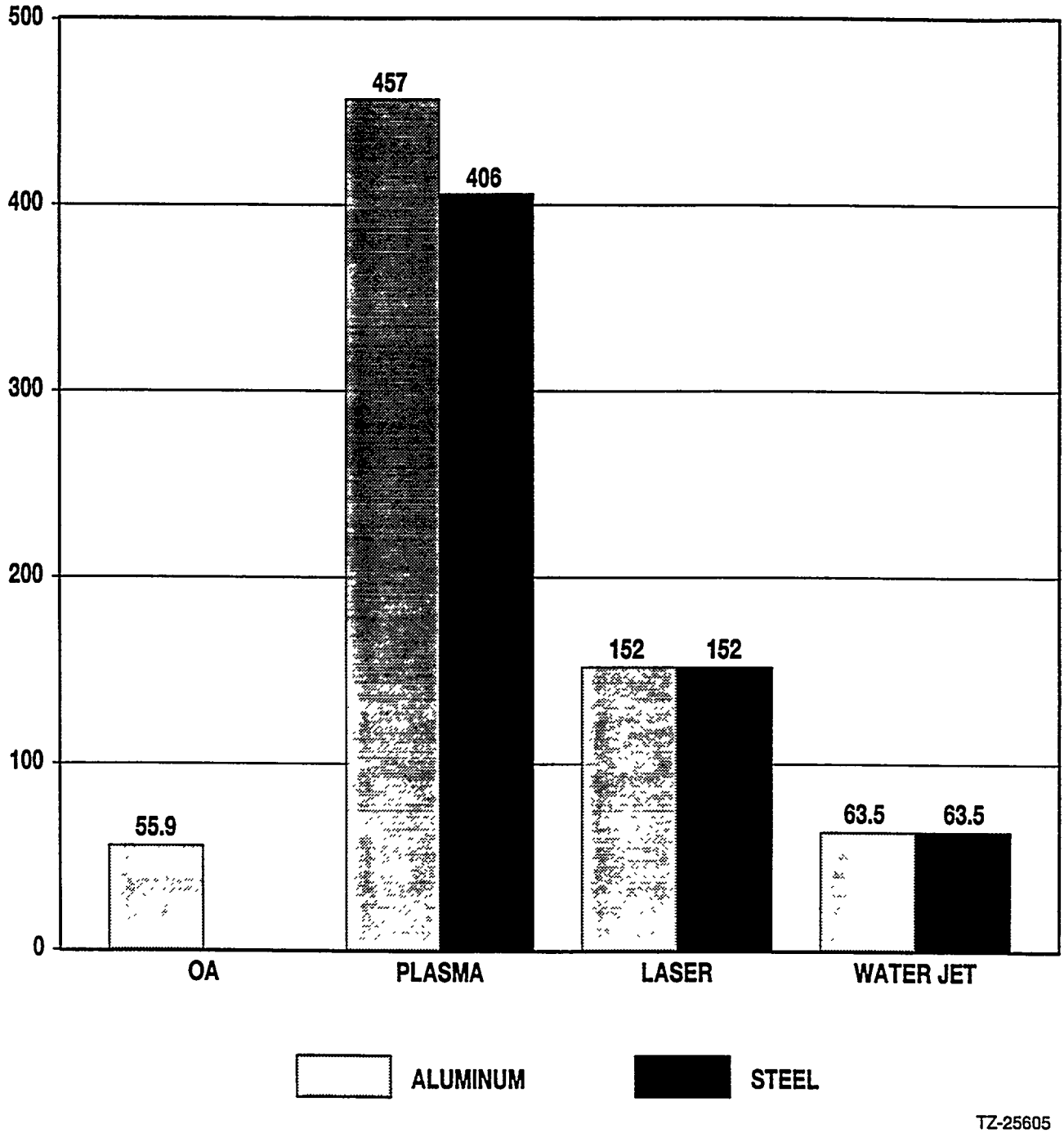

GRAPH 2

Out-of-plane Distortion for Steel:

Oxyacetylene	3.81 cm (1.5 in.)
Plasma	-2.5 to +2.5 mm (-0.10 to +0.10 in.)
Laser	0.5 mm (0.02 in.)
Water Jet	-0.8 to +0.2 mm (-0.03 to +0.01 in.)

Hardness (500 gram Vickers) range for steel across the HAZ starting 4 roils from cut edge: Oxyacetylene - 166 to 238; Plasma - 161 to 320; Laser - 149 to 253; Water Jet - 220 to 232.

CONCLUSIONS

[illegible] cutting produced the least distortion in cutting of 3 mm aluminum plates, 0.8 mm (0.03 in.).

The fastest cutting of 3 mm (0.118 in.) aluminum plates was by Plasma arc at 457 cm/min. (180 in./min.).

The laser cutting of aluminum, at 152 cm/min. (59.8 in./min.), produced 1.0 mm (0.04 in.) out-of-plane distortion.

Water jet cutting of aluminum at 63.5 cm/min. (25 in./min.) produced out-of-plane distortion of -1.3 mm to +0.76 mm (-0.05 in. to +0.03 in.)

The [illegible]er process produced the least distortion, 0.5 mm (0.02 in.), in cutting of 3 mm steel plate.

The fastest cutting of steel was with the plasma process at 406 cm/min. (160 in./min.), which produced distortion from -2.5 mm to +2.5 mm (0.10 in.).

Oxyacetylene cutting of steel, at 55.9 cm/min. (22 in./min.), produced the most distortion, 3.81 cm (1.5 in.) when compared to

plasma, laser, and water jet cutting.

Plasma arc was the fastest and most cost effective method of cutting 3 mm (0.118 in.) aluminum and steel plates with acceptable low levels of distortion.

The greatest base metal heat effect on steel was from plasma cutting which produced a range of hardness across the HAZ of Vickers (500 g) 161 to 320.

The least variation in hardness effects on steel across the HAZ was from water jet which produced a range of hardness of Vickers (500 g) 220 to 232.

No excessive base metal damage was produced in aluminum or steel by any of the cutting processes tested.

Contour plots produced in this project demonstrate that photogrammetry can be used effectively in measurement of out-of-plane distortion in thin plates.

Photogrammetry can be used where high density data is needed for measurement of out-of-plane contours as small as 0.25 mm (0.01 in.).

C. DISCUSSION

The process which produced the least amount of distortion in cutting steel used only 1500 watts from a $C0_2$ laser; however, the plasma process cut the 3 mm (0.118 in.) steel plates over twice as fast. Further study of faster rates of cutting with more powerful lasers than that available with this project should be undertaken to determine whether or not faster rates could be achieved while holding the distortion to below that of plasma. The distortion

produced by plasma at the much faster rate was still acceptable for most shipbuilding construction using thin plates. A major trade off consideration before converting from existing plasma cutting systems to laser cutting would necessarily be the relative cost of a laser versus a plasma cutting system. A conservative estimate based on available information indicates that a laser system would cost from 3 to 4 times more than a plasma system. The water jet system which produces low levels of distortion and clean cuts was from 2 to 6 times slower than laser and plasma respectively. From the productivity standpoint, the slow cutting rate of water jet does not warrant further consideration of that process for cutting of aluminum and steel plates for ship construction. Cutting of other materials, not feasible with thermal processes, such as Kevlar, rubber and composites may be cost effective for shipbuilding using water jet and should not be ruled out.

The success in this project of measuring small and large displacements of out-of-plane distortion in plates by photogrammetry indicates that those techniques could become a more widely used tool in distortion control. Research and development of real time photogrammetry would be justified for use as a mechanism for robotic control for weld joint tracking or for correction of distortion. The development of software programs to perform rapid computations of stereo images of a work field would be a useful area of research toward that end.

APPENDIX A

METALLOGRAPHIC EVALUATIONS OF 3MM ALUMINUM AND STEEL PLATES

CUT BY OXYACETYLENE, PLASMA, LASER AND WATER JET

CONTENTS :

Sample Identities:

WE-lA-A715A	Plasma Cut Steel
WE-lA-B209	Plasma Cut Aluminum
WE-lB-A715A	Water Jet Cut Steel
WE-lB-B209A	Water Jet Cut Aluminum
WE-lC-A715A	Laser Cut Steel
WE-lC-B209A	Laser Cut Aluminum
WE-lD-A715A	Oxyacetylene Cut Steel

MATERIALS EVALUATION LABORATORY
INCORPORATED
17695 Perkins Road
Baton Rouge, Louisiana 70810

Telephone (504) 752-6070 Fax (504) 752-6097

GENERAL INFORMATION

Work Performed For: Ingalls Shipbuilding, Inc.

Report Date: February 16, 1993

Report Number: 10571

WORK PERFORMED

Samples representing the effects of four industrial cutting processes were submitted for examination. As appropriate, both steel and aluminum specimens had been machined. This work was done at the request of Mr. Russ McClellan.

Each of seven samples was subjected to a series of tests. These included: macroscopic evaluation of a cut edge profile; scanning electron microscopic (SEM) study Of the cut surface; microscopic examination of sections parallel and perpendicular to a cut edge; and, a microhardness traverse inward from the cut edge.

RESULTS

Macroscopic Evaluation

Specimens were prepared from each sample which would display a profile of the cut edge. These were examined visually and with a stereographic microscope. Typical features are described in the following:

WE-lA-A715A . There was a pronounced groove made during the cut . It had a roughly 45 degree included angle with the widest opening on the top. A heat-affected-zone on the cut face is 8-10 mils thick.

WE-lA-B209A . A groove was formed by the cutting action. It had a roughly 35 degree included angle with the widest opening on the top.

WE-lB-A715A. The cut edge was straight and perpendicular to the two faces.

WE-lB-B209A . The majority of the cut edge was straight and perpendicular to the two faces. The top edge had a rounded shoulder with a radius of 50 roils.

WE-lC-A715A. The cut edge was straight and perpendicular to the two faces. A heat-affected-zone on the cut face ranged from 4-6 Mils in thickness.

WE-IC-B209B. The majority of the cut edge was straight and perpendicular to the two faces. Both edges were slightly rounded to a radius of 70 mils.

WE-lD-A715A. The cut edge was rounded with a radius of 1/4 inch. A heat-affected-zone on the cut face ranged from 25 to 40 mils in thickness.

Figures 1, 5, 9, 13, 17, 21 and 25 show the cut edge profiles.

SEM Study

A length of the cut edge was removed from each sample. These specimens were studied using a scanning electron microscope (SEM) . That provided high depth of field viewing of the surface , texture. Features observed are discussed in the following:

WE-lA-A715A. The cut face was smooth with very little adherent debris. There were parallel lines on the surface. These were due to a waviness with a crest spacing of 10 roils. The upper 1/2 of the lines were straight, while the lower 1/2 curved on a 1 inch radius.

WE-lA-B209A. The cut face had a smeared appearance. There were poorly defined lines of waviness with crest spacing of 10 mils. The lines were parallel but had a 2 inch radius curvature across the face.

WE-lB-A715A. There was an irregular, slightly roughened texture. Small nodules of metal adhered to the surface. No distinct cutting pattern was observed.

WE-lB-B209A. There was an irregular, slightly roughened texture. A faint pattern of parallel cut lines was visible on the surface.

WE-lC-A715A. The surface displayed closely spaced, parallel lines of waviness. The crests were 5 mils apart. A very fine network of craze-cracks covered much of the surface.

WE-lC-B209B. The surface had a smeared appearance. There were poorly defined wavy lines with 5 mil crest spacing. A random pattern of small debris adhered to the metal.

WE-lD-A715A . The surface was slightly roughened with no distinct pattern of cut lines. Random clumps of oxide scale adhered to the metal.

Figures 2, 6; 10, 14, 18, 22 and 26 show the cut face textures.

Microscopic Examination

Specimens were removed from the samples, mounted, polished and etched. They were examined microscopically using a light optical metallograph. Viewing orientations were in the transverse and longitudinal directions. Comments from this examination are provided in the following:

TRANSVERSE

WE-lA-A715A . There was a smooth edge with a thin layer of adherent oxide scale. A heat-affected-zone extended inward roughly 8-10 roils.

WE-lA-B209A . The cut edge was smooth. Random spots of resolidified metal adhered to the surface.

WE-lB-A715A. Plastic grain flow in a downward direction across the cut face was evident. A thin layer of oxide adhered to the surface.

WE-lB-B209A . The cut edge was straight and clean.

WE-lC-A715A. The cut edge was straight and free of any oxide scale. A faint heat-affected-zone extended inward for about 5 mils.

WE-lC-B209B. The cut edge was straight and clean.

WE-lD-A715A. The cut surface was flat with some oxide scale. Grain coarsening in the heat-affected-zone could be seen to a depth of 1/10 inch.

Figures 3, 7, 11, 15, 19, 23 and 27 show a transverse edge.

LONGITUDINAL

WE-lA-A715A. A heat-affected-zone with mild coarsening of the grains extended inward 10-12 roils. Oxide scale 2-4 roils thick adhered to the surface.

WE-1A-B209A. The edge was generally clean and smooth. The crests from waviness in the cutting pattern could be seen.

***WE-1B-A715A*. The cut edge was very clean. There was a slightly jagged contour with variations of ±5 mils.**

***WE-1B-B209A*. The cut edge was clean, but had an uneven contour. There was a suggestion of waviness and an overlaid roughness with ±5 mil variation.**

WE-lC-A715A. The cut edge was smooth and clean. A region of coarsened grains formed a heat-affected-zone 5 roils deep.

WE-lC-B209B. The cut edge was smooth, clean and straight.

WE-lD-A715A. The cut edge was smooth. There was a 10 mil thick, adherent layer of oxide scale. A 1/8 inch deep heat-affected-zone was indicated by grain coarsening.

Figures 4, 8, 12, 16, 20, 24 and 28 show a longitudinal edge.

Microhardness Traverse

Microhardness measurements were made on each sample. A Vicker's type indenter with either a 200g or 500g primary load was used. The first impression was 4 mils from the cut edge. Subsequent impressions were at 6 mil intervals. Test results, grouped by the primary load, are tabulated in the following:

500g Load

WE-1A-A715A	320	231	189	177	164	161
WE-1B-A715A	220	228	229	225	229	232
WE-1C-A715A	253	174	156	149	149	149
WE-1D-A715A	197	238	223	214	174	166

200g Load

WE-1A-B209A	85.4	86.2	93.4	90.8	98.4	102
WE-1B-B209A	103	102	101	101	110	102
WE-1C-B209B	76.8	86.2	90.8	96.2	84.9	87.5

CONCLUSIONS

The following comments are the Author's opinions based upon the results of this investigation:

1. The cutting process that produced samples WE-lB-* was the least intrusive. It produced a clean edge with little distortion, scale formation, or microstructural change.

2. A ranking of the remaining processes, in order of increasing alteration of the metal, would be: WE-lC-*; WE-1A-*; and, WE-lD-*.

STATE OF LOUISIANA
CLAUDE R. MOUNT
REG. No. 23321
REGISTERED PROFESSIONAL ENGINEER
METALLURGICAL ENGINEER

Materials Evaluation Laboratory, Inc.

Claude R. Mount, PE

Reviewed By: Archie L. Tuttle

Date: 2-19-93

NOTE: Specimen(s) and material remnants from this project will be discarded after thirty (3o) days from the date of this report. Any requests for alternative handling must be submitted in writing and received prior to that deadline.

Figure 1: A profile view of sample WE-lA-A715A, the *top* surface is to the right. (30X)

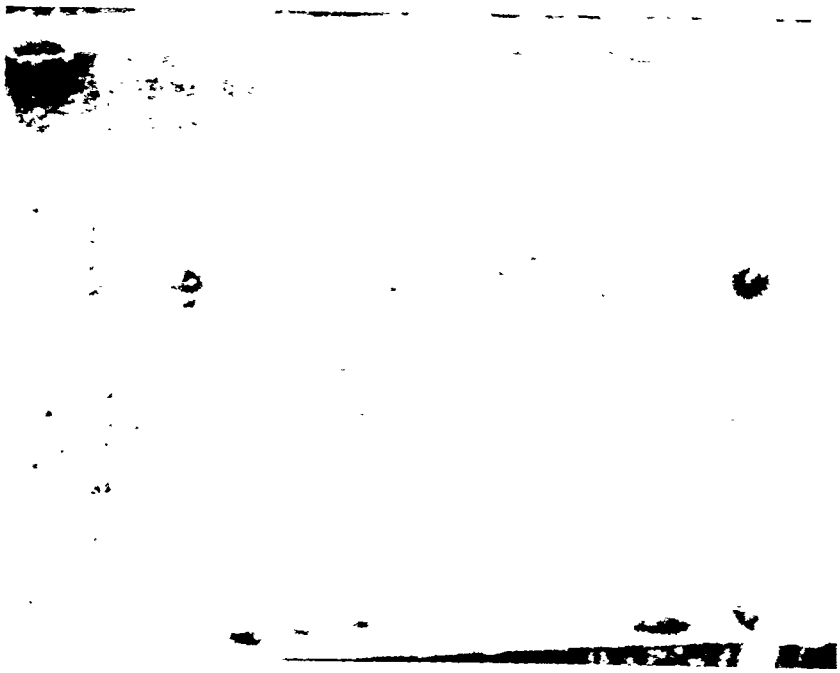

Figure 2: A face-on view using an SEM of sample WE-lA-A715A, the cutting direction was left-to-right. (30X)

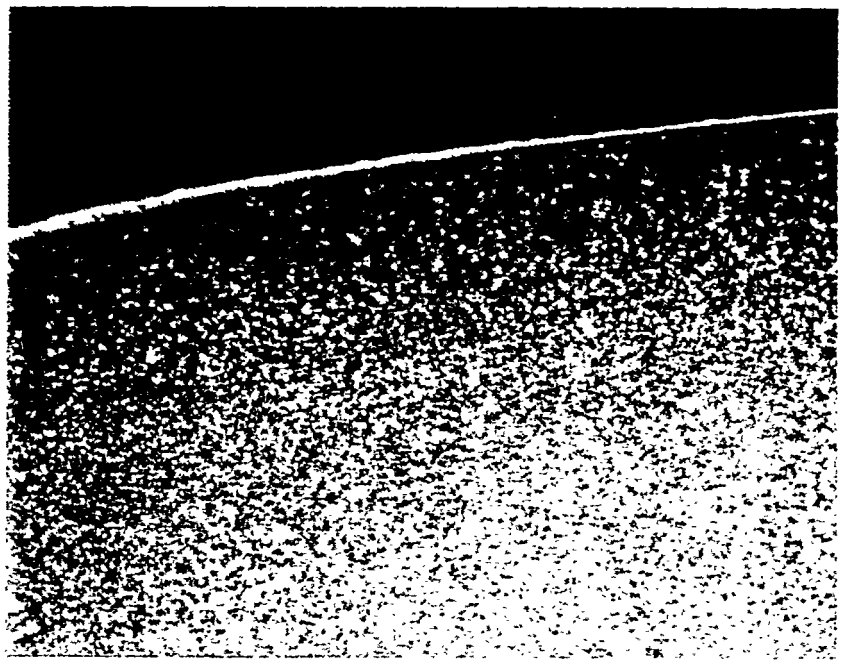

Figure 3: A photomicrograph showing a transverse edge of sample WE-1A-A715A . (lOOX, Nital Etch)

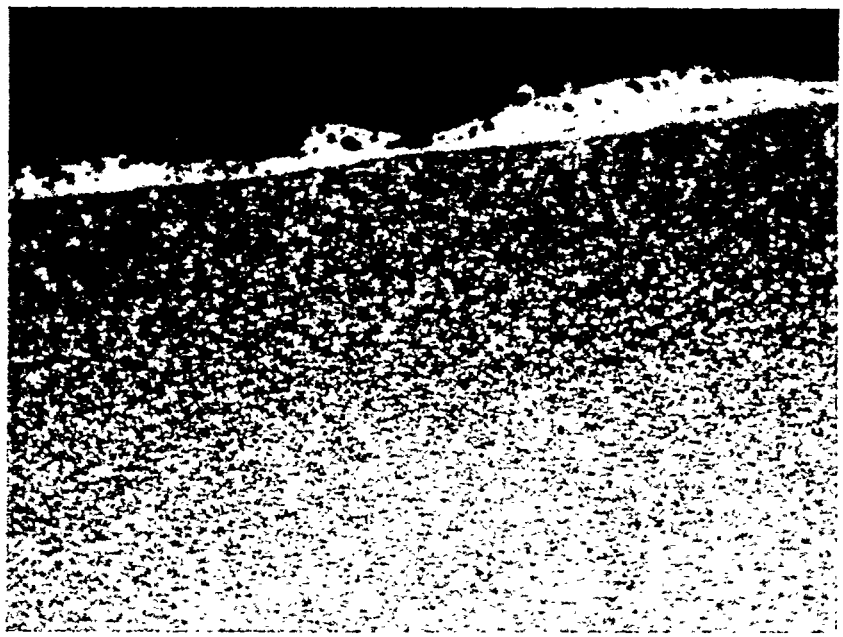

Figure 4: A photomicrograph showing a longitudinal edge from sample WE-1A-A715A. (1OOX, Nital Etch)

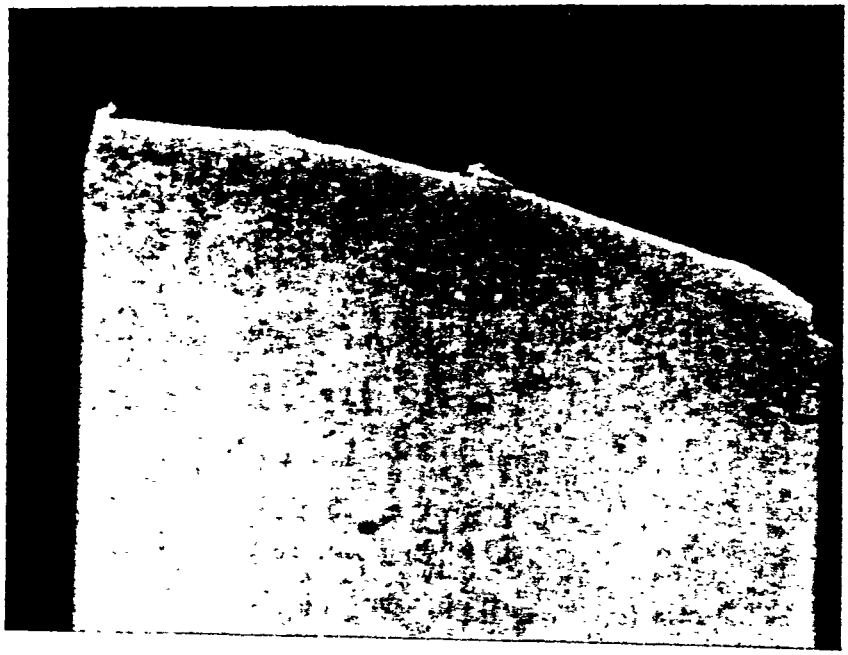

Figure 5: A profile view of sample WE-lA-B209A, the top surface is to the right. (30X)

Figure 6: A face-on view using an SEM of sample WE-1A-B209A, the cutting direction was left-to-right. (3OX)

Figure 7: A photomicrograph showing a transverse edge of sample WE-lA-B209A . (100X, 1/2% HF .Etch)

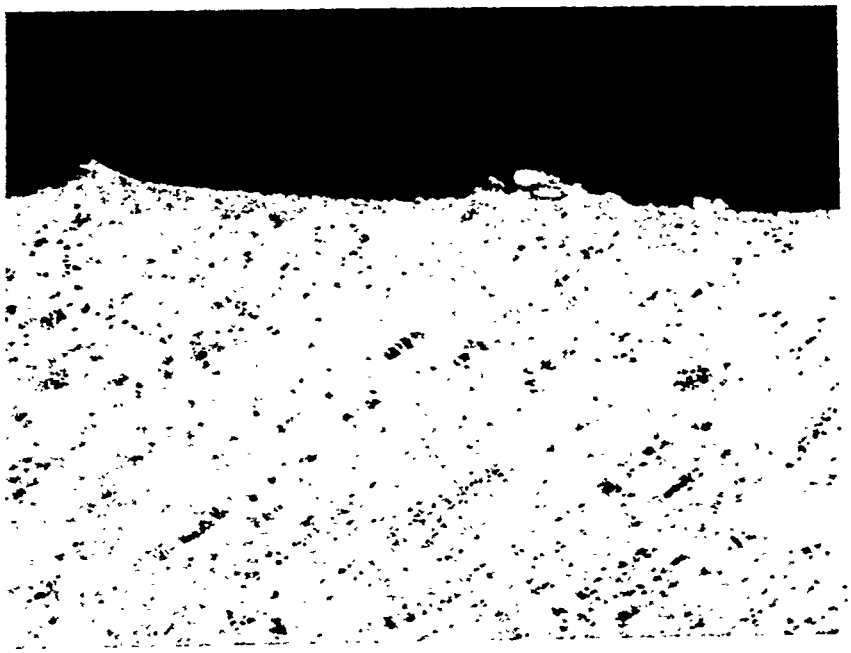

Figure 8: A photomicrograph showing a longitudinal edge from sample WE-lA-B209A. (100X, 1/2% HF Etch)

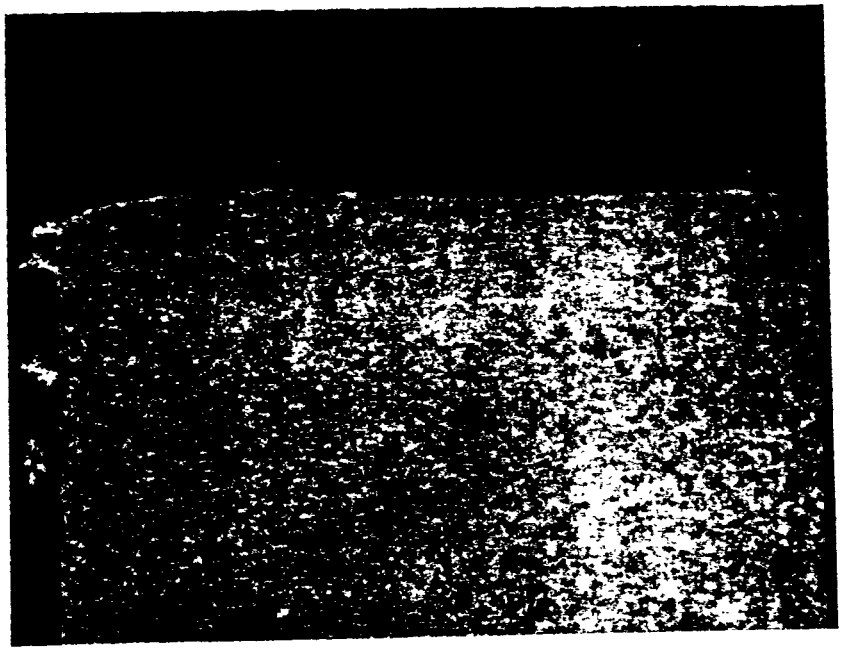

Figure 9: A profile view of sample WE-1B-A715A, the *top* surface is to the right. (30X)

Figure 10: A face-on view using an SEM of sample WE-1B-A715A, the cutting direction was left-to-right. (30X)

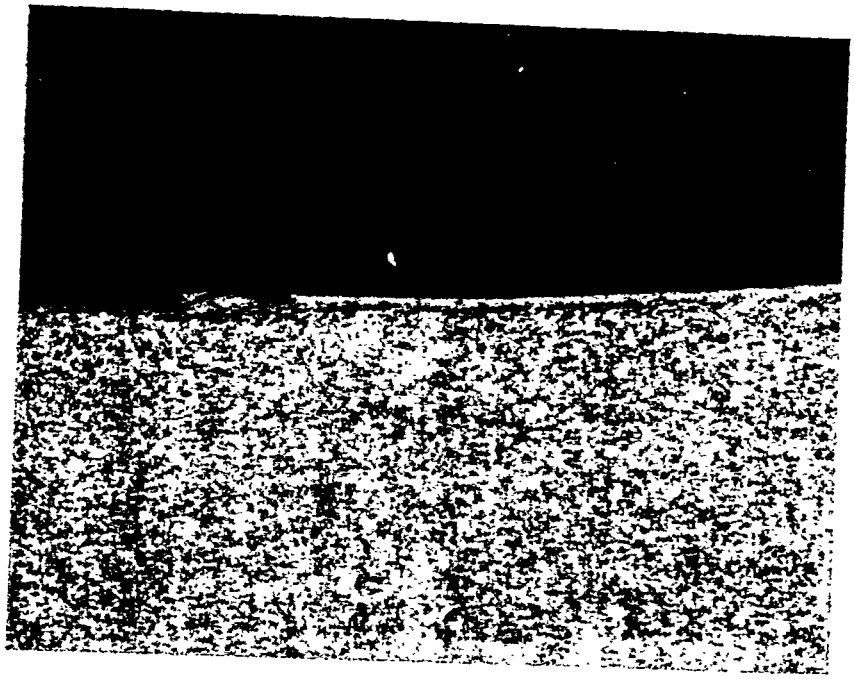

Figure 11: A photomicrograph showing a transverse edge of sampl WE-1B-A715A. (100X, Nital Etch)

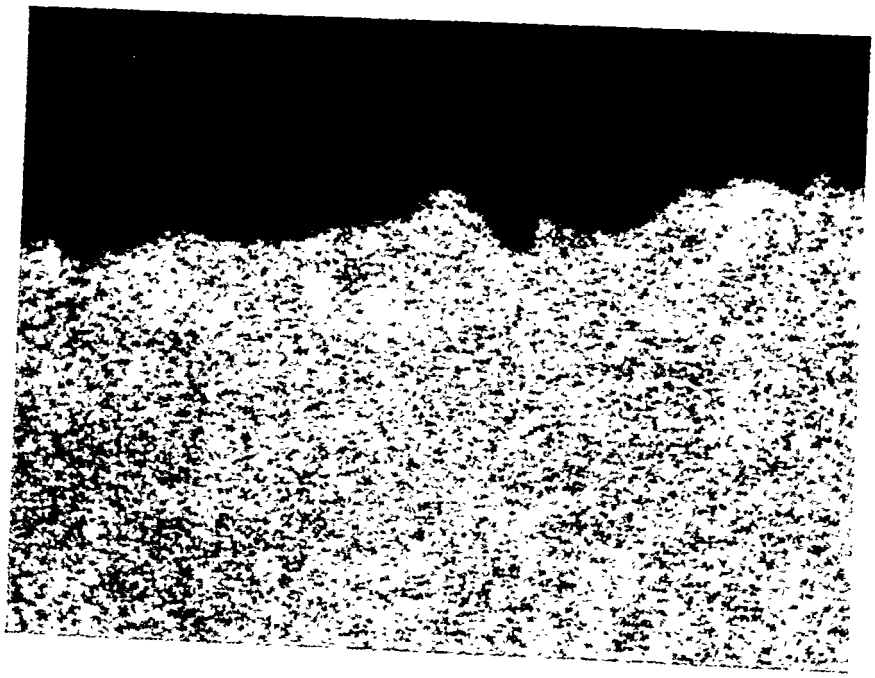

Figure 12: A photomicrograph showing a longitudinal edge from sample WE-1B-A715A. (100X, Nital Etch)

Figure 13: A profile view of sample WE-1B-B209A, the *top* surface is to the left. (30X)

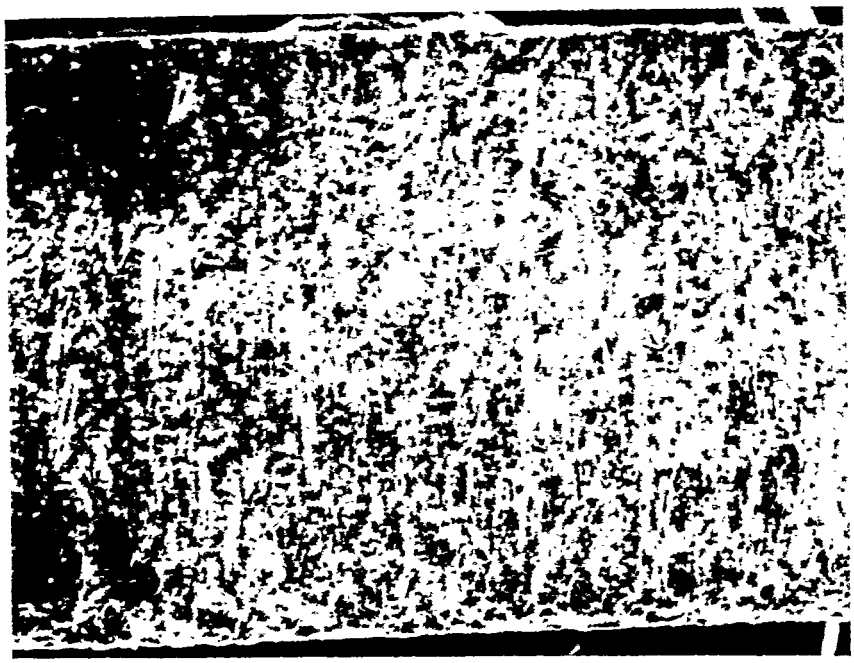

Figure 14: A face-on view using an SEM of sample WE-1B-B209A, the cutting direction was left-to-right. (30X)

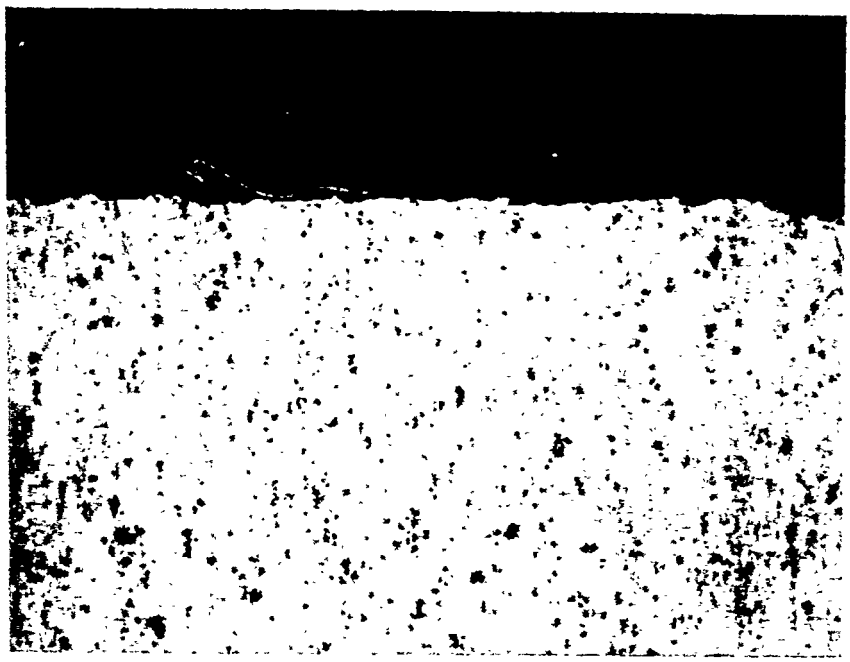

Figure 15: A photomicrograph showing a transverse edge of sample WE-lB-B209A . (100X, 1/2% HF Etch)

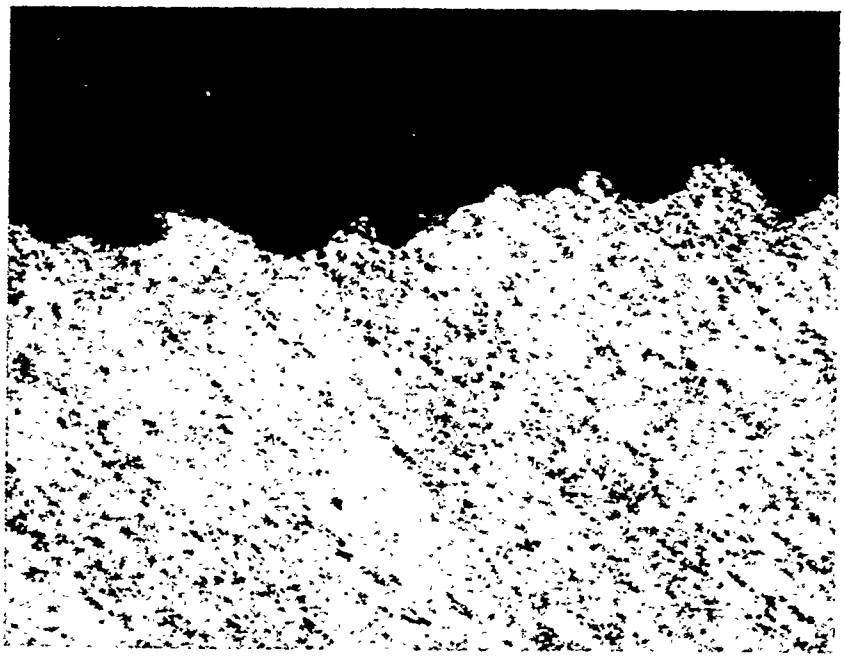

Figure 16: A photomicrograph showing a longitudinal edge from sample WE-lB-B209A. (100X, 1/2% HF Etch)

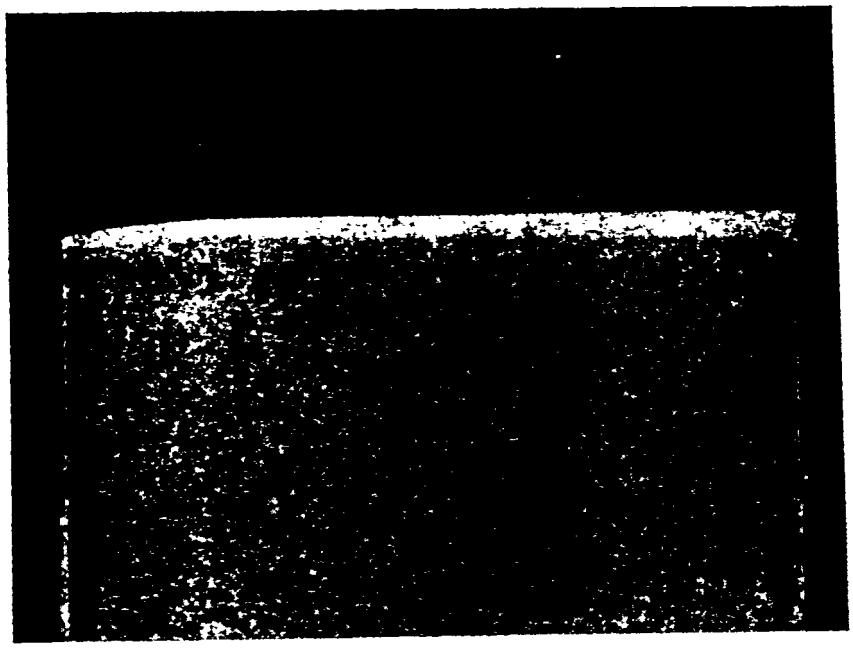

Figure 17: A profile view of sample WE-lC-A715A, the top surface is to the right. (30X)

Figure 18: A face-on view using an SEM of sample WE-lC-A715A, the cutting direction was left-to-right. (30X)

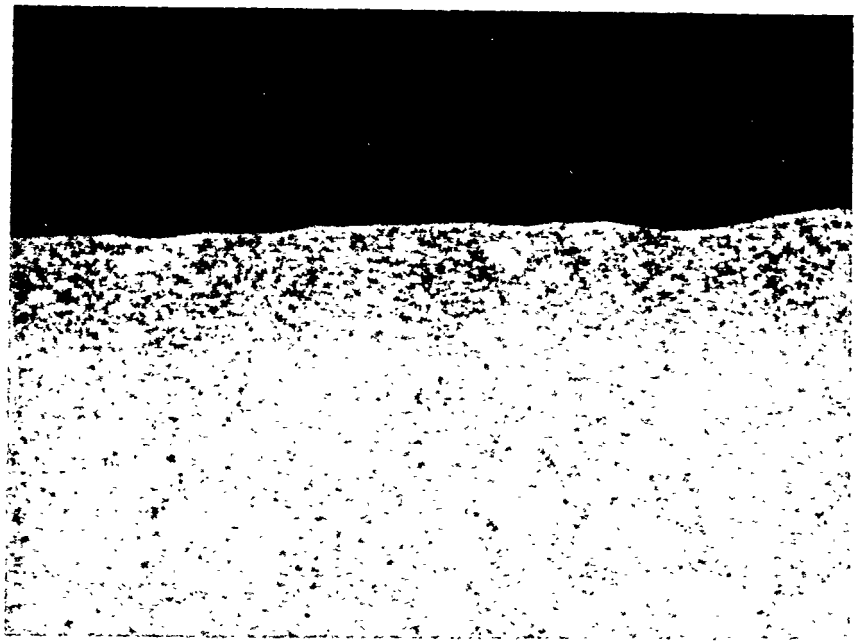

Figure 19: A photomicrograph showing a transverse edge of sample WE-1C-A715A. (100X, Nital Etch)

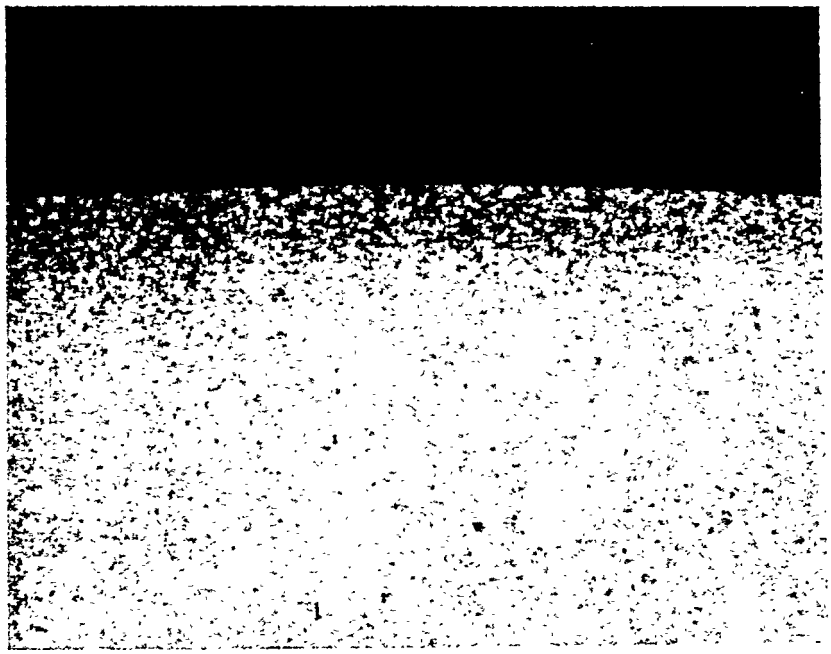

Figure 20: A photomicrograph showing a longitudinal edge from sample WE-lC-A715A. (100X, Nital Etch)

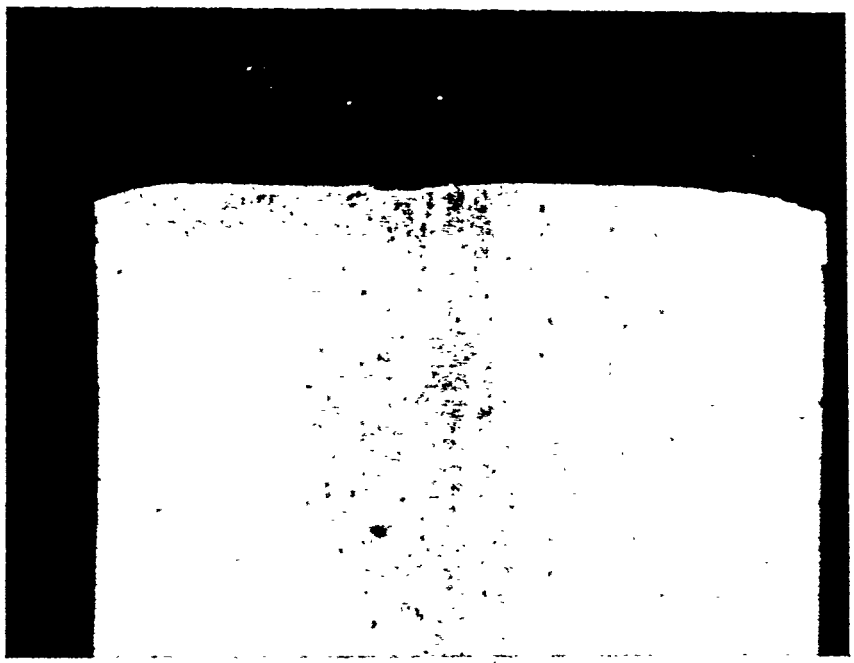

Figure 21: A profile view of sample WE-lC-B209A, the top surface is to the right. (30X)

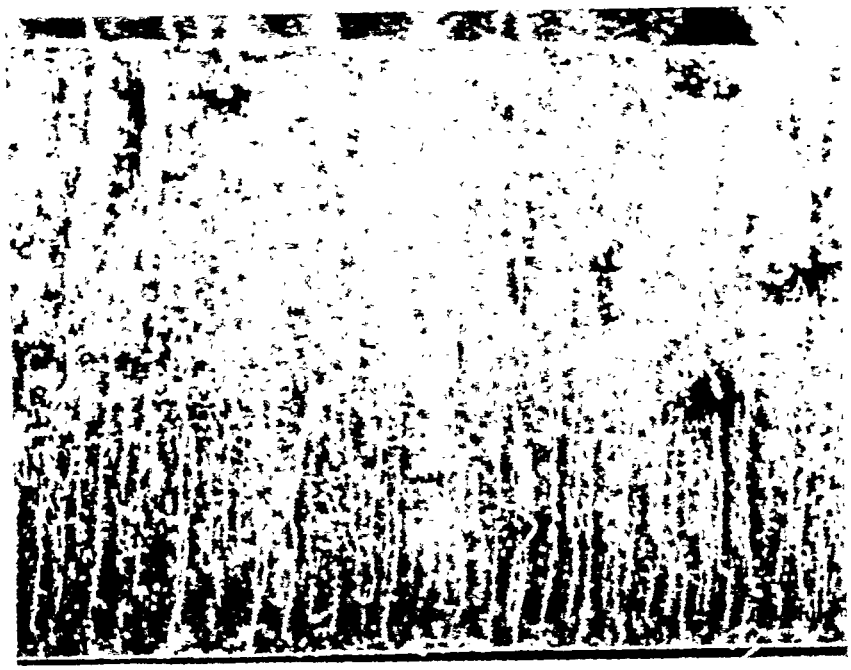

Figure 22: A face-on view using an SEM of sample WE-lC-B209A, the cutting direction was left-to-right. (30X)

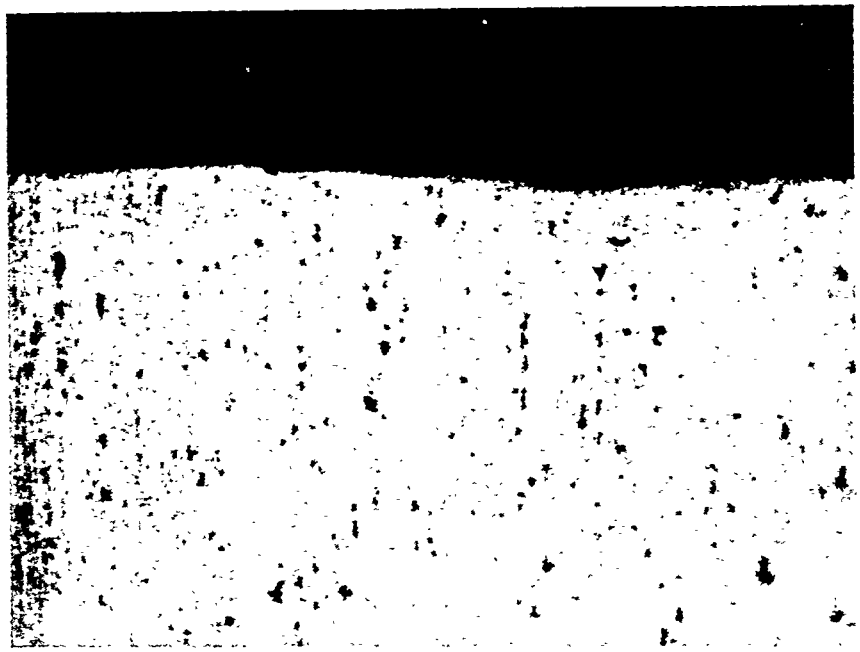

Figure 23: A photomicrograph showing a transverse edge of sample WE-1C-B209A. (100X, 1/2% HF Etch)

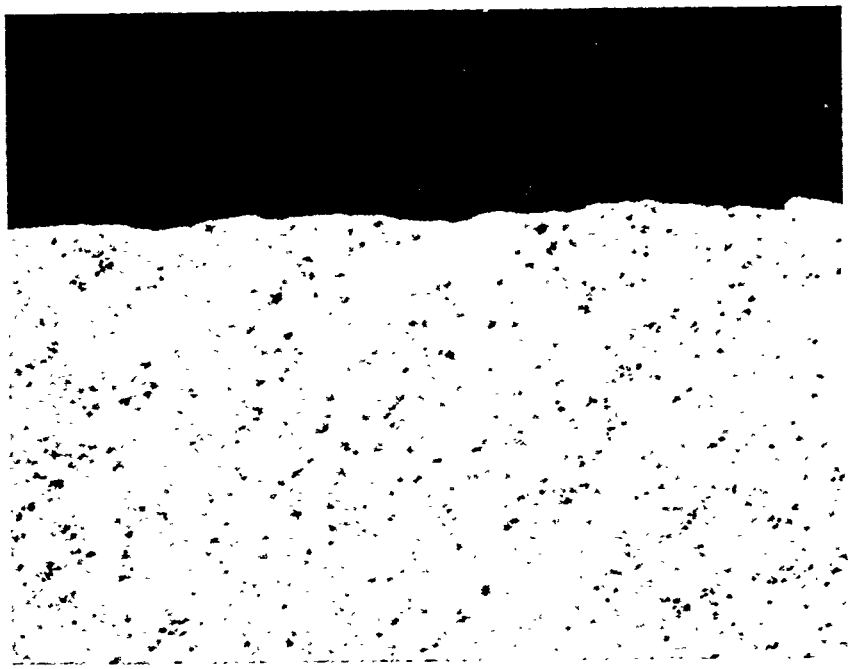

Figure 24: A photomicrograph showing a longitudinal edge from sample WE-1C-B209A. (100X, 1/2% HF Etch)

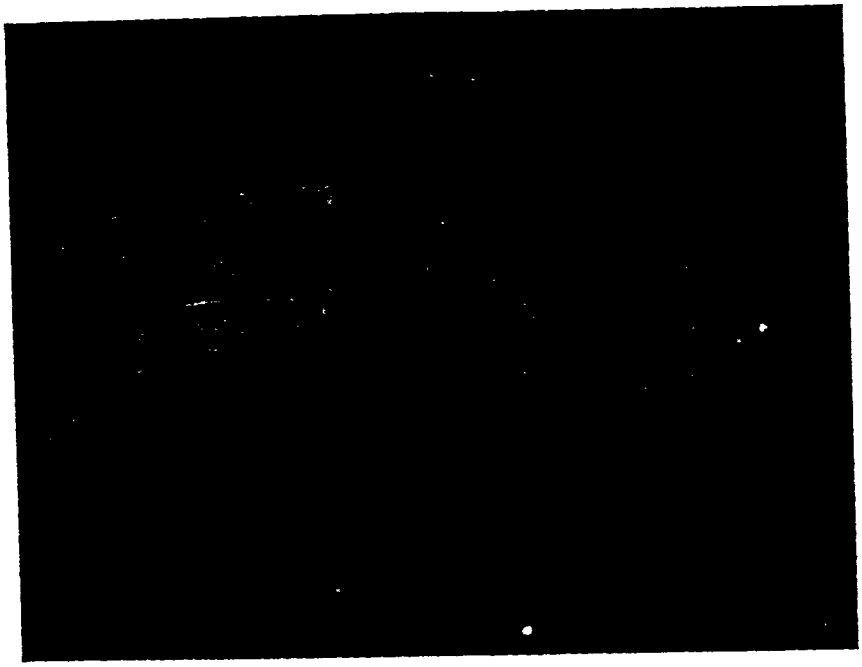

Figure 25: A profile view of sample WE-1D-A715A, the *top* surface is to the right.. (30X)

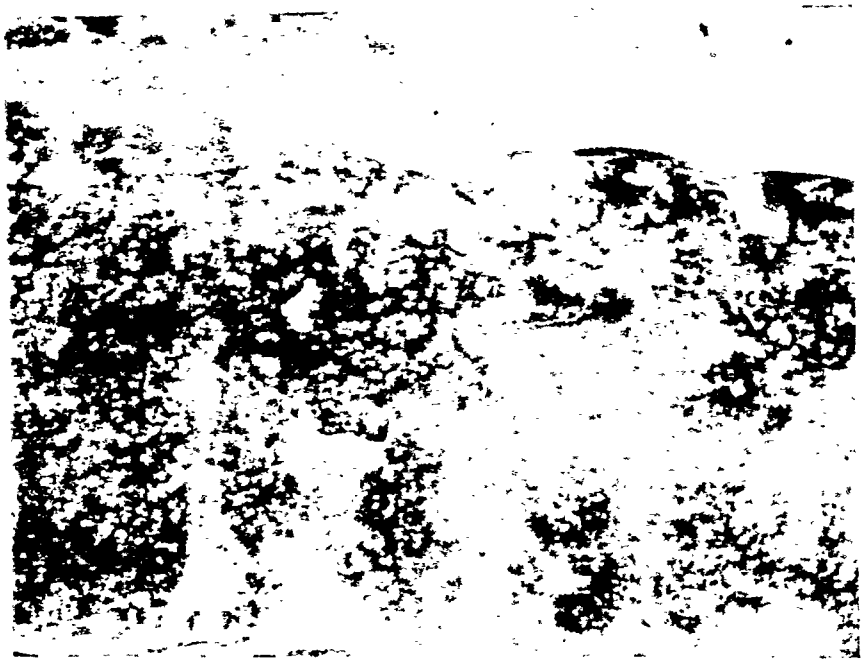

Figure 26: A face-on view using an SEM of sample WE-1D-A715A, the cutting direction was left-to-right. (30X)

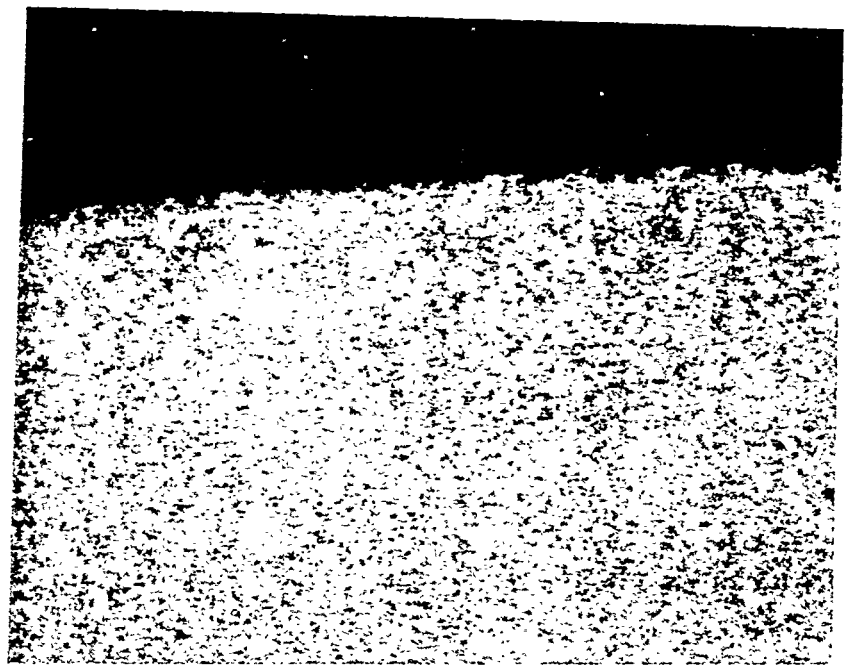

Figure 27: A photomicrograph showing a transverse edge of s WE-1D-A715A. (100X, Nital Etch)

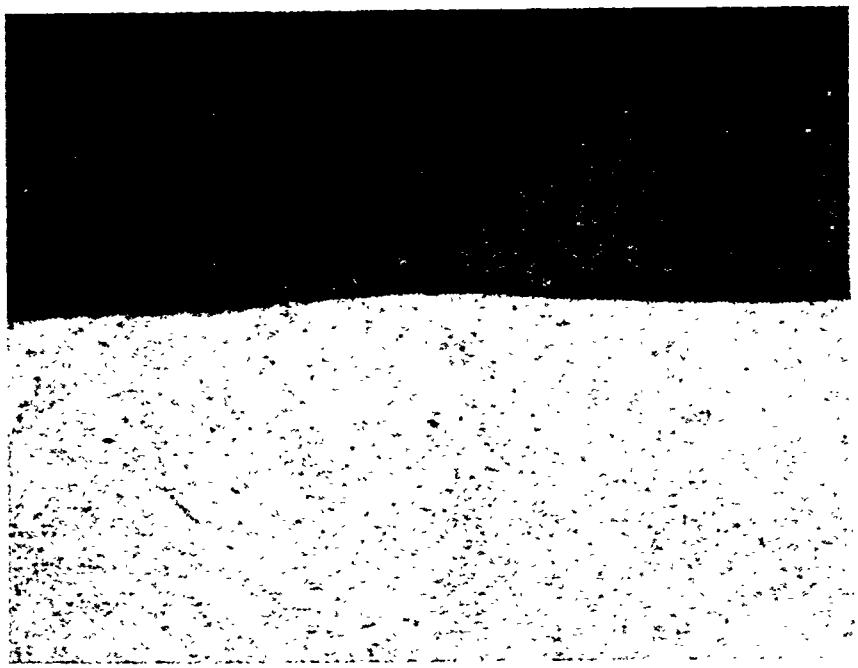

Figure 28: A photomicrograph showing a longitudinal edge from sample WE-1D-A715A. (100X, Nital Etch)

Additional copies of this report can be obtained from the National Shipbuilding Research Program Coordinator of the Bibliography of Publications and Microfiche Index. You can call or write to the address or phone number listed below.

NSRP Coordinator
The University of Michigan
Transportation Research Institute
Marine Systems Division
2901 Baxter Rd.
Ann Arbor, MI 48109-2150
Phone: (313) 763-2465
Fax (313) 936-1081